5-11-2002

Evaluating the Design Process of a Four-Bar-Slider Mechanism Using Uncertainty Techniques

Elizabeth Kay Bartlett

Evaluating the Design Process of a Four-bar-slider Mechanism Using Uncertainty Techniques

By

Elizabeth Kay Bartlett

A Thesis
Submitted to the Faculty of
Mississippi State University
in Partial Fulfillment of the Requirements
for the Degree of Master of Science
in Mechanical Engineering
in the Department of Mechanical Engineering

Mississippi State, Mississippi

May 2002

EVALUATING THE DESIGN PROCESS OF A FOUR-BAR-SLIDER MECHANISM

USING UNCERTAINTY TECHNIQUES

By

Elizabeth Kay Bartlett

Approved:

Susan T. Hudson Assistant Professor of Mechanical Engineering (Director of Thesis)	Carl James Assistant Research Professor Mechanical Engineering (Committee Member)
James C. Newman III Assistant Professor of Aerospace Engineering (Committee Member)	Jeffrey Shenefelt Research Engineer I Mechanical Engineering (Committee Member)
Rogelio Luck Associate Professor of Mechanical Engineering Director of Graduate Studies in the Department of Mechanical Engineering	Robert Taylor Associate Dean Dean of the College of Engineering

Name: Elizabeth Kay Bartlett

Date of Degree: May 11, 2002

Institution: Mississippi State University

Major Field: Mechanical Engineering

Major Professor: Dr. Susan T. Hudson

Title of Study: EVALUATING THE DESIGN PROCESS OF A FOUR-BAR-SLIDER MECHANISM USING UNCERTAINTY TECHNIQUES

Pages in Study: 112

Candidate for Degree of Master of Science

With limited resources and time available for a typical design project, it is difficult to decide how to allocate these resources and time to produce an optimum design. Also, the question arises, "Given the design process, available resources, and available time, will the design meet the program goals?" Uncertainty analyses of design processes addresses these issues and could substantially improve design quality, cost, and cycle time. Research to examine uncertainty in the design process employs previous experience in experimental, model, and manufacturing uncertainty in an innovative approach for analyzing the entire design process. This research was initiated with a pilot project, a four-bar-slider mechanism. Three new theories for the research have arisen from this pilot project. First, design optimization techniques could be used to compare steps of the design process. Second, the design optimization techniques could also be

used to help determine the overall uncertainty of the final manufactured product. Third, manufacturing uncertainty can be included as an additional random uncertainty in the analysis of the final manufactured product. While more research needs to be completed to test, apply, and expand on these theories, the pilot project has been a positive step forward. This research, although in its beginning stages, could substantially improve the design process.

Table of Contents

LIST OF TABLES

LIST OF FIGURES

LIST OF VARIABLES AND SYMBOLS

VARIABLE		DEFINITION
d	=	Piston displacement
l_1	=	Inner length on the connecting rod
l_2	=	Outer length on the connecting rod
l_{cr}	=	Average length of the connecting rod
l_{cs}	=	Length of the crank shaft
d_{cr}	=	Diameter of the connecting rod collar for crankshaft
d_{cs}	=	Diameter of the crank shaft pin
l_p	=	Length of the piston
d_p	=	Diameter of the connecting rod collar for piston
θ	=	Crank angle
s_x	=	Slop
Ci	=	Constant "i" from regression analysis
S_x	=	Systematic uncertainty in variable x
R_x	=	Random uncertainty in variable x
U_x	=	Total uncertainty in variable x

t_x	=	Manufacturing tolerance for variable x
V	=	Voltage
F(x)	=	Function of variable(s) x

CHAPTER I

INTRODUCTION

Uncertainty analysis is a relatively new field of study. The field of uncertainty analysis was conceived as an experimental strategy. Experimental uncertainty analysis is well established though still evolving. More recently, researchers have begun to examine its usefulness as applied to manufacturing and modeling. This project, analyzing the design process of a four-bar slider mechanism, will begin a new stage of development, analyzing the entire design process using uncertainty techniques.

Objectives of the Study

Every design process has the following four basic steps in the design process: experiment, model, manufacture, and comparison. Methods of uncertainty analysis for each stage have been established, but the overall uncertainty for the entire design process is a new area of research. The three foremost objectives of this research were to compare the uncertainty of each step in the design process, find the overall uncertainty of the manufactured product, and determine the relative contribution of each step. The benefit of this research is that the design process can be improved by reducing the cost and cycle time without compromising the performance of the final manufactured product.

The first goal was to define a method to compare the results and uncertainty analyses of each step in the design process. Manufacturing uncertainty effects on both the model and experimental results and uncertainty were examined. Various assumptions must be made in every experiment and model. Therefore, the results and uncertainties of both the model and experiment were compared directly to determine the accuracy in each.

The second objective was to determine the overall uncertainty of the manufactured product. Using the four steps (model, experiment, manufacture, and comparisons), the expected results and uncertainty of the final manufactured product were determined.

The third objective was to determine how each step in the design process contributed to the uncertainty of the manufactured product. This understanding will lead to more efficient and reliable design processes.

Methodology of Design Process Uncertainty Analysis

For experimental uncertainty analysis,[1] the result, r, is determined by a **data reduction equation** and is a function of J measured variables

$$r = f(X_1, X_2, X_3, ..., X_J) \tag{1-1}$$

The uncertainty in the result, U_r, is a function of the uncertainties in the measured variables

$$U_r = f(U_{X_1}, U_{X_2}, U_{X_3}, ..., U_{X_J}) \tag{1-2}$$

The design process is analogous to the experiment. Consider the sample design process given in Table 1.1. For the design process, the final design, d, is a function of n-2 steps in the process. Next, the design has to be manufactured (step n-1) to produce a final product, p. The final product is, therefore, a function of n-1 steps in the process,

$$p = f(Step_1, Step_2, Step_3, ..., Step_{n-1}) \tag{1-3}$$

Using the analogy to experimental uncertainty analysis, the uncertainty of the final product, U_p, is a function of the uncertainties in the n-1 steps in the process

$$U_p = f(U_{Step_1}, U_{Step_2}, U_{Step_3}, ..., U_{Step_{n-1}}) \tag{1-4}$$

Step n is then an independent check to verify that the final product is as expected.

Table 1.1

SAMPLE DESIGN PROCESS

Step in Process	Step No.
1-D Meanline Code	1
2-D/3-D Steady Codes	2
Baseline Design	3
3-D Steady/Unsteady Codes	4
Design II	5
Cold-flow Testing/Code Validation	6
Design III	7
Prototype Manufacture	8
Hot-fire Testing	9
Final Design	10 or n-2
Product Manufacture	11 or n-1
Flight Test/Design Validation/Certification	12 or n

But, what is the **data reduction equation** for the process? Design process uncertainty analysis research addresses this question. Although each phase of a design process as well as each process itself is unique in the actual steps taken, the steps can generally be described by those given in Table 1.2. Research related to the steps in Table 1.2 as well as uncertainty in design will be addressed in the next section.

Table 1.2

GENERAL STEPS IN A DESIGN PROCESS

Step in Process	**Step No.**
Model	1
Experiment	2
Manufacture	3
Comparisons	4

Literature Survey

Research has been conducted on each stage of the design process, the unification of the design process, and robust design. Design process uncertainty analysis research aims to incorporate these ideas to reduce design cost and cycle time.

For step 1, modeling, limited work has been done on evaluating the uncertainty. The technical community is just beginning a push to quantify uncertainties associated with modeling. An American Institute of Aeronautics and Astronautics (AIAA) technical committee, for example, has been working to document a method of evaluating uncertainties associated with modeling. The Joint Army, Navy, NASA, and Air Force Interagency Propulsion Committee (JANNAF) has also established a Modeling and Simulation Subcommittee. Mississippi State University has been involved in the limited work that has been done on evaluating the uncertainties associated with modeling. For example, MSU researchers have previously applied experimental uncertainty analysis methodology to modeling and to improving design techniques.[2, 3] Also, Hudson has recently done work with NASA Marshall Space Flight Center (MSFC) to evaluate the uncertainty of results calculated using a one-dimensional model along with experimental test data input.[4]

For step 2, experimentation, the field of uncertainty analysis is well documented and constantly evolving as much work is being done in the area. Uncertainty analysis techniques have been defined by Coleman and Steele in accordance with engineering standards.[1]

For step 3, manufacturing, uncertainties have typically been viewed in terms of manufacturing tolerances. This view needs to be expanded to involve manufacturing in the complete design process. This will allow the effect of uncertainties in manufacturing on the uncertainty of the overall design to be evaluated.

For step 4, comparisons, very limited work has been done in this area. A program sponsored by the Office of Naval Research has begun to study this subject.[5] Hudson has also been involved with several programs at NASA/MSFC incorporating experimentation with modeling with the goal of improving the use of Computational Fluid Dynamics (CFD) as a design tool (references 6-12).

In addition to design steps uncertainty, research has been done in robust design. Genichi Taguchi began research in robust design by modeling both the controllable and uncontrollable design parameters with a signal to noise ratio.[13, 14, 15] The development of robust design attracted a lot of attention from researchers in several disciplines.[16, 17] This research is similar to design process uncertainty analysis in that it incorporates real world effects in the model. The goal of design process uncertainty is to determine the performance of the final manufactured product using information from all stages in the design process and to simplify each stage of the design process without significant losses in the robustness of the design.

Furthermore, research is being conducted to unify the design process. This research uses model data to define the optimum experiment.[18,19] In addition research has been conducted on experimental cost optimization at Rice University.[20] This research is also similar to design process uncertainty in that it attempts to design the best experiment from model data.

This research in similar areas contributes to research on uncertainty in the design process; however, none of the research addresses the total uncertainty in the final manufactured product as a function of the uncertainty in each step. Also, research on design process uncertainty is different because it is the first research to determine how the uncertainty in each stage in the design process contributes to the uncertainty in the final manufactured product.

CHAPTER II

EXPERIMENTAL UNCERTAINTY OVERVIEW

This chapter includes an overview of experimental uncertainty analysis methods that were employed for this pilot project. More information on experimental uncertainty analysis techniques can be found in Coleman and Steele.[1]

Experimental Uncertainty Analysis

Accuracy is defined as the difference between an experimentally-determined value of a quantity and its true value. Uncertainty, U, is an estimate of accuracy. The estimate must have a level of confidence associated with it. For example, a 95% level of confidence means that the true value of the quantity is expected to fall within the ±U interval about the measured variable 95 times out of 100. According to experimental uncertainty analysis techniques, there are two types of uncertainty – random and systematic. Systematic uncertainty is a fixed component of error that is constant throughout an experiment. Random uncertainty, on the other hand, is a measure of repeatability.

The experimental result is usually a function of several measured quantities. This function is called a data reduction equation (DRE). The general representation of a data reduction equation is repeated here for convenience as Equation 2-1.

$$r = f(X_1, X_2, X_3, \ldots, X_J) \tag{2-1}$$

The experimental result, r, is determined from J independent measured variables X_i. Each of these measured variables contains systematic uncertainties and random uncertainties. The uncertainty in the result is a function of the uncertainty in each of the measured variables.

The systematic uncertainty, B_i, for each variable, X_i, is the root-sum-square combination of its elemental systematic uncertainties as shown in Equation 2-2

$$B_i = \left[\sum_{j=1}^{M} \left(B_i \right)_j^2 \right]^{1/2} \tag{2-2}$$

where M is the number of elemental systematic uncertainties. In addition, systematic uncertainties can be correlated. Correlation occurs when some of the measured variables share common elemental sources. To handle the correlation, covariance terms are defined as

$$B_{ik} = \sum_{\alpha=1}^{L} \left(B_i \right)_\alpha \left(B_k \right)_\alpha \tag{2-3}$$

where L is the number of correlated elemental sources of systematic uncertainty.

Random uncertainty is a variable uncertainty in the precision, or repeatability, of a measurement. The 95% confidence large sample (t=2) random uncertainty for a variable is estimated as

$$P_i = 2S_i \tag{2-4}$$

where, S_i, is the sample standard deviation which is defined as

$$S_i = \left[\frac{1}{N-1} \sum_{k=1}^{N} [(X_i)_k - \overline{X}_i]^2 \right]^{1/2} \tag{2-5}$$

N is the number of measurements, and the mean value for X_i is defined as

$$\overline{X}_i = \frac{1}{N} \sum_{k=1}^{N} (X_i)_k \tag{2-6}$$

Whenever possible, measurements are repeated to reduce the random uncertainty, and the mean is used as the measured quantity. The large sample random uncertainty estimate then becomes

$$P_{\overline{Xi}} = \frac{2S_{\overline{Xi}}}{\sqrt{N}} \tag{2-7}$$

As stated previously, the uncertainty in the result is a function of the systematic and random uncertainties in each measured variable. The equations for the systematic and random uncertainties in the result are

$$B_r^2 = \sum_{i=1}^{J} \theta_i^2 B_i^2 + 2 \sum_{i=1}^{J-1} \sum_{k=i+1}^{J} \theta_i \theta_k B_{ik} \tag{2-8}$$

$$P_r^2 = \sum_{i=1}^{J} \theta_i^2 P_i^2 + 2 \sum_{i=1}^{J-1} \sum_{k=i+1}^{J} \theta_i \theta_k P_{ik} \tag{2-9}$$

where θ is the partial derivative, as shown in Equation 2-10. Note that the correlation terms in Equation 2-9 are generally considered to be zero since the uncertainties are random.

$$\theta_i = \frac{\partial r}{\partial X_i} \tag{2-10}$$

The root-sum-square method then gives the 95% confidence expression for U_r

$$U_r^2 = B_r^2 + P_r^2 \tag{2-11}$$

Multiple Tests

The random uncertainty defined in Equations 2-4 or 2-7 and used in Equation 2-9 are applicable to a single test—that is, at a given test condition, the result is determined once using the data reduction equation, and the measured variables are considered single measurements. If a test is repeated a number of times so that multiple results at the same test condition are available, then the best estimate of the result r would be $\bar{r}$.

$$\bar{r} = \frac{1}{M} \sum_{k=1}^{M} r_k \tag{2-12}$$

M is the number of separate test results. The random uncertainty for this result would be $P_{\bar{r}}$ calculated as

$$P_{\bar{r}} = \frac{K\,S_r}{\sqrt{M}} \tag{2-13}$$

K is the coverage factor and is taken as 2 for large sample sizes. As before, S_r is the standard deviation of the sample of M results and is defined as

$$S_r = \left[\frac{1}{N-1} \sum_{k=1}^{N} [r_k - \bar{r}\,]^2 \right]^{1/2} \tag{2-14}$$

Obviously, this cannot be computed until multiple results are obtained. Also note that the standard deviation computed is only applicable for those random error sources that were "active" during the repeat measurements. For example, if the test conditions were not changed and then reestablished between the multiple results, the variability due to resetting to a given test condition would not be accounted for in the precision estimate.

Regression Uncertainty

A regression equation is an equation determined from several data points. The least squares approximation is a common method used to perform a polynomial regression. The least squares approximation determines the constants that minimize the sum of the square of the difference, η, between the Y_i data points and the result, Y_0, of the regression equation for the corresponding X_i data points. However, the data reduction equations must be expressed in terms of all the measured variables. Therefore, the data reduction equation for regression is defined as a function of the new measured variable, X_{new}, and the regression data points, X_i and Y_i. For regression uncertainty analysis, there are just three measured variables that contribute to the uncertainty in the result. The Y_i and X_i values come from the data used to determine the regression, and the X_{new} values come from the experiment. Therefore, the equations for the systematic and random uncertainties in the result of the regression equation are Equations 2-15 and 2-16, respectively.

$$B_Y = \sqrt{\begin{aligned}&\sum_{i=1}^{J}\left[\left(\frac{\partial Y}{\partial X_i}\right)^2 {B_{X_i}}^2\right] + 2\sum_{i=1}^{J-1}\sum_{k=i+1}^{J}\left[\left(\frac{\partial Y}{\partial X_i}\right)\left(\frac{\partial Y}{\partial X_k}\right)B_{X_i}B_{X_k}\right]\ldots \\ &+\sum_{i=1}^{J}\left[\left(\frac{\partial Y}{\partial Y_i}\right)^2 {B_{Y_i}}^2\right] + 2\sum_{i=1}^{J-1}\sum_{k=i+1}^{J}\left[\left(\frac{\partial Y}{\partial Y_i}\right)\left(\frac{\partial Y}{\partial Y_k}\right)B_{Y_i}B_{Y_k}\right]\ldots \\ &+2\sum_{i=1}^{J}\sum_{k=1}^{J}\left[\left(\frac{\partial Y}{\partial X_i}\right)\left(\frac{\partial Y}{\partial X_k}\right)B_{X_i}B_{X_k}\right]\ldots \\ &+\left(\frac{\partial Y}{\partial X_{new}}\right)^2 {B_{X_{new}}}^2 + \sum_{i=1}^{J}\left[\left(\frac{\partial Y}{\partial X_{new}}\right)\left(\frac{\partial Y}{\partial X_i}\right)B_{X_{new}}B_{X_i}\right]\ldots\end{aligned}} \tag{2-15}$$

$$P_Y = \sqrt{\sum_{i=1}^{J}\left[\left(\frac{\partial Y}{\partial X_i}\right)^2 {P_{X_i}}^2\right] + \sum_{i=1}^{J}\left[\left(\frac{\partial Y}{\partial Y_i}\right)^2 {P_{Y_i}}^2\right] + \left(\frac{\partial Y}{\partial X_{new}}\right)^2 {P_{X_{new}}}^2} \tag{2-16}$$

The P_{Xi}, B_{Xi}, P_{Yi}, and B_{Yi} terms are the random and systematic uncertainties in the X_i and Y_i data points, respectively. The P_{Xnew} and B_{Xnew} terms are the random and systematic uncertainties in the new experimental X value.

For this brief overview the symbols were selected to match those in Coleman and Steele, the referenced text. However, in the following chapters, “R” will be used to indicate a random uncertainty instead of “P” and “S” will be used to define a systematic uncertainty instead of “B.”

CHAPTER III

PILOT PROJECT

To begin design process uncertainty research, a four-bar-slider mechanism was chosen for a pilot project. The pilot project was selected to satisfy several criteria. First, it needed to be accomplished in a relatively short amount of time– one year. Next, the project needed to include the four general steps in a design process: model, experiment, manufacture, and comparisons. Finally, each of the four general steps in the design process needed to be relatively simple so that the focus of the study could be on the comparisons and determining the uncertainty of the final manufactured product. A four-bar-slider mechanism was selected for the pilot project. A four bar slider mechanism is a linkage used to convert rotational energy to translational energy or vice versa. A common example is the crankshaft, connecting rod, and piston from a reciprocating, internal combustion engine. An in-house, single-cylinder engine was available for the baseline design (Figure 3.1).

Figure 3.1: Single Cylinder Engine

The pilot project consisted of completing an entire design process and determining the uncertainty associated with each step in the design process, as well as evaluating the overall design process. Therefore, the design process of the four-bar-slider mechanism was defined with the objectives of design process uncertainty research goals in mind. The objectives of this pilot project are listed in Table 3.1. First, each simple, individual stage of the design process was defined. For the model, the displacement of the piston was the result of a kinematic equation. To make comparisons, the experiment measured piston displacement. For manufacture, the connecting rod was selected for redesign and manufacture. Next, the objectives of determining the relationships between the steps in the design process and determining the relative contribution of each step to the overall uncertainty of the manufactured product were addressed. To be able to compare the model and the experiment and to study the manufacturing effects, the input parameters of the model and the experiment were varied. For the redesigned connecting rod, the length was changed. The effect of this change was evaluated in the model-experiment comparisons. Also, to understand the effects of manufacturing on both the experiment and the model, the collar diameter of the connecting rod was altered by a small margin. This exaggerated the effects of manufacturing tolerances. The results of the pilot project calculations for one set of data are included in Appendix A, MathCad Worksheets.

Table 3.1

PILOT PROJECT OBJECTIVES

(1) Develop computational model, design mechanism, develop necessary uncertainty analysis techniques, and complete uncertainty analysis of model.
(2) Plan and execute experiment, and complete uncertainty analysis of experimental data.
(3) Develop necessary techniques and compare model and experiment.
(4) Manufacture the product and complete uncertainty analysis for manufacturing.
(5) Determine the expected results and uncertainty of the final manufactured product
(6) Define the Data Reduction Equation for the process.
(7) Determine the relative contribution of each step to the overall uncertainty of the final manufactured product.

CHAPTER IV

MODEL

The first stage in the pilot project design process was the model. This stage included several items. First, a relationship for the model was developed. Then, the expected results of the model were evaluated. Next, the assumptions were defined. Finally, the results were calculated. An uncertainty analysis of the model was then conducted. The following paragraphs describe the model and uncertainty analysis.

Model Definition

Using MathCad software, the four-bar-slider mechanism was modeled kinematically as a function of the crank angle, θ, (Equation 4-1).

$$d(\theta) = l_{cs}\cos(\theta) + \sqrt{\frac{l_1 + l_2}{2} - l_{cs}{}^2 \sin^2(\theta)} + l_p + s_x \qquad (4\text{-}1)$$

This model was based on the geometry of the four-bar-slider mechanism. More information on this linkage and other linkages can be found in Shigley and Vicker.[21] Figure 4.1 identifies the variables, and as shown in the figure, the mechanism is made from three manufactured pieces: the crankshaft, the connecting rod, and the piston. The total displacement is considered the fourth bar, hence the name four-bar-slider mechanism. The lengths of each of these pieces are labeled as l_{cs}, l_{cr}, and $l_{p,}$ respectively. In accordance with uncertainty analysis protocol, the data reduction equation (4-1) was written in terms of the measured variables. The center-to-center distance of the connecting rod, l_{cr}, was not measured directly. The outer length l_2 and the inner length l_1 were measured to find the center-to-center distance. The average of these measurements was used in the data reduction equation. The diameter of the crankshaft, d_{cs}, and the diameter of the connecting rod, d_{cr}, are also labeled in the figure. This connection is called a pin joint because it allows movement in the plane of the paper but does not allow movement in the z-plane, ideally. These diameter measurements describe the fit in the pin joint. The diameter of the crankshaft is the diameter of the "pin." The diameter of the connecting rod is the diameter of the collar for the crankshaft "pin." For a perfect fit, these two diameters are equivalent. If there is not a perfect fit, then there is slop. The "slop," s_x, was included in the data reduction equation because it will contribute to the uncertainty. However, it was assumed that the slop was negligible for the model.

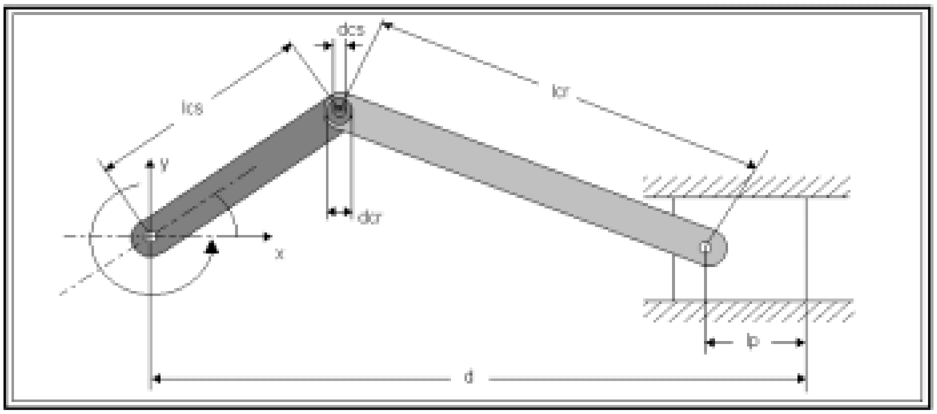

Figure 4.1: Schematic Drawing of the Four-bar-slider Mechanism

To establish the baseline design, the lengths and diameters of the existing parts were measured. After the primary dimensions of the original connecting rod were measured ten times, the mean and standard deviation of each measurement were calculated. The dimensions of the other elements of the linkage, the crankshaft and the piston, were recorded also. The baseline design variables are listed in Table 4.1.

Table 4.1

BASELINE PARAMETERS

l_{cr} (in)	l_{cs} (in)	l_1 (in)	l_2 (in)	d_{cr} (in)	d_{cs} (in)	l_p (in)
3.250	0.777	2.871	3.738	0.778	0.747	1.101

Two of the primary goals of uncertainty analysis of the design process were to evaluate the effects of manufacturing uncertainty and to compare the model and experiment. To help meet these goals, the connecting rod was selected for manufacture. For the manufactured connecting rods, the length was changed since this change would affect the displacement determined by the model and measured in the experiment. It was expected that the changes in length would affect the model and experimental results and uncertainty differently. The model results were used to estimate differences in connecting rod length that would cause measurable changes in displacement.

The collar diameter of the connecting rod was also varied since this dimension affects the slop in the fit and hence the displacement measured during the experiment. The model assumed a perfect fit; therefore, the slop did not affect the model results. One half of the difference in the diameters was added to the maximum model displacement and subtracted from the minimum model displacement to predict the experimental effects. The collar diameter changes exaggerated the effects of manufacturing tolerances and were expected to aid in model-experiment comparisons. Tables 4.2 and 4.3 show the maximum and minimum displacement, respectively, for three different lengths and diameters.

Table 4.2

MAXIMUM DISPLACEMENT MEASUREABLE EFFECTS

Maximum Displacement	l_1 (3.25 in)	l_2 (3.15 in)	l_3 (3.35 in)
d_1 (.75 in)	5.154	5.054	5.254
d_2 (.80 in)	5.179	5.079	5.279
d_3 (.85 in)	5.204	5.104	5.304

Table 4.3

MINIMUM DISPLACEMENT MEASUREABLE EFFECTS

Minimum Displacement	l_1 (3.25 in)	l_2 (3.15 in)	l_3 (3.35 in)
d_1 (.75 in)	3.545	3.445	3.745
d_2 (.80 in)	3.520	3.420	3.720
d_3 (.85 in)	3.495	3.395	3.595

Based on these displacement values, nine connecting rods were redesigned. The new lengths and diameters of the nine redesigned connecting rods are listed in Table 4.4.

Table 4.4

CONNECTING ROD LENGTHS AND DIAMETERS

Length 1 (inches)	3.25	Diameter 1 (inches)	.75
Length 2 (inches)	3.15	Diameter 2 (inches)	.80
Length 3 (inches)	3.35	Diameter 3 (inches)	.85

After the nine new connecting rods were manufactured, the mean and standard deviation of the lengths and diameters of each were calculated using the same techniques as with the previous measurements of the existing parts. The model was analyzed for each of the connecting rods. The detailed model analysis for the first connecting rod is included in the Appendix, MathCad Worksheets. This analysis and the experiments were run in the order shown in Table 4.5. The second connecting rod was the original connecting rod.

Table 4.5

EXPERIMENT AND MODEL NUMBERS

1	Length 1	Diameter 1
2	Length 1	Diameter 2
3	Length 1	Diameter 3
4	Length 2	Diameter 1
5	Length 3	Diameter 1
6	Length 2	Diameter 2
7	Length 3	Diameter 2
8	Length 2	Diameter 3
9	Length 3	Diameter 3

Figure 4.2 displays the model results of the nine connecting rods. The model results of the connecting rods with the same length but various diameters were graphed together. The model results from the connecting rods with the same diameter but different lengths were equivalent because the model results were not a function of the collar diameter. From the figure it can be seen that the increase in length increased the total displacement.

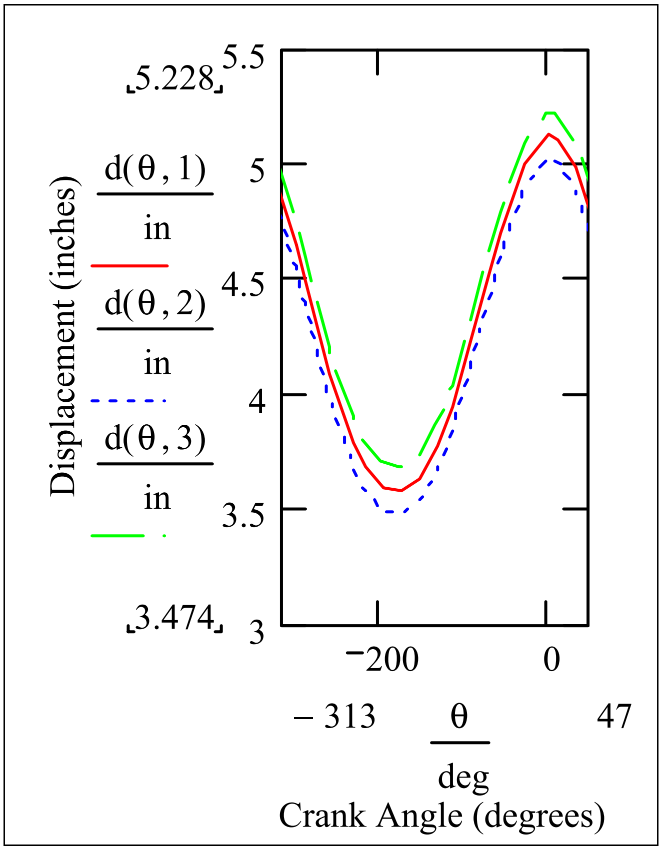

Figure 4.2: Model Results of Lengths 1, 2, and 3

Model Uncertainty

For the uncertainty in the overall design process it was important to evaluate all of the major assumptions in each step in the design process. The first major model assumption was zero slop in the crankshaft connecting rod joint. Second, it was assumed that all other connections, excluding the connecting rod-crankshaft joint, were a "perfect fit" (the collar diameter exactly matched the pin diameter of the connection). For example, the diameter of the wrist pin that links the piston to the connecting rod is equal to the diameter of the journals in the piston and the connecting rod. Next, it was assumed that the engine speed remained constant and there was no uncertainty in the crank angle, θ. Finally, it was assumed that there was zero displacement in the z-direction.

Experimental uncertainty analysis techniques from Coleman and Steele[1] were applied to analyze the uncertainty of the model, considering the systematic and random components of uncertainty for each quantity. The total uncertainty was the root-sum-square combination of the random and systematic uncertainties.

There were two sources of uncertainty in the traditional model analysis: random uncertainty in the length of the connecting rod and fossilized systematic uncertainty from the baseline measurements. To determine these uncertainties, first, the standard deviation (Equation 2-5) in each of the measurement sets was calculated. The standard deviations were used with a 95% confidence interval for a Gaussian distribution to calculate the random uncertainty associated with each measurement as shown in Equation 2-7. Because the number of measurements, N, was greater than or equal to ten for every dimension, the large sample assumption was used ($t = 2$). Table 4.6 displays the calculated random uncertainties for l_1 and l_2 of each connecting rod. For the crankshaft and the piston dimensions, the random uncertainties in the length measurements were classified differently from the connecting rod length uncertainties because these parts were already manufactured and were not changed for the project. Therefore, the random uncertainties for these parts were treated as fixed or “fossilized” systematic uncertainties for this project. The fossilized systematic uncertainty was .0006 in. for the crankshaft length and .0007 in. for the length of the piston.

Table 4.6

RANDOM UNCERTAINTIES IN CONNECTING ROD LENGTHS

SOURCES	R_{l1} (inches)	R_{l2} (inches)
Model 1	.0014	.0023
Model 2	.0012	.0012
Model 3	.0009	.0018
Model 4	.0012	.0014
Model 5	.0025	.0030
Model 7	.0014	.0012
Model 7	.0011	.0015
Model 8	.0014	.0010
Model 9	.0013	.0012

To prepare for the comparisons, an additional uncertainty was included for the slop in the connecting rod-crankshaft joint. For the uncertainty analysis, the slop in this joint was included in the model equation. However, it was considered negligible for the model results. This slop will allow the collar to "float" on the pin. The exact location of the pin in the collar cannot be determined at every instant. Therefore, there is an uncertainty in the pin location that is constrained geometrically by the collar according to Equation 4-3.

$$R_{s_x} = \frac{d_{cr} - d_{cs}}{2} \tag{4-3}$$

This uncertainty is random, not systematic, because the pin location could be different at any instant. However, there is also a systematic uncertainty. The size of both diameters constrains the movement of the pin. Therefore, if the manufactured pin or collar diameter dimensions are not exactly as specified, then the uncertainty in slop will change also. This systematic uncertainty is defined in Equation 4-4.

$$S_{sx} = \sqrt{\frac{1}{4}U_{d\,cr}{}^{2} + \frac{1}{4}U_{d\,cs}{}^{2}} \tag{4-4}$$

Each element of uncertainty from the different sources was calculated and then combined using the uncertainty analysis techniques discussed in Chapter 2 to determine the total model uncertainty. Equation 4-5 gives the random uncertainty in the model, Equation 4-6 gives the systematic uncertainty in the model, and Equation 4-7 gives the total model uncertainty. For the model, there were no correlated uncertainties. The model results and uncertainties are displayed in Figure 4.2. The model results are labeled according to Table 4.5.

$$R_d(\theta) = \sqrt{\begin{array}{l} \left(\frac{\partial d(\theta)}{\partial l_{cs}}\right)^2 R_{l\,cs}{}^2 + \left(\frac{\partial d(\theta)}{\partial d_{cs}}\right)^2 R_{d\,cs}{}^2 + \left(\frac{\partial d(\theta)}{\partial l_1}\right)^2 R_{l1} + \left(\frac{\partial d(\theta)}{\partial l_2}\right)^2 R_{l2} \ldots \\ {}^2 + \left(\frac{\partial d(\theta)}{\partial d_{cr}}\right)^2 R_{d\,cr}{}^2 + \left(\frac{\partial d(\theta)}{\partial l_p}\right)^2 R_{l\,p}{}^2 + \left(\frac{\partial d(\theta)}{\partial s_x}\right)^2 R_{s\,x}{}^2 \end{array}} \tag{4-5}$$

$$S_d(\theta) = \sqrt{\begin{array}{l} \left(\frac{\partial d(\theta)}{\partial l_{cs}}\right)^2 S_{l\,cs}{}^2 + \left(\frac{\partial d(\theta)}{\partial d_{cs}}\right)^2 S_{d\,cs}{}^2 + \left(\frac{\partial d(\theta)}{\partial l_1}\right)^2 S_{l1}{}^2 + \left(\frac{\partial d(\theta)}{\partial l_2}\right)^2 S_{l2}{}^2 \ldots \\ + \left(\frac{\partial d(\theta)}{\partial d_{cr}}\right)^2 S_{d\,cr}{}^2 + \left(\frac{\partial d(\theta)}{\partial l_p}\right)^2 S_{l\,p}{}^2 + \left(\frac{\partial d(\theta)}{\partial s_x}\right)^2 S_{s\,x}{}^2 \end{array}} \tag{4-6}$$

$$U_d(\theta) = \sqrt{S_d(\theta)^2 + R_d(\theta)^2} \tag{4-7}$$

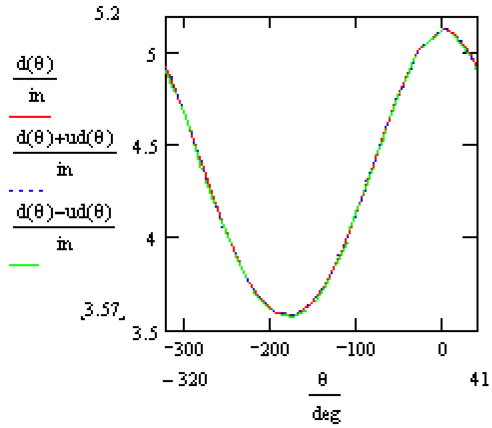

(a) Model 1

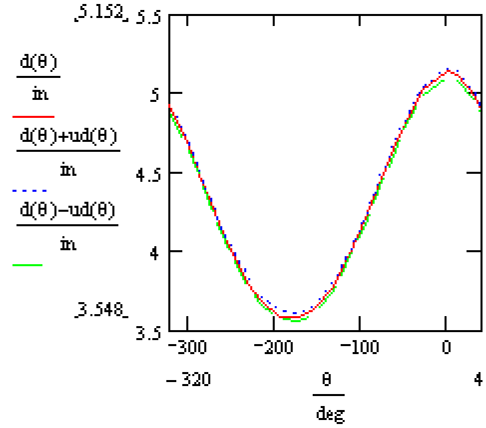

(b) Model 2

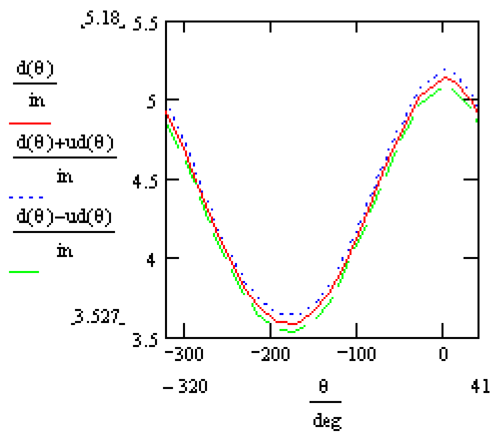

(c) Model 3

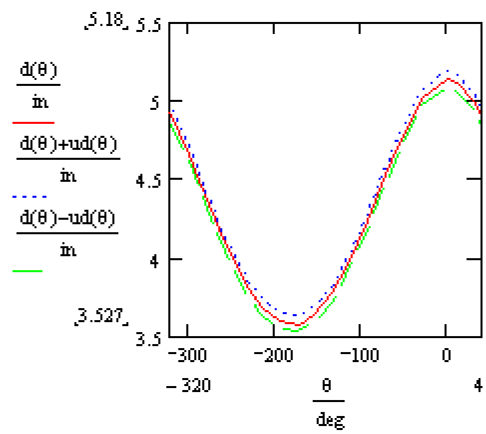

(d) Model 4

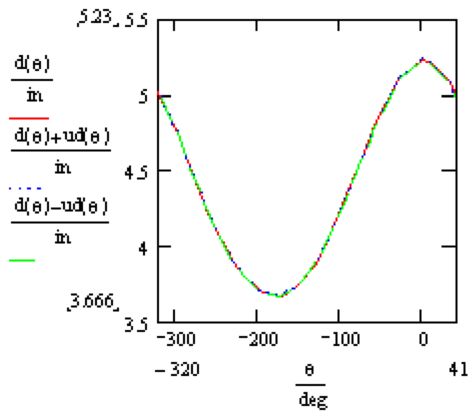

(e) Model 5

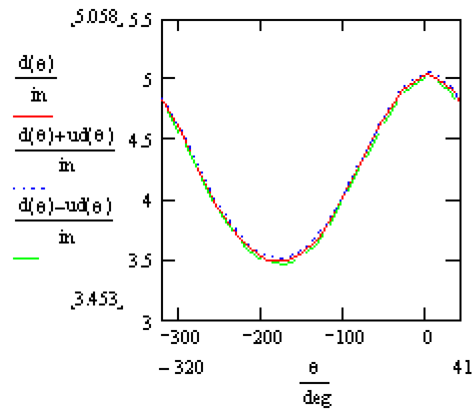

(f) Model 6

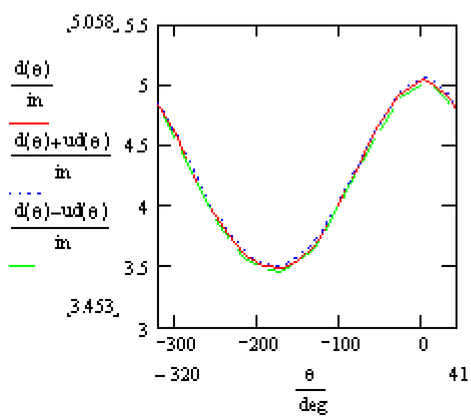

(g) Model 7

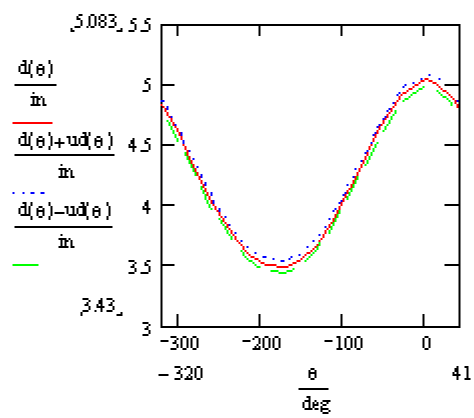

(h) Model 8

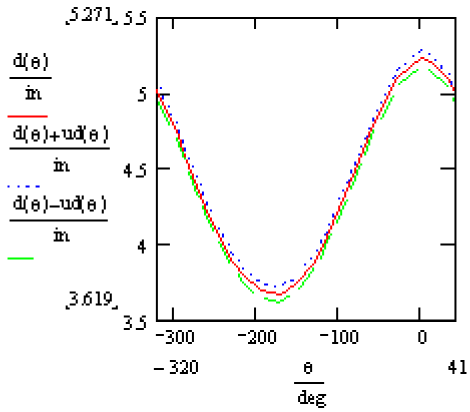

(i) Model 9

Figure 4.3 (a-i): Model Results and Uncertainties

In Figure 4.3, the solid trace represents the model results, and the dotted lines represent the model uncertainty. The actual model results could fall anywhere within the area between these two dotted lines. The increase in length increases the model displacement. The diameter, as expected, does not affect the model results since the model assumed a perfect fit with no slop. However, the diameter does affect the model uncertainty. Both the increases in length and diameter increase the model uncertainty.

CHAPTER V

MANUFACTURE

Manufacturing was the second stage in the pilot project design process. Three different connecting rod lengths were defined with three different diameters per connecting rod length resulting in nine different connecting rods for testing.

Manufacture Description

The connecting rods were manufactured at Patterson Engineering Laboratories using a vertical mill. They were machined out of 1 x 2 in. aluminum bar stock. The technical drawing of the original connecting rod is shown in Figure 5.1. Here, the length of the connecting rod was specified by the center-to-center distance, l_{cr}, in accordance with machine capabilities. The tolerance was also specified for the center-to-center distance. However, in order to relate the manufacture to the model, the uncertainty in the connecting rod length had to be specified in terms of the inner and outer lengths, l_1 and l_2, respectively. Therefore the data reduction equations were determined from the geometry of the connecting rod and are included as Equations 5-1 and 5-2.

$$l_1 = l_{cr} - \frac{d_{cr} + d_p}{2} \tag{5-1}$$

$$l_2 = l_{cr} + \frac{d_{cr} + d_p}{2} \tag{5-2}$$

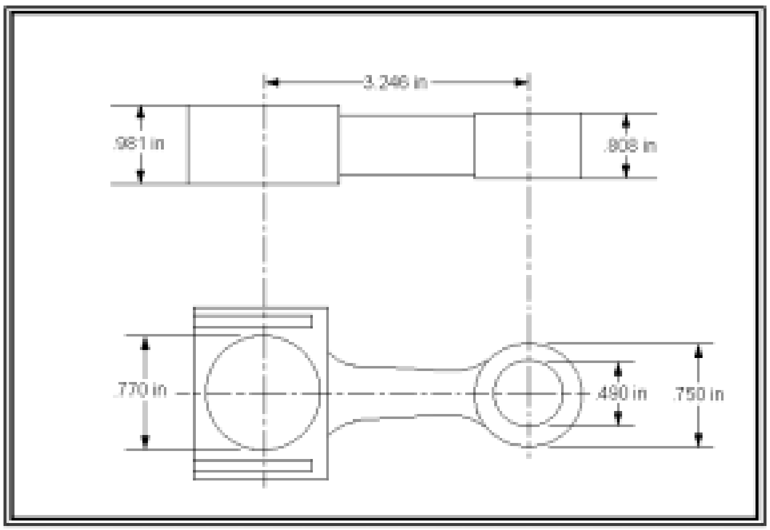

Figure 5.1: Technical Drawing of the Connecting Rod

Instead of manufacturing nine connecting rods, the different length connecting rods were first manufactured with the smallest diameter. After the first run of experiments, the diameters were bored out. Then the experiments were run again for two more sets of diameters. Note that this is only the first stage of manufacturing. In most applications, there is an initial manufacture stage for test purposes. However, after the experimentation is complete, the piece is put into mass production. This stage of manufacture will not be completed, but it will be accounted for in the uncertainty analysis of the final manufactured product.

Manufacturing Uncertainty

The manufacturing tolerances were the only manufacturing sources of uncertainty considered for this simple design process. The manufacturing tolerances were estimated by machine capabilities and are presented in Table 5.1. Again, experimental uncertainty techniques were applied to find the systematic uncertainty in l_1 and l_2 from the uncertainties in l_{cr}, d_{cr} and d_p as shown in equations 5-3 and 5-4. For the dimensions of the other links, the systematic uncertainty is equal to the tolerance.

$$S_{l1} = \sqrt{t_{l\,cr}^{\;2} + \frac{1}{4} t_{d\,cr}^{\;2} + \frac{1}{4} t_{d_p}^{\;2}} \tag{5-3}$$

$$S_{l2} = \sqrt{t_{l\,cr}^{\;2} + \frac{1}{4} t_{d\,cr}^{\;2} + \frac{1}{4} t_{d_p}^{\;2}} \tag{5-4}$$

Table 5.1

MANUFACTURING TOLERANCES

SOURCES	t_{lcs} (inches)	t_{lcr} (inches)	t_{dcr} (inches)	t_{dp} (inches)	t_{lp} (inches)
Manufacturing Tolerances	.010	.005	.005	.005	.001

These uncertainties in the manufactured pieces replaced the measurement capability elemental source of uncertainty for the final manufactured product because not all parts will be measured, but they will be machined according to these tolerances. As in the initial model, the elemental sources are combined using the root-sum-square method. Then the elemental uncertainty is again used in Equations 4-5 through 4-7 to demonstrate how manufacturing uncertainties affect the model. The detailed analysis of the manufacturing results and uncertainty is included in the Appendix, MathCad Worksheets. The manufacturing uncertainty effects will be discussed in the comparisons, Chapter 7. Note that the manufacturing uncertainty was already accounted for within the experimental uncertainty bands because the experiments were conducted on manufactured pieces.

CHAPTER VI

EXPERIMENT

The third stage in the pilot project design process was the experiment. In the following paragraphs the experimental set-up, equipment list, preparations, procedure, and results are covered.

Experiment Definition

The purpose of the experiment was to measure the displacement of the piston head. The displacement was found with respect to time. To make comparisons, the crank angle was also determined from the experiment using a proximity sensor. This data was recorded every .005 seconds using a data acquisition system. Each repetition lasted five seconds, and, therefore, contained several cycles. The first cycle of data was used for the analysis. The following cycles were used as trial runs for the comparisons. The experiment was repeated three times for all nine of the connecting rods.

Experiment Construction

First, the experimental apparatus was constructed as shown in Figure 6.1. Two aluminum blocks were used to mount the engine. To stabilize the engine, it was anchored to a wood board. A hole was drilled through the center of the board to add oil for each experimental run. The linear transducer was fixed to the top of the cylinder wall with brackets, and the follower was screwed into the head of the piston. The proximity sensor was also mounted to the top of the cylinder across from the linear transducer. The wires from both of these instruments were connected to a 12-volt power source and the break-out box of the data acquisition according to the manufacturers' diagrams. The break-out box was connected to the computer, and the data acquisition card was installed. A hose connected the air wrench to the air compressor and a pressure regulator was added to the line to control the engine speed.

Figure 6.1: Experimental Apparatus

Data Acquisition Program

A Labview program was written to acquire the experimental data. The experiment was a two-channel experiment; one input channel for the linear transducer voltage and a second for the proximity sensor voltage. Labview was programmed to write the experimental output to a text file. The output file included elapsed time (s), transducer voltage (V), proximity sensor voltage (V), and engine speed (rpm).

The Labview program was written such that the linear transducer was the input for channel one. The linear transducer uses variable resistance to output voltage measurements that are directly proportional to the displacement. The transducer was calibrated to determine this exact relationship. The data acquisition was used to simply record the transducer voltage.

The proximity sensor voltage was the input for channel two. The proximity sensor is a switch that turns "on" once per cycle at some angle. This angle was determined in the calibration. In addition, the proximity sensor data was used to determine the engine speed. Because the transducer triggers at the same angle for every cycle, 360 degrees (one cycle) was divided by the difference in switch-times.

A "run" and "stop" button were included on the control panel. Fields for the data rate and measurement duration were also included on the control panel. The instruments were calibrated using the following procedures before each experimental run.

Linear Transducer Calibration

The linear transducer was calibrated before each test run so that the displacement could be determined from the voltage measurement during the experiment. For the calibration, the piston was displaced .25 in. down from the top of the cylinder wall using a micrometer. The voltage output was measured with the linear transducer hooked to the data acquisition system to avoid installation effects. In the Labview program, the data rate was set significantly lower for the calibration: 20 measurements in five seconds. Next, the mean of these measurements was calculated. This process was repeated for .5, .75, 1, and 1.25 in. displacements. This process was repeated ten times at each of the five set displacements to minimize the random uncertainty in the voltage measurements. These displacements were set from both the counter-clockwise and clockwise directions to avoid hysteresis. All of the voltage measurements for a distance set point were averaged. Displacement versus average voltage was then plotted. A linear regression was performed to solve for the coefficients, C_1 and C_2, of the regression equation.

$$d(V) = C_1 V + C_2 \tag{6.1}$$

This regression equation was then used to determine displacement from the voltage measurements during the experiment. Figure 6.2 is the graph of the calibration data and the linear regression for the first experiment. The x's represent the five mean data points from the calibration. The solid line is the curve fit.

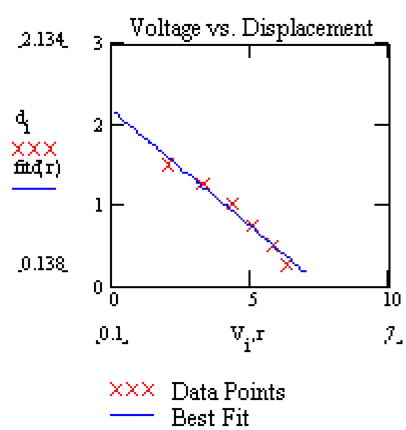

Figure 6.2: Curve Fit for the Linear Transducer Calibration

Proximity Sensor Calibration

As stated previously, the experiment measured displacement versus time, but the model calculated displacement versus crank angle, θ. Therefore, a conversion from time to crank angle was needed for the experiment to be able to compare the results with the model. The proximity sensor calibration was used to obtain the reference angle, θ_0, the crank angle where the model and experiment matched. The value of θ_0 depended on the top dead center location, θ_{TDC}, and the angle where the proximity sensor "turned on," θ_{on}.

With a degree wheel fastened to the crankshaft, Top Dead Center was found by slowly turning the crankshaft counter-clockwise. The angle, θ_1, where the piston stopped was recorded. The crankshaft was rotated further until the piston started to move again, then this angle, $\delta\theta_1$, was recorded also. Next the crankshaft was turned slowly in the clockwise direction. The angle, θ_2, where the piston stopped, was recorded. And again, the crankshaft was turned until the piston began to move. This angle, $\delta\theta_2$, was also recorded. This process was repeated 4 more times. Then, top dead center was found using Equation 6-2.

$$\theta_{TDC} = \frac{\left(\theta_1 + \frac{\delta\theta_1}{2}\right) + \left(\theta_2 + \frac{\delta\theta_2}{2}\right)}{2} \tag{6-2}$$

To find the angle when the proximity sensor turned "on," θ_{on}, the crankshaft was slowly turned counter clockwise, the same direction the experiment was run, until the data acquisition system showed the beginning of a square wave for the proximity sensor voltage, and that angle was recorded. This process was repeated ten times, and the mean and standard deviation were calculated.

The angle measurements in the experiment depended on the arbitrary initial position of the degree wheel; however, in the model, Top Dead Center is zero degrees. Therefore, the angle of interest or reference angle, θ_0, is the difference between the recorded value for θ_{on} and θ_{TDC} as shown in Equation 6-3.

$$\theta_0 = \theta_{on} - \theta_{TDC} \tag{6-3}$$

Experimental Procedure

The following experimental procedure was followed for all nine connecting rods. After the calibrations were complete, with the power source already turned on and the Labview program in use, the data rate was established at 200 measurements per second. Oil was squirted into the engine through the drilled access hole with an oilcan. A nut was screwed onto the crankshaft, and a socket was applied to the air wrench. The pressure regulator was adjusted, the air wrench was connected to the crankshaft, and the air wrench was turned on. The parameters were allowed to settle. The Labview program was “run” to record the data. The experiment was completed for all nine connecting rods, and then the results were calculated.

It is important to note that during the running of the experiment it was obvious that the air impact wrench was not able to maintain a constant speed. The engine speed varied noticeably at different points in rotation, especially at TDC. The model assumed a constant engine speed, and the calculations of the experimental crank angle depend upon a constant engine speed. These points are important in the Comparisons, Chapter 7.

Experiment Analysis

As previously stated, a data acquisition system was used to record the experimental data. The data acquisition system consisted of a break out box with channels to connect the instrumentation to a computer, a DAQ card to interpret the incoming data, and a Labview program to set experiment control parameters and to record data.

The displacement of the head of the piston was measured using a linear transducer fixed to the top of the cylinder. In MathCad, the voltage from the transducer was converted to a displacement using the least squares approximation for a linear function. Equation 6-1 is the linear regression equation.

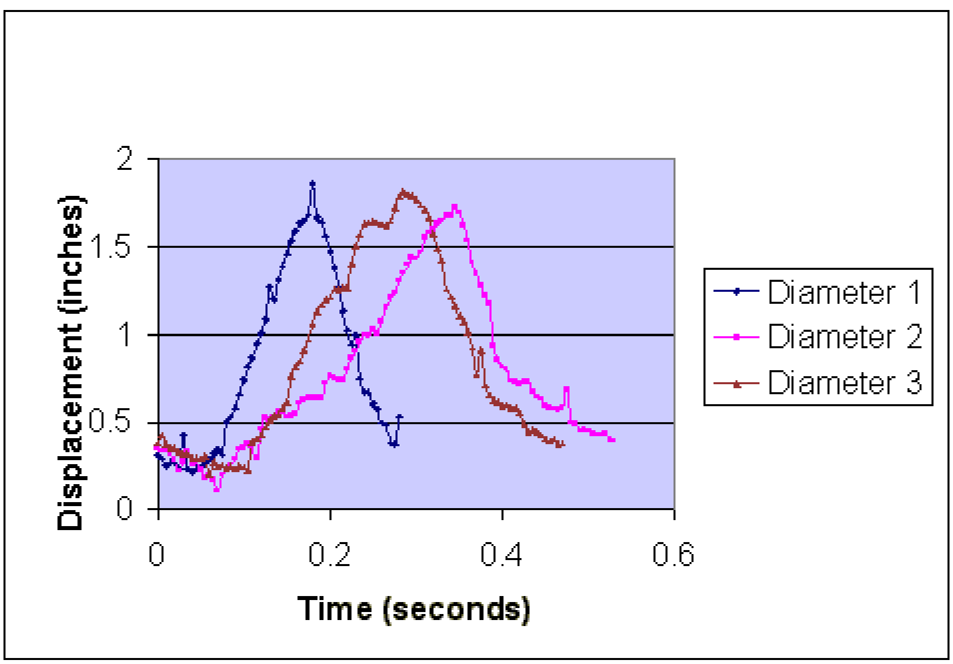

(a) Length 1

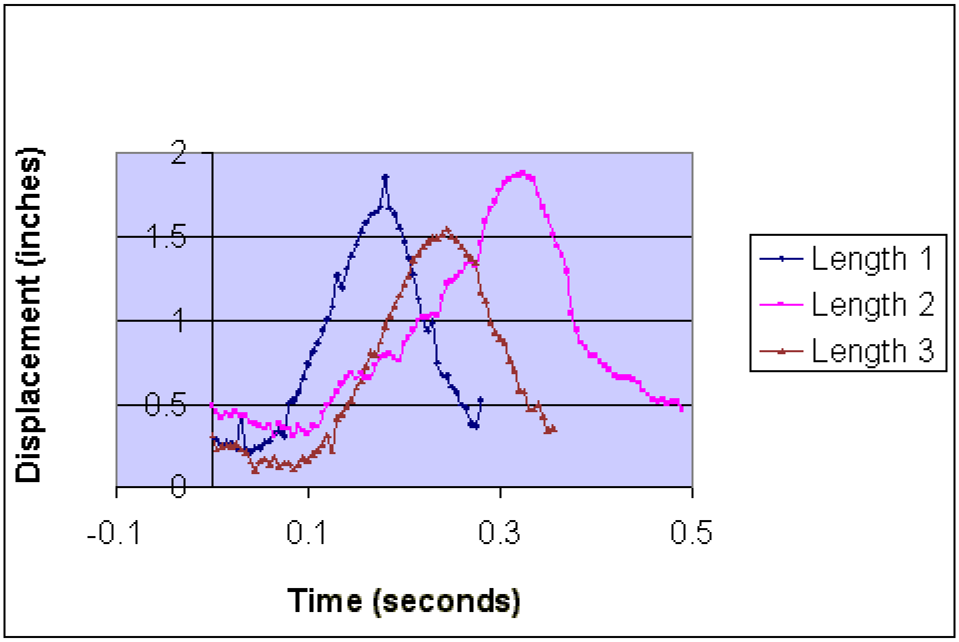

(b) Diameter 1

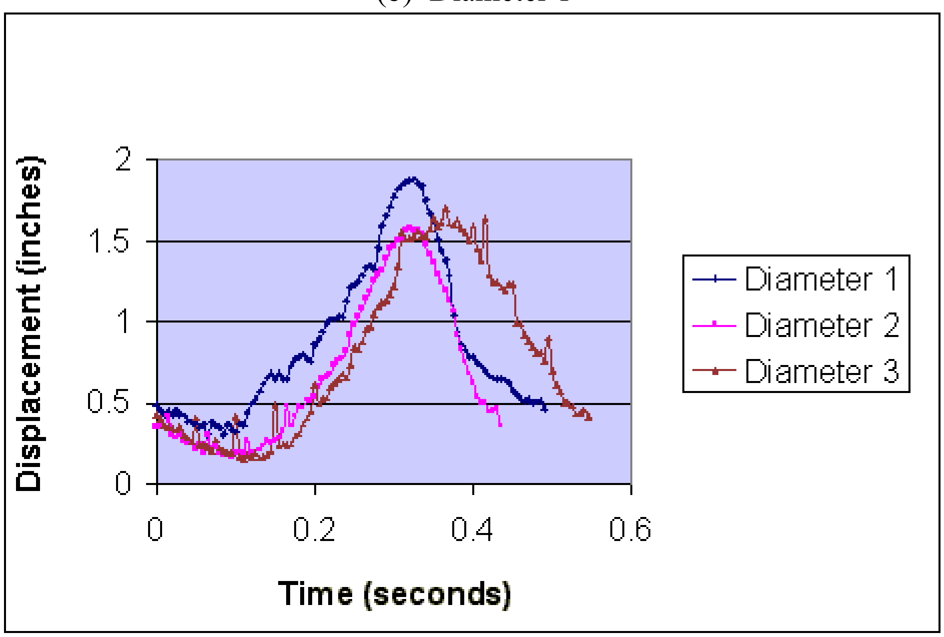

(c) Length 2

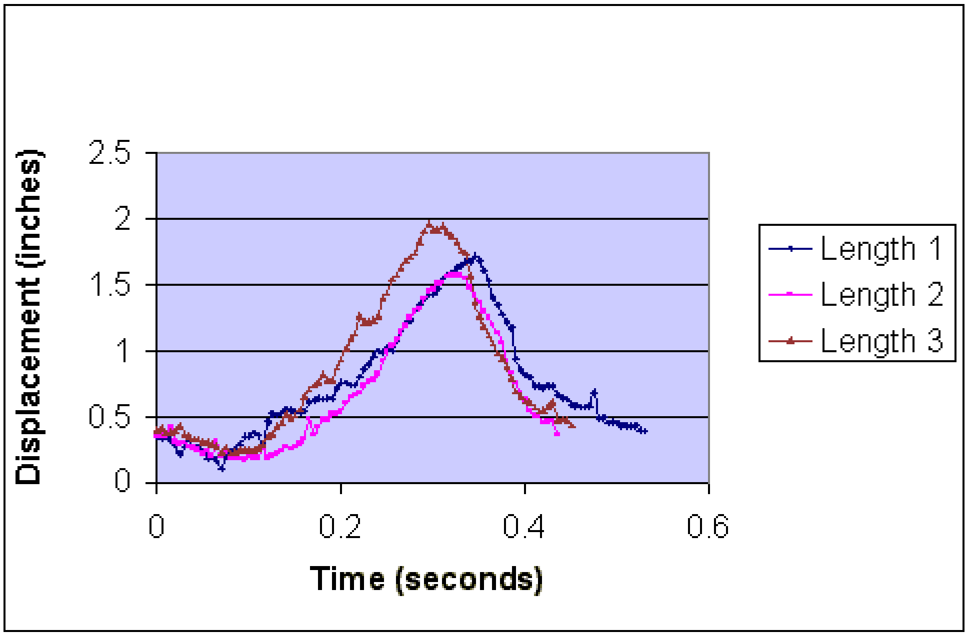

(d) Diameter 2

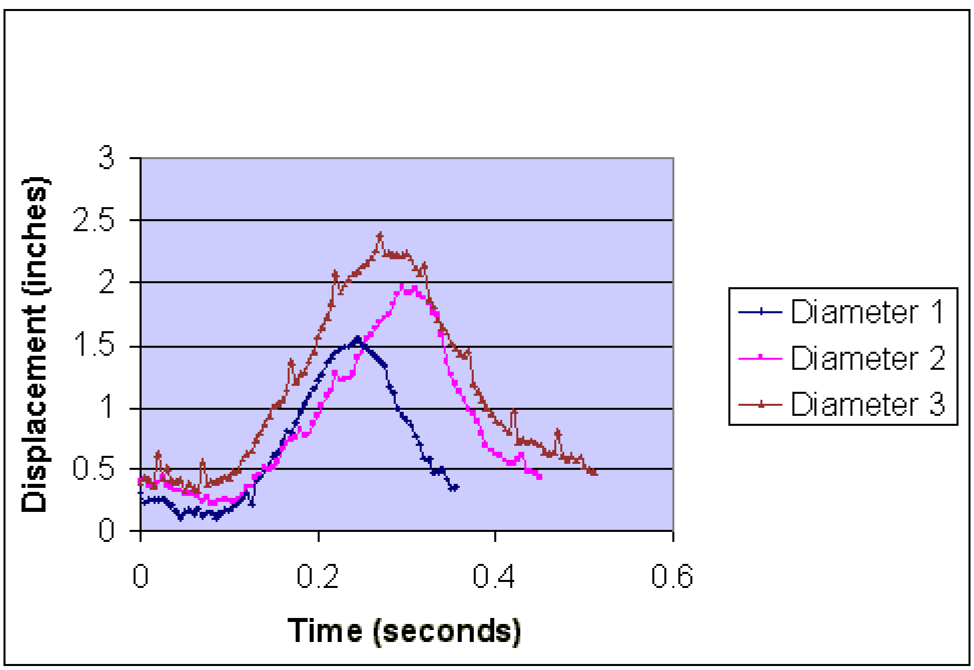

(e) Length 3

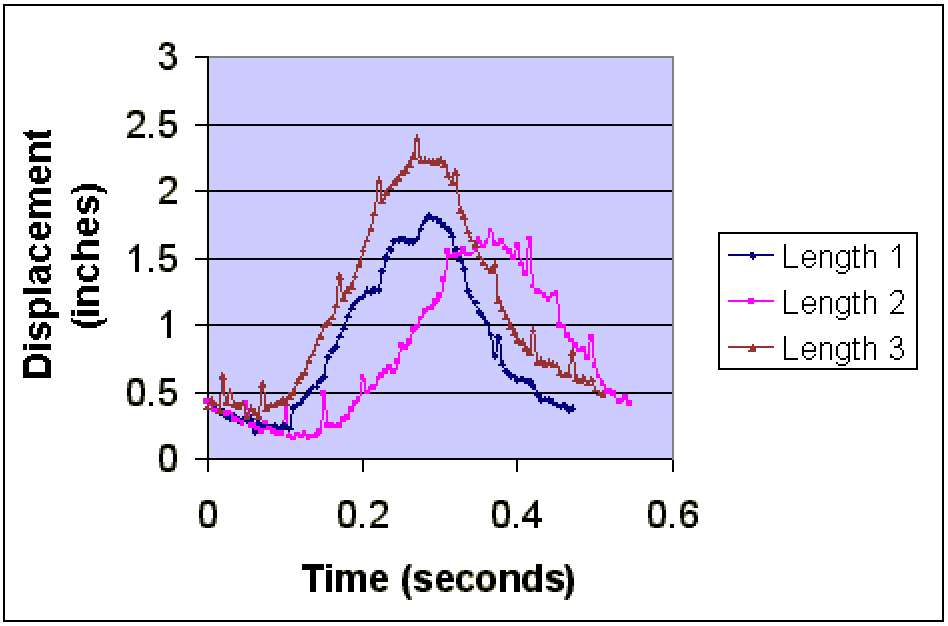

(f) Diameter 3

Figure 6.3 (a-f): Experimental Results

Figure 6.3 displays the results of all nine experiments. Again, the experimental results of the connecting rods with the same length but various diameters are graphed together. Also, the experimental results from the connecting rods with the same diameter but different lengths are graphed together to make comparisons easier. From the figure it can be seen that the increases in length increased the total displacements. The changes in diameter also had an affect on the experimental results. The increases in diameter increased the maximum displacements and slightly decreased the minimum displacements.

Experimental Uncertainty

The displacement of the piston was measured directly in the experiment; therefore, all of the uncertainty in this stage is a result of the accuracy and precision of the linear transducer. A curve fit was performed to determine displacement as a function of the voltage from the linear transducer. Then a linear regression uncertainty analysis was performed. The general equation for linear regression uncertainty analysis is in Chapter 2. For the calibration, the voltage is the independent variable (X) and the displacement is the dependent variable (Y).

All sources of uncertainty were included in the equations for linear regression uncertainty. The regression uncertainty, therefore, represents the total uncertainty in the experimental displacement, $U_Y=U_d$. The random regression uncertainty sources for this application included the random uncertainty in the transducer voltage measurements from calibration, R_{Vi}, and the random uncertainty in the new voltage measurement from the experiment, R_{Vnew}. The calibration voltage random uncertainty, R_{Vi}, was calculated using the standard deviation of all 200 calibration measurements from Equation 2-5 for 95% confidence of a Guassian distribution. The random uncertainty in displacement, R_{di}, was accounted for in the voltage calibration random uncertainty by resetting the displacement ten times according to the calibration procedure. The random uncertainty in the new experimental voltages, R_{Vnew}, was obtained from the calibration data but did not include the uncertainty in displacement from calibration. To estimate the random uncertainty of the experiment voltage measurements from the calibration data, the standard deviations of the voltage measurements for each setting of the displacement (only 20 measurements) were calculated. Then the random uncertainties were calculated for all 50 set displacements. Based on these calculations, the standard deviation was estimated as .001 V. Finally, the standard deviation was used to calculate the random uncertainty in the new voltage measurements. In this way, the displacement uncertainty was eliminated from the new voltage uncertainty, but all of the calibration data was still used for the best estimate of uncertainty in the new voltage measurements. These two sources of uncertainty were combined in the random regression uncertainty analysis, discussed in Chapter 2. The calculated random uncertainties are listed in Table 6.1. The linear regression random uncertainty reduced to Equation 6-2 for this calibration.

$$R_d = \sqrt{\sum_{i=1}^{J}\left[\left(\frac{\partial d}{\partial V_i}\right)^2 R_{V_i}{}^2\right] + \left(\frac{\partial d}{\partial V_{new}}\right)^2 R_{V_{new}}{}^2} \tag{6-2}$$

TABLE 6.1

EXPERIMENTAL UNCERTAINTIES

EXPERIMENT NUMBER	R_{Vi} (VOLTS)
1	.0015
2	.0033
3	.0021
4	.0030
5	.0021
7	.0023
7	.0017
8	.0018
9	.0015

The only systematic regression uncertainty source for this application was the systematic uncertainty in the calibration displacements, S_{di}. One-half least count for the micrometer used to set the calibration displacements was used for the displacement systematic uncertainty, S_{di}. The least count for the micrometer was .001 inches; therefore, the calibration displacement systematic uncertainty, S_{di} was .0005 in.. The systematic uncertainty in the linear transducer, S_{Vnew} and S_{Vi}, were negligible because both the calibration and the experimental data were found using the same linear transducer. The elemental sources of uncertainty were combined in the regression uncertainty analysis, in Chapter 2. The linear regression systematic uncertainty reduced to Equation 6-3 for this calibration.

$$S_d = \sqrt{\sum_{i=1}^{J}\left[\left(\frac{\partial d}{\partial d_i}\right)^2 S_{d_i}{}^2\right] + 2\sum_{i=1}^{J-1}\sum_{k=i+1}^{J}\left[\left(\frac{\partial d}{\partial d_i}\right)\left(\frac{\partial d}{\partial d_k}\right)S_{d_i}S_{d_k}\right]} \tag{6-3}$$

Finally, the total uncertainty in the experimental displacement was calculated from the root-sum-square method discussed in Chapter 2.

The detailed analysis of the experimental data and related uncertainty is also included in the Appendix, MathCad Worksheets. The experimental results and uncertainties for the first cycles of each experiment are shown in Figure 6.4. The experimental results are labeled according to Table 4.5. The maximum displacement of the piston was between 1.5 and 2 inches and the minimum displacement ranged between 0 and .25 inches.

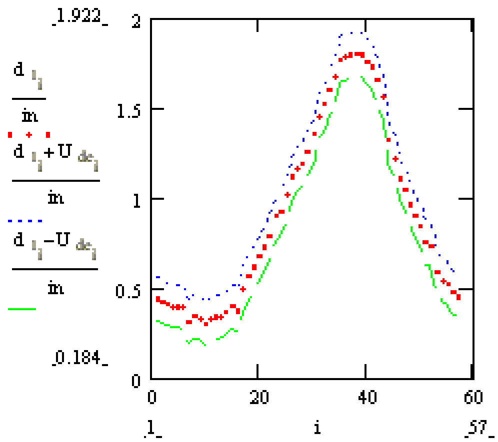

(a) Experiment 1

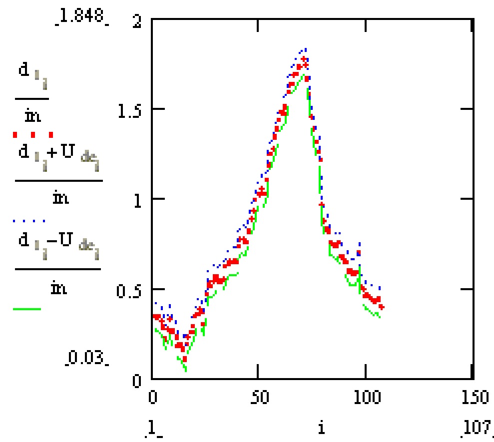

(b) Experiment 2

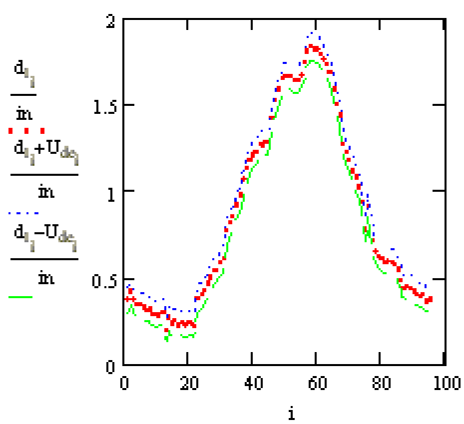

(c) Experiment 3

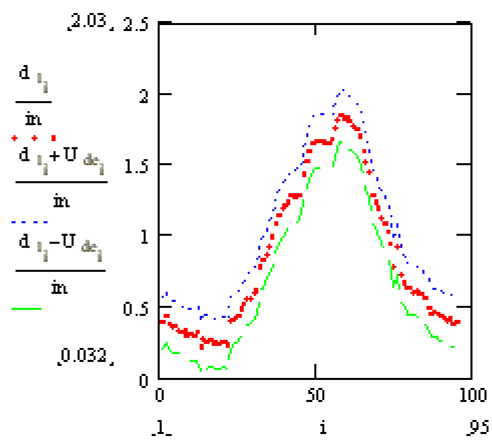

(d) Experiment 4

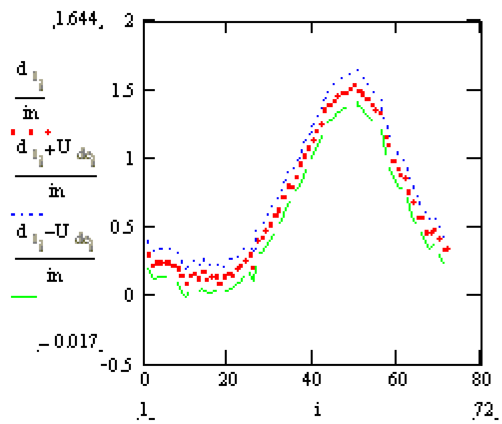

(e) Experiment 5

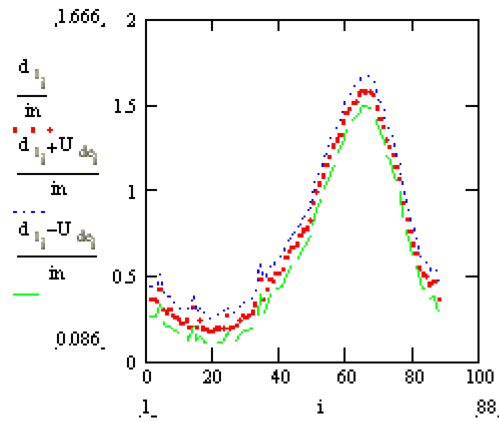

(f) Experiment 6

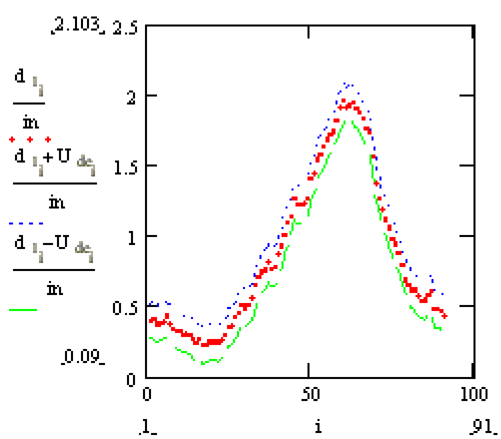

(g) Experiment 7

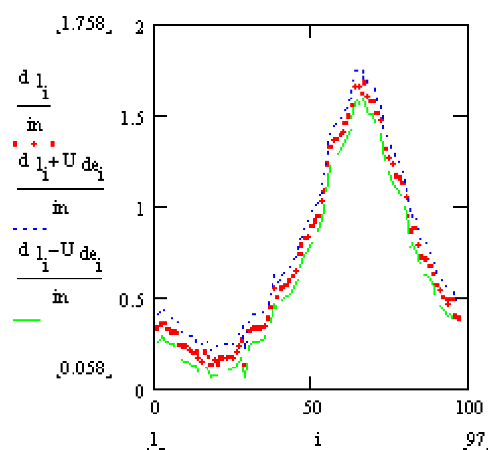

(h) Experiment 8

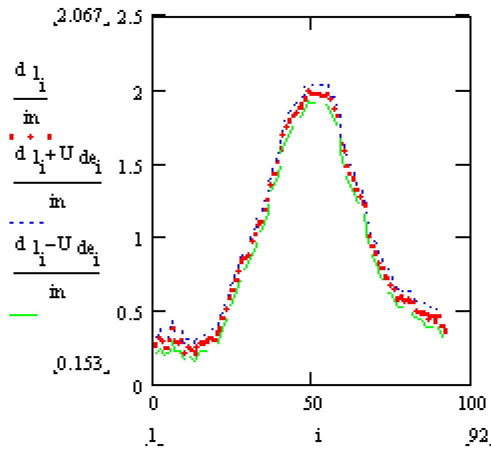

(i) Experiment 9

Figure 6.4 (a-i): Experimental Results and Uncertainties

The reference angle was calculated from the proximity sensor calibration data. The uncertainty in the reference angle was treated as an experimental result and was also calculated using experimental uncertainty analysis techniques. Here, the data reduction equation was written as a function of the measured variables, θ_1, $\delta\theta_1$, θ_2, $\delta\theta_2$, and θ_{on} because they were not independent. The systematic uncertainties of all the measured angles was estimated as 1 degree ($S_{\theta 1} = S_{\theta 2} = S_{\theta\delta 1} = S_{\theta\delta 2} = S_{\theta on} = S_\theta = 1$ deg) because of degree wheel capabilities. Therefore, the systematic uncertainties of all the measured angles were correlated. Next the systematic uncertainty in the result, the reference angle, was calculated using uncertainty techniques. For this result, the equation for systematic uncertainty reduced to

$$S_{\theta 0} = \sqrt{\begin{aligned}&\left(\frac{\partial\theta_0}{\partial\theta_{on}}\right)^2 S_\theta{}^2 + \left(\frac{\partial\theta_0}{\partial\theta_1}\right)^2 S_\theta{}^2 + \left(\frac{\partial\theta_0}{\partial\delta\theta_1}\right)^2 S_\theta{}^2 + \left(\frac{\partial\theta_0}{\partial\theta_2}\right)^2 S_\theta{}^2 \ldots\\ &+ \left(\frac{\partial\theta_0}{\partial\delta\theta_2}\right)^2 S_\theta{}^2 + 2\left(\frac{\partial\theta_0}{\partial\theta_{on}}\right)\left(\frac{\partial\theta_0}{\partial\theta_1}\right)S_\theta{}^2 + 2\left(\frac{\partial\theta_0}{\partial\theta_{on}}\right)\left(\frac{\partial\theta_0}{\partial\delta\theta_1}\right)S_\theta{}^2 \ldots\\ &+ 2\left(\frac{\partial\theta_0}{\partial\theta_{on}}\right)\left(\frac{\partial\theta_0}{\partial\theta_2}\right)S_\theta{}^2 + 2\left(\frac{\partial\theta_0}{\partial\theta_{on}}\right)\left(\frac{\partial\theta_0}{\partial\delta\theta_2}\right)S_\theta{}^2 + 2\left(\frac{\partial\theta_0}{\partial\theta_1}\right)\left(\frac{\partial\theta_0}{\partial\delta\theta_1}\right)S_\theta{}^2 \ldots\\ &+ 2\left(\frac{\partial\theta_0}{\partial\theta_1}\right)\left(\frac{\partial\theta_0}{\partial\theta_2}\right)S_\theta{}^2 + 2\left(\frac{\partial\theta_0}{\partial\theta_1}\right)\left(\frac{\partial\theta_0}{\partial\delta\theta_2}\right)S_\theta{}^2 + 2\left(\frac{\partial\theta_0}{\partial\delta\theta_1}\right)\left(\frac{\partial\theta_0}{\partial\theta_2}\right)S_\theta{}^2 \ldots\\ &+ 2\left(\frac{\partial\theta_0}{\partial\delta\theta_1}\right)\left(\frac{\partial\theta_0}{\partial\delta\theta_2}\right)S_\theta{}^2 + 2\left(\frac{\partial\theta_0}{\partial\theta_2}\right)\left(\frac{\partial\theta_0}{\partial\delta\theta_2}\right)S_\theta{}^2 \ldots\end{aligned}} \qquad (6\text{-}3)$$

The total systematic uncertainty in θ_0 was calculated from Equation 6-3 as 3.385 degrees.

Once again, the random uncertainty was calculated using the standard deviations of each angle. The random uncertainty from the calibration angles θ_1, $\delta\theta_1$, θ_2, $\delta\theta_2$, and θ_{on} are included in Table 6.2. These random uncertainties were combined in Equation 6-4 for the random uncertainty in the reference angle.

$$R_{\theta 0} = \sqrt{\begin{aligned}&\left(\frac{\partial\theta^0}{\partial\theta_{on}}\right)^2 R_\theta{}^2 + \left(\frac{\partial\theta_0}{\partial\theta_1}\right)^2 R_\theta{}^2 + \left(\frac{\partial\theta_0}{\partial\delta\theta_1}\right)^2 R_\theta{}^2 \ldots\\ &+ \left(\frac{\partial\theta_0}{\partial\theta_2}\right)^2 R_\theta{}^2 + \left(\frac{\partial\theta_0}{\partial\delta\theta_2}\right)^2 R_\theta{}^2\end{aligned}} \qquad (6\text{-}4)$$

Table 6.2

CALIBRATION ANGLE UNCERTAINTIES

ANGLE	$R_{\theta 1}$ (deg)	$R_{\delta\theta 1}$ (deg)	$R_{\theta 2}$ (deg)	$R_{\delta\theta 2}$ (deg)	$R_{\theta on}$ (deg)	$R_{\theta 0}$ (deg)	$U_{\theta 0}$ (deg)
Experiment 1	.340	.213	.213	.342	.153	.272	3.397
Experiment 2	.359	.521	.249	.307	.300	.401	3.409
Experiment 3	.233	.177	.258	.173	.133	.227	3.393
Experiment 4	.258	.173	.307	.180	.153	.430	3.412
Experiment 5	.371	.307	.593	.348	.221	.430	3.412
Experiment 7	.700	.233	.423	.233	.180	.417	3.411
Experiment 7	.748	.233	.300	.233	.180	.422	3.411
Experiment 8	.733	.213	.359	.233	.149	.442	3.414
Experiment 9	.593	.417	.327	.211	.224	.422	3.411

The random uncertainty in the reference angle is also included in Table 6.2. The total uncertainty in the reference angle was calculated using the root-sum-square method (Equation 6-5) and is also included in Table 6.2.

$$U_{\theta 0} = \sqrt{R_{\theta 0}^{\;2} + S_{\theta 0}^{\;2}} \tag{6-5}$$

CHAPTER VII

COMPARISONS

Comparison was the fourth stage in the pilot project design process. This stage is often overlooked in design processes, however. Part of the goal of this new area of research is to develop distinct methods for this stage in the design process. The comparisons stage has several aspects. First, how does manufacturing affect the model results? Second, how does manufacturing affect experimental results? And finally, how are the experimental results related to the model results?

Manufacturing Effects on the Model

The first aspect of comparisons is evaluating manufacturing's effect on the model. The connecting rods were modeled with various diameters to evaluate these effects. The results and uncertainties of the nine models were included in the Model, Chapter 4. Now, how can these effects be accounted for in the uncertainty analysis without constructing a new model for each connecting rod? It is proposed that the manufacturing uncertainty can be included in the model as an additional systematic uncertainty. Figure 7.1 is the graph of model 3 (length 1 and diameter 3) to illustrate this idea. The figure gives the model results along with the model uncertainty bands for the largest diameter case (d3). The figure also shows the dotted-line uncertainty bands, which include the manufacturing uncertainty. The model uncertainty bands that include the manufacturing tolerances are slightly larger, as expected.

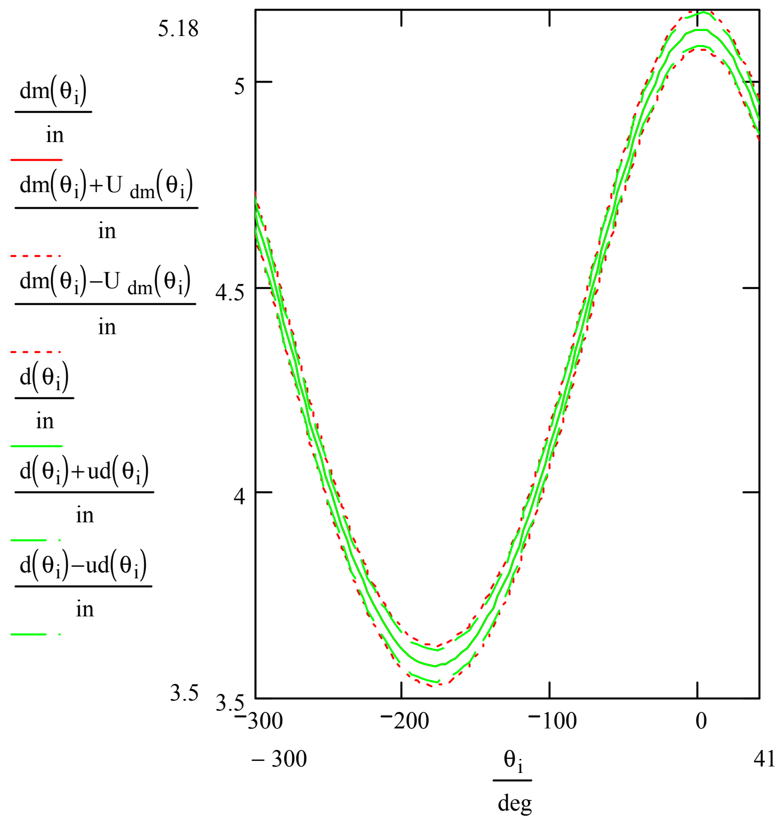

Figure 7.1: Manufacture Effects Compared to the Model Results

Manufacturing Effects on the Experiment

The next step of comparing was to evaluate the effects of manufacturing uncertainty on the experimental data. Once again, to exaggerate manufacturing uncertainty effects, connecting rods of various diameters were manufactured and used for experimentation. To further test the idea of including manufacturing tolerances as an elemental source of uncertainty, length one experimental results with the largest diameter were plotted with the model-manufacturing uncertainty in Figure 7.2. The dashed lines represent the model uncertainty with manufacturing uncertainty included. The dotted lines are the experimental uncertainties. These uncertainty bands do not match because of the variations in engine speed mentioned in the Experiment. This problem will be addressed in the following sections. However, the maximum and minimum experimental displacement matches closely to the maximum and the minimum manufacturing tolerance uncertainty bands from the model. These results help prove the validity of including manufacturing uncertainties as additional random uncertainties in the model.

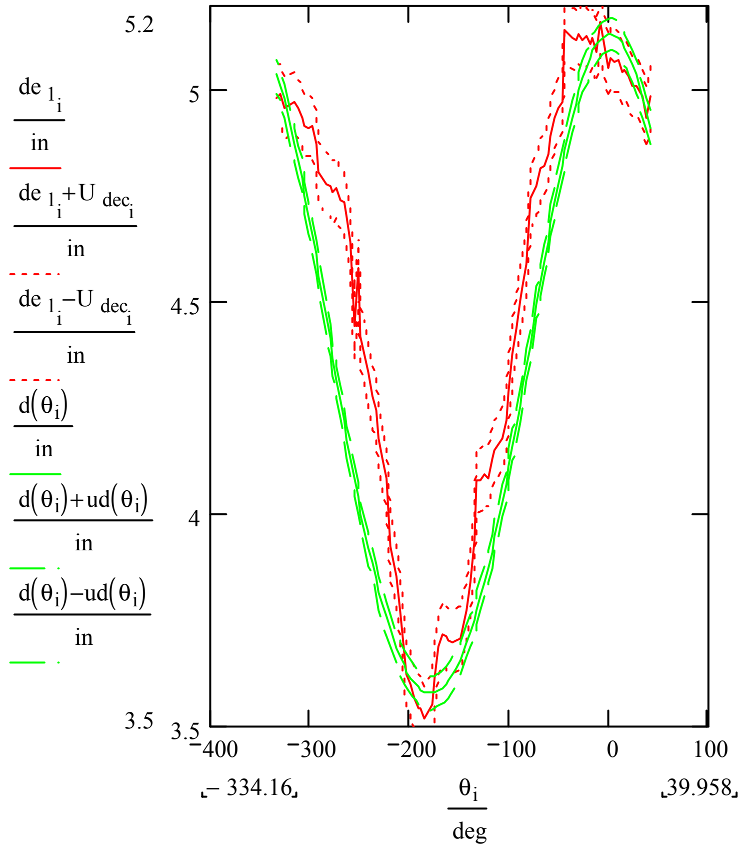

Figure 7.2: Manufacture Effects Compared to the Experimental Results

Model and Experiment Comparisons

<u>Initial Comparisons</u>

For model and experiment comparisons, the independent variable, t, of the experiment had to be converted to crank angle, θ_i. During the experiment, the experimental data was collected every .005 seconds. Therefore, the displacement data was collected with respect to time. The model equation, on the other hand, expressed the piston displacement as a function of crank angle. Therefore, to make comparisons between the model and the experiment, a crank angle had to be determined for each experimental displacement data point. Equation 7-1 was used to determine the crank angle for each experimental displacement data point.

$$\theta_i = \theta_0 + \sum_{j=1}^{i} \omega_j \times \left(t_j - t_{j-1}\right) \tag{7-1}$$

In Equation 7-1, the reference angle, θ_0, was determined from Equation 6-3, the engine speed was calculated in the Labview program, and time was kept by the computer clock in the Labview program.

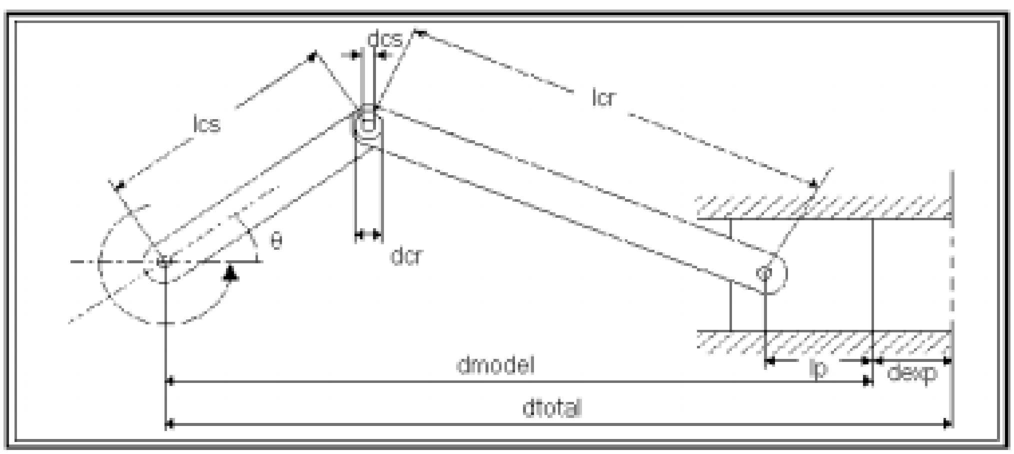

Figure 7.3: New Frame of Reference

The final step needed for comparing the model and experiment involved correcting the frame of reference of the experiment to match the model. The experimental displacement was measured from the top of the cylinder to the top of the piston head as shown in Figure 7.3. In contrast, the model displacement was measured from the crankshaft to the top of the piston. The sum of the model displacement and the experimental displacement ideally equals a constant total displacement. However, the different assumptions in the model and the experiment complicate these calculations. The uncertainty in the crank angle made a summation of all points incredibly inaccurate. For a better value of this total displacement, the average maximum experimental displacement of all eight cycles of data for each experimental run, max(d), which does not depend on an accurate estimate of the crank angle, was added to the minimum model displacement, d(180). To eliminate hysteresis, the total displacement was also determined using the average minimum experimental displacement, min(d), plus the maximum model displacement, d(0). These two estimates of the total displacement were then averaged for the final value of the total displacement as shown in Equation 7-2.

$$d_t = \frac{[d_{\max} + d(180)] + [d_{\min} + d(0)]}{2} \tag{7-2}$$

Initial Comparisons Uncertainty

The data reduction equation, Equation 7-1, for the crank angle, θ_i, was expressed in terms of θ_0, ω, and t. Therefore, Equation 7-3, derived from general uncertainty analysis techniques, describes the uncertainty in θ_i as a function of the uncertainty of each of these elements. Even though θ_0 was not a measured variable, the data reduction equation was expressed this way because θ_0 was independent of the other variables. The uncertainty in engine speed, ω, was estimated as 300 deg/s to account for the fluctuations in engine speed. The total uncertainty in the reference angle was determined from

Equation 6-5. The uncertainty in time was assumed to be negligible. Therefore the general uncertainty equation became

$$U_{\theta_i} = \sqrt{{U_{\theta_0}}^2 + \left(\frac{\partial \theta_i}{\partial \omega}\right)^2 {U_\omega}^2} \tag{7-3}$$

To determine the uncertainty with respect to the new frame of reference, the sources of uncertainty were evaluated. It was not known if the recorded maximum and minimum experimental displacements were the "true" maximums and minimums. Therefore, the random uncertainties in these points were calculated using eight cycles of each experiment using Equation 2-7. For the random uncertainty in the model, the model uncertainty at 180 degrees and 0 degrees ($U_d(180)$ and $U_d(0)$) were used because there were no additional sources of uncertainty. As in the model, the uncertainty in the experimental data points, d_i, were used because there were no additional uncertainties in these values either. The random uncertainty of the minimum and maximum model displacement and the random uncertainty in the experimental data points were combined in the uncertainty analysis Equation 7-4.

$$R_d = \sqrt{\frac{1}{4}{R_{d\max}}^2 + \frac{1}{4}R_d(180)^2 + \frac{1}{4}{R_{d\min}}^2 + \frac{1}{4}R_d(0)^2 + {R_{di}}^2} \tag{7-4}$$

Also the systematic uncertainty of each value from the model and the experiment was combined to determine the systematic uncertainty in the new frame of reference data using Equation 7-5.

$$S_d = \sqrt{\frac{1}{4}{S_{d\max}}^2 + \frac{1}{4}S_d(180)^2 + \frac{1}{4}{S_{d\min}}^2 + \frac{1}{4}S_d(0)^2 + {S_{di}}^2} \tag{7-5}$$

Finally, the root-sum-square method (Equation 7-5) was used to determine the total uncertainty.

$$U_d = \sqrt{R_d^{\,2} + S_d^{\,2}} \tag{7-6}$$

The constant engine speed assumption caused the experimental data to deviate from the model. Estimating the uncertainty in engine speed as 300 deg/s to accommodate the fluctuations enlarged the total uncertainty to such an extent that the comparisons became meaningless. How could a meaningful comparison be obtained?

Final Comparisons

It is proposed that design optimization techniques can be used to make comparisons between the model and the experiment. Design optimization techniques are currently used to minimize the difference between the model and the design goals by determining the "optimum" value for each design variable. Design optimization problems are grouped in one of two categories: constrained or unconstrained. Constraints are design limitations that must be met for the design to be feasible. In using design optimization for comparisons, the optimization techniques will be used to minimize the difference between the model and the experiment by determining the most probable value of each unknown parameter. The variable uncertainty bands are analogous to design limitations and will also be handled by imposing constraints.

For the pilot project, design optimization techniques were used to minimize the **absolute error** between the model and experiment, where the crank angle, θ, was the unknown parameter or design variable. Equation 7-7 is the function that was optimized.

In Equation 7-7, nde is the experimental result, and the term in the brackets is the model result. Here, z was used as a "dummy" variable to represent the design variable, the crank angle. Therefore, the difference between the two results is the function being minimized. It is important to note that the slop was not treated as a design variable to simplify the comparisons stage.

$$F(z, nde) := \left| nde - \left[nl_{cs} \cdot \cos(z) + \sqrt{\left(\frac{nl_1 + nl_2}{2}\right)^2 - nl_{cs}^{\,2} \cdot (\sin(z))^2} + nl_p \right] \right| \tag{7-7}$$

The golden section method was selected because of its simplicity and ability to handle absolute functions. The golden section method does have one significant disadvantage; upper and lower bounds on the design variable must be identified. The golden section method can only find the minimum of a function within these specified bounds. In addition, if the bounds include more than one local minimum, the golden section method will not necessarily find the global minimum. Therefore, for the golden section method, the bounds must be specified to include only the global minimum.

To begin the golden section optimization, bounds for the crank angle were specified that included the crank angle that minimized Equation 7-7. The bounds were specified according to Figure 7.4. From the reference angle to the angle that corresponds to the minimum piston displacement from the experiment, the bounds were 90 to 0 degrees. From the angle of minimum displacement to maximum displacement, the bounds were 0 to (-180) degrees. And from the maximum to the end of the run, the bounds were established (-180) to (-360) degrees. These bounds do have uncertainties related to the maximum and minimum values.

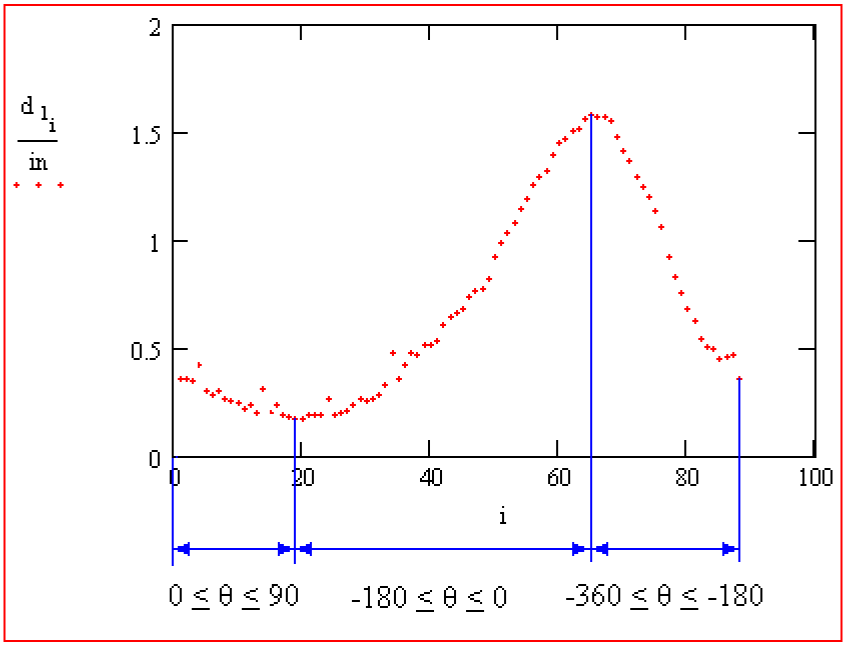

Figure 7.4: Establish Bounds on the New Estimate of the Crank Angle

The classification of this particular optimization was unconstrained with one-variable. When necessary, a constrained optimization (e.g., exterior or interior penalty function methods) could be employed using uncertainty bands for constraints. However, for this case, the optimization served to validate the experimental results, model results, and performance of the optimization process itself.

The most probable crank angle is compared to the average engine speed in Figure 7.5 for all nine cases. Again, the comparisons results are labeled according to Table 4.5. The solid line is the original value of the crank angle calculated from Equation 7-1. The points are the most probable crank angles from the optimization process. To verify the new values of the crank angle, the graphs were examined. The area between the average velocity line and the instantaneous velocity curve is approximately zero. Additionally, the optimized data forms a relatively good curve consistent with the fact that the velocity is continuous. The most probable crank angle does fall within the original uncertainty bands for crank angle. If it had not, this would then have indicated that an additional source of error existed between the experiment and the model that had not yet been identified.

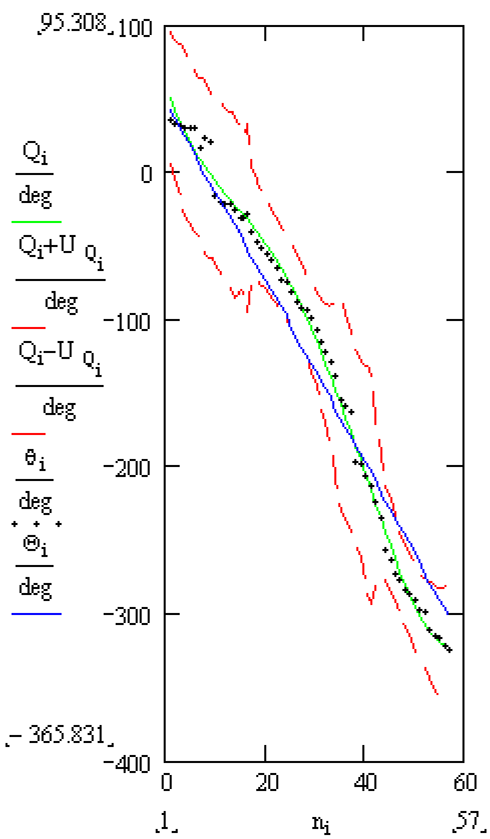

(a) Comparison 1

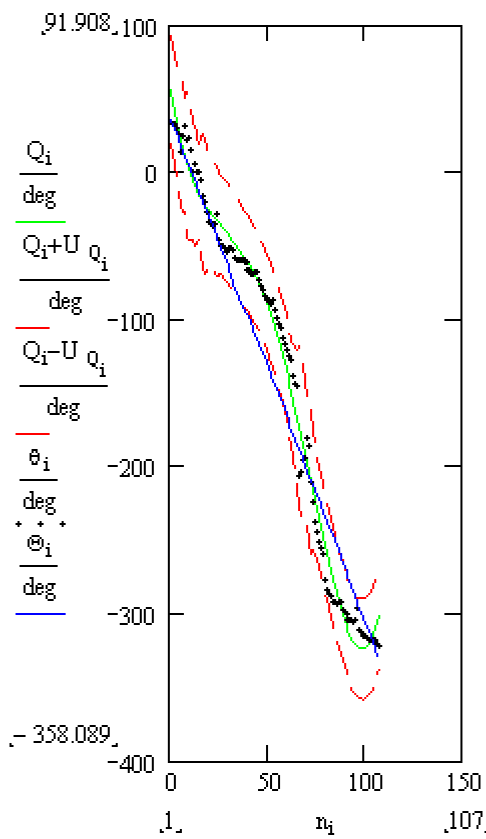

(b) Comparison 2

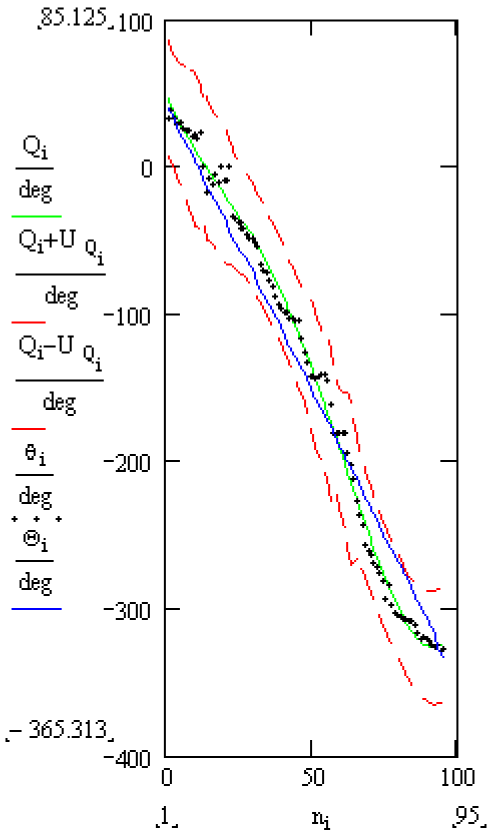

(c) Comparison 3

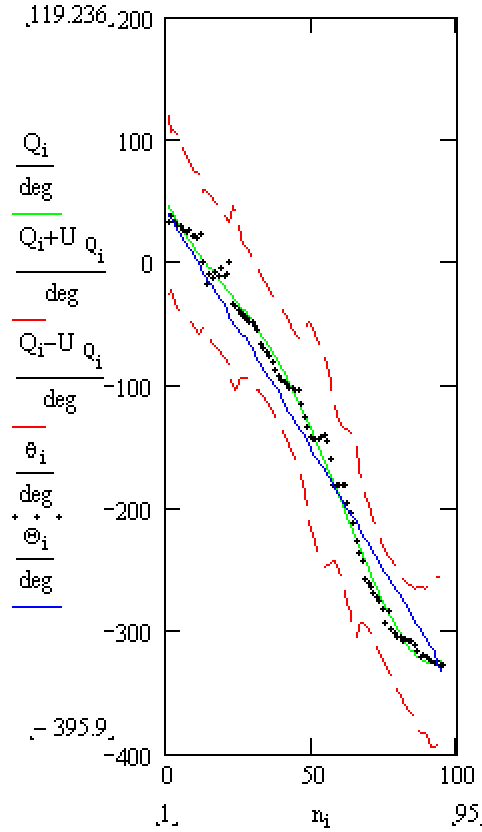

(d) Comparison 4

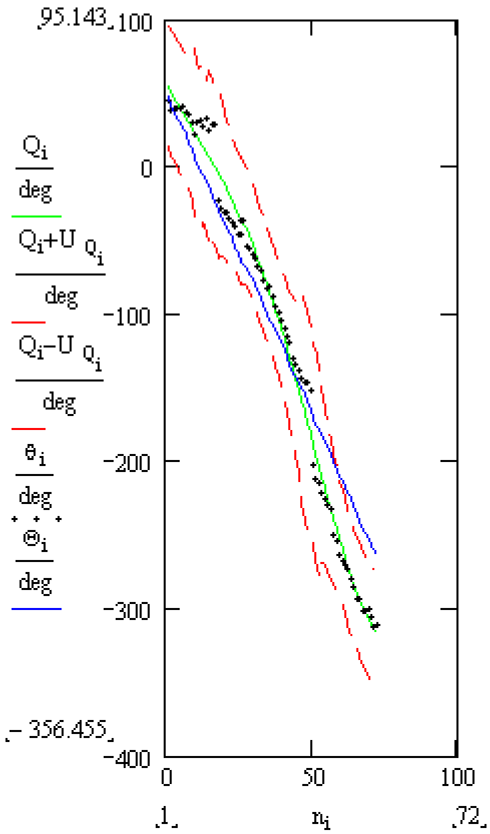

(e) Comparison 5

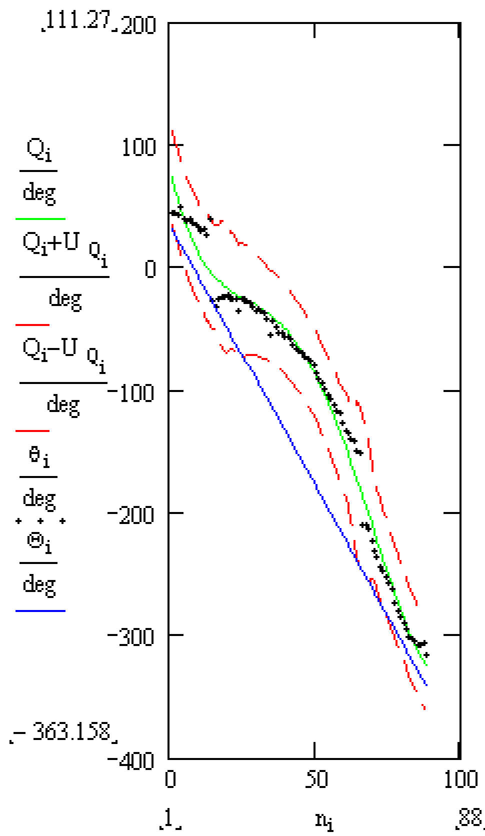

(f) Comparison 6

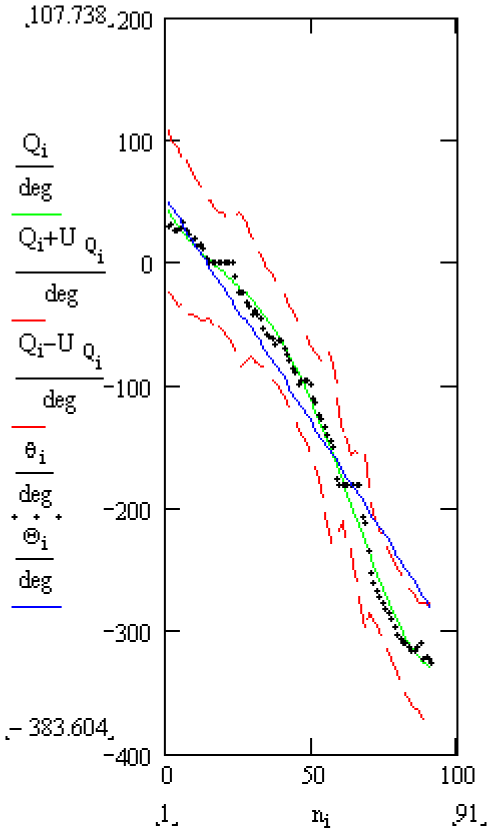

(g) Comparison 7

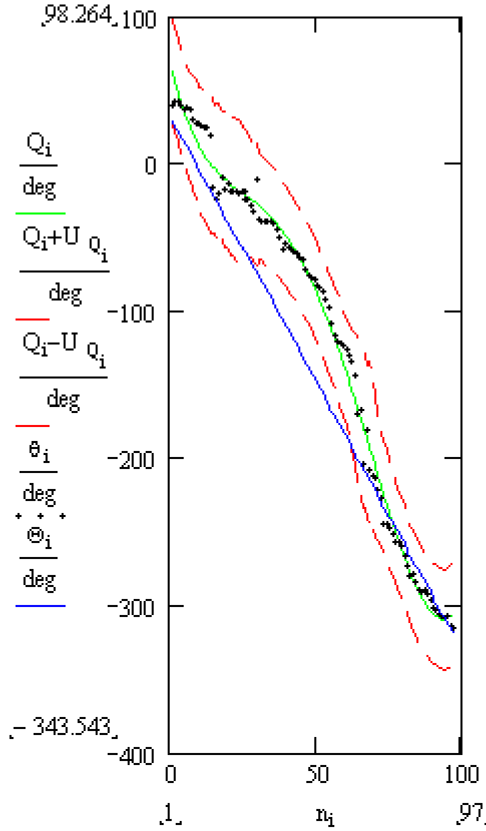

(h) Comparison 8

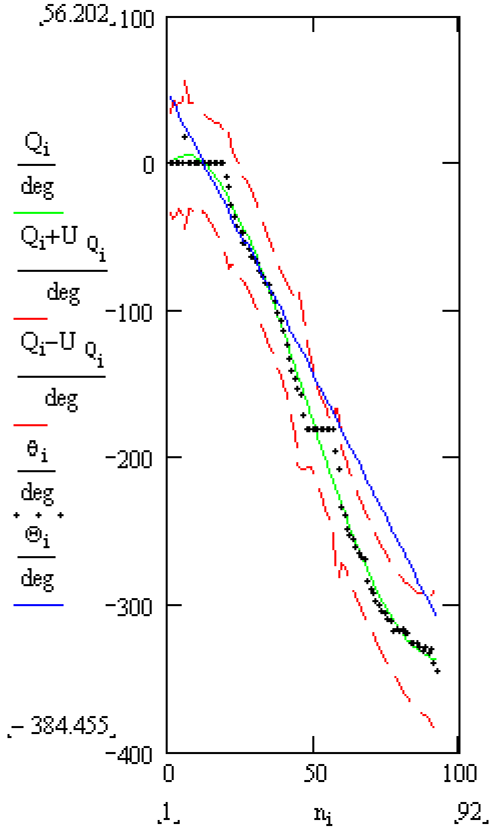

(i) Comparison 9

Figure 7.5 (a-i): Comparisons of Crank Angles

To predict the crank angle for future experimentation, the most probable crank angle, θ, values were fit in a 4th order equation versus the counter, "i" for simplicity ("i" is a function of time). This curve is also graphed in Figure 7.5. The curve fit data is the green line. Equation 7-8 is the fourth order polynomial. Where C_1, C_2, C_3, C_4, and C_5 are the constants that were determined from the curve fit.

$$\theta(i) = C_1 * i^4 + C_2 * i^3 + C_3 * i^2 + C_4 * i + C_5 \qquad (7\text{-}8)$$

Final Comparisons Uncertainty

Because of the large value of uncertainty in the instantaneous engine speed, the uncertainty in the crank angle was unacceptably large. In order to improve the estimate of uncertainty, the design optimization was employed. However, the improved estimate of the crank angle does have uncertainty associated with it.

The uncertainty in the new estimate of the crank angle had two sources of uncertainty; the uncertainty in the optimization function F(z,nde) and the uncertainty in the optimization process itself.

First, the uncertainty in the model and the experiment were independent. Therefore, the data reduction equation was expressed simply as the difference between the experiment and the model. The model uncertainty was considered negligible in comparison to the uncertainty in the experiment. The experimental uncertainty bands, as well as the experimental results, were optimized to obtain the first source of uncertainty in the improved estimate of the crank angle. By performing the optimization process on the uncertainty bands, the experimental uncertainty in displacement was converted to a source of the uncertainty in the crank angle, R_θ, for the comparisons and, eventually, the uncertainty in the final manufactured product.

Second, the optimization itself contributed to the systematic uncertainty. The tolerance of the optimization was set at .0001. The tolerance of the optimization algorithm specifies how close the consecutive iterations must be in order to stop the algorithm and claim that an improved estimate has been determined. However, because of the fuzzy bounds, the systematic uncertainty, S_θ, was approximated as .1 deg.

Finally, the improved estimate of the crank angle was curve fit using the least squares approximation for a fourth order polynomial. Another regression uncertainty analysis was performed to find the total uncertainty using the calculated random and systematic uncertainty in the most probable crank angle. For this linear regression, the counter, i, was the independent variable (X), and the crank angle was the dependent variable (Y). It was assumed that the uncertainty in the counters (or time) was negligible. The only uncertainty was from the uncertainty in the crank angle data points (R_θ, and S_θ from the previous paragraph). The equations for regression uncertainty for this application reduce to Equations 7-9 and 7-10.

$$S_Q = \sqrt{\sum_{i=1}^{J}\left[\left(\frac{\partial Q}{\partial \theta_i}\right)^2 {S_{\theta_i}}^2\right] + 2\sum_{i=1}^{J-1}\sum_{k=i+1}^{J}\left[\left(\frac{\partial Q}{\partial \theta_i}\right)\left(\frac{\partial Q}{\partial \theta_k}\right) S_{\theta_i} S_{\theta_k}\right]} \tag{7-9}$$

$$R_Q = \sqrt{\sum_{i=1}^{J}\left[\left(\frac{\partial Q}{\partial \theta_i}\right)^2 {R_{\theta_i}}^2\right]} \tag{7-10}$$

The only uncertainty was from the uncertainty in the crank angle data points. Therefore, the only partial derivative that was required for the general uncertainty analysis was the curve fit crank angle with respect to the crank angle data points $\left(\frac{\partial Q}{\partial \theta_i}\right)$.

A jitter program was used to estimate this partial derivative to ease calculations. The jitter program is included in Figure 7.6. The perturbation size, $\delta\theta$, was .01.

$$\theta u(i,j) := \theta_i \cdot \left[1 + (\delta\theta \cdot \mathrm{identity}(P))_{i,j} \right] \qquad \theta l(i,j) := \theta_i \cdot \left[1 - (\delta\theta \cdot \mathrm{identity}(P))_{i,j} \right]$$

```
Qu := | for j ∈ 1..P                                Ql := | for j ∈ 1..P
      |   | for i ∈ 1..P                                  |   | for i ∈ 1..P
      |   |   θ_i ← θu(i, j)                              |   |   θ_i ← θl(i, j)
      |   | C ← linfit(n, θ, F)                           |   | C ← linfit(n, θ, F)
      |   | Qu_j ← Q(n_i, C_1, C_2, C_3, C_4, C_5)        |   | Ql_j ← Q(n_i, C_1, C_2, C_3, C_4, C_5)
      | Qu                                                | Ql
```

$$d\theta fit_j := \frac{Qu_j - Ql_j}{2 \cdot \delta\theta} \qquad U_Q := \sqrt{\sum_{i=1}^{P} (d\theta fit_i)^2 \cdot R_Y{}^2 + \sum_{i=1}^{P} (d\theta fit_i)^2 \cdot B_Y{}^2 + 2 \cdot \sum_{i=1}^{P-1} \sum_{k=i+1}^{P} d\theta fit_i \cdot d\theta fit_k \cdot B_Y{}^2}$$

Figure 7.6: Jitter Program

The curve fit function of theta (Q-solid line) and its uncertainty bands (dashed lines), the optimized crank angle (θ-data points), and the original theta (Θ-solid straight line) are all shown in Figure 7.5. The uncertainty in the new estimate of the crank angle is smaller than the original uncertainty. The calculations for the comparisons and comparisons uncertainty for the first connecting rod are included in the Appendix.

CHAPTER VIII

FINAL MANUFACTURED PRODUCT

Finally, the uncertainty of the final manufactured product must be determined. The four stages of the design process were used to accumulate the most accurate information. The model's primary advantage was an accurate value of displacement. There were two major disadvantages that had an effect on the results. First, the crank angle and its uncertainty were undetermined. Second, the slop was assumed to be zero. The experiment's primary advantage was that the effects of the slop do affect the displacement. The experimental disadvantages were the inaccurate value of the crank angle and, less so, the displacement. However, the comparisons combined the model and experimental data to find the most probable crank angle.

The expected results of the final manufactured product were calculated using Equation 8-1 which incorporates information from all four stages in the design process. First, the model equation was used as the equation for the final manufactured product because of the accurate displacement. Note that the slop was assumed to be zero for the final manufactured product also. Second, the manufacturing tolerances were included in the model uncertainty (Equation 8-2). Therefore, the model-manufacture uncertainty discussed in Chapter 7 makes up the total uncertainty of the displacement of the final manufactured product. Third, the experimental displacement was used in the comparisons. And last, the comparisons were used with experimental and model data (as discussed in Chapter 7) to determine the best estimate of the crank angle as a function of the counter (or time) and to reduce the crank angle uncertainty. Therefore, the experimental uncertainty and the uncertainty from the comparisons itself make up the total uncertainty in the crank angle of the final manufactured product (Equation 8-3). Figure 8.1 displays the expected results and uncertainty of the final manufactured product. Again, the results are labeled according to Table 4.5.

$$d_{fmp} = d_{model}(\theta_{comparison}) \tag{8-1}$$

$$U_{d\mathit{fmp}} = f(U_{d\mathit{model}}, U_{d\mathit{manufacture}}) \tag{8-2}$$

$$U_{\theta \mathit{fmp}} = f(U_{\theta \mathit{experiment}}, U_{\theta \mathit{comparisons}}) \tag{8-3}$$

The solid curves are the expected results. The dashed lines are the uncertainty in the crank angle and the dotted lines are the uncertainty in the distance. All of these graphs show that the expected results of the final manufactured product agree with the first cycle results. In addition, the trial runs for each experiment are similar. The minimum displacement occurs between –150 and –200 degrees and the maximum displacement occurs around 0 degrees. Again, the detailed calculations for the first final manufactured product are included in the Appendix.

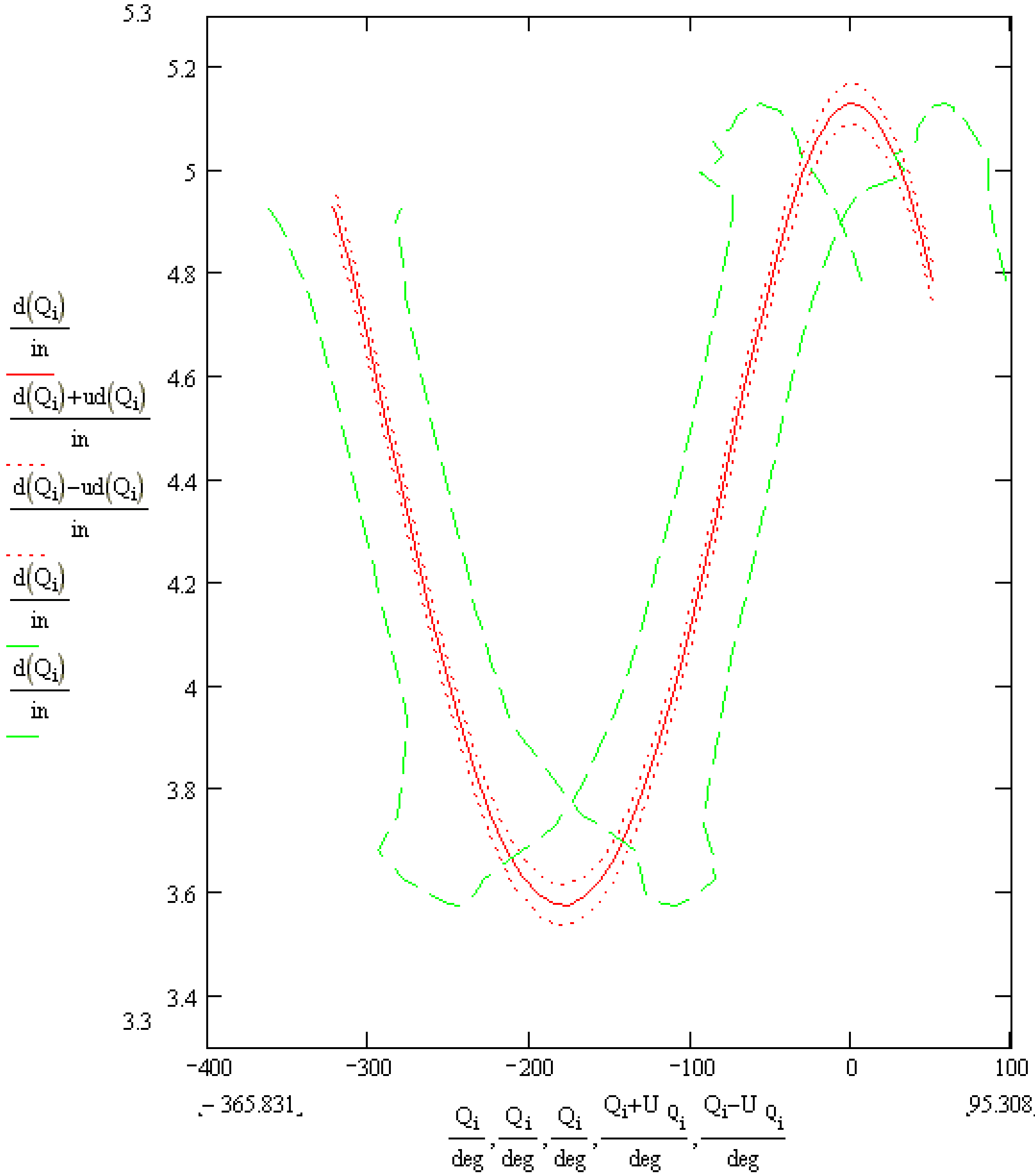

(a) Final Product 1

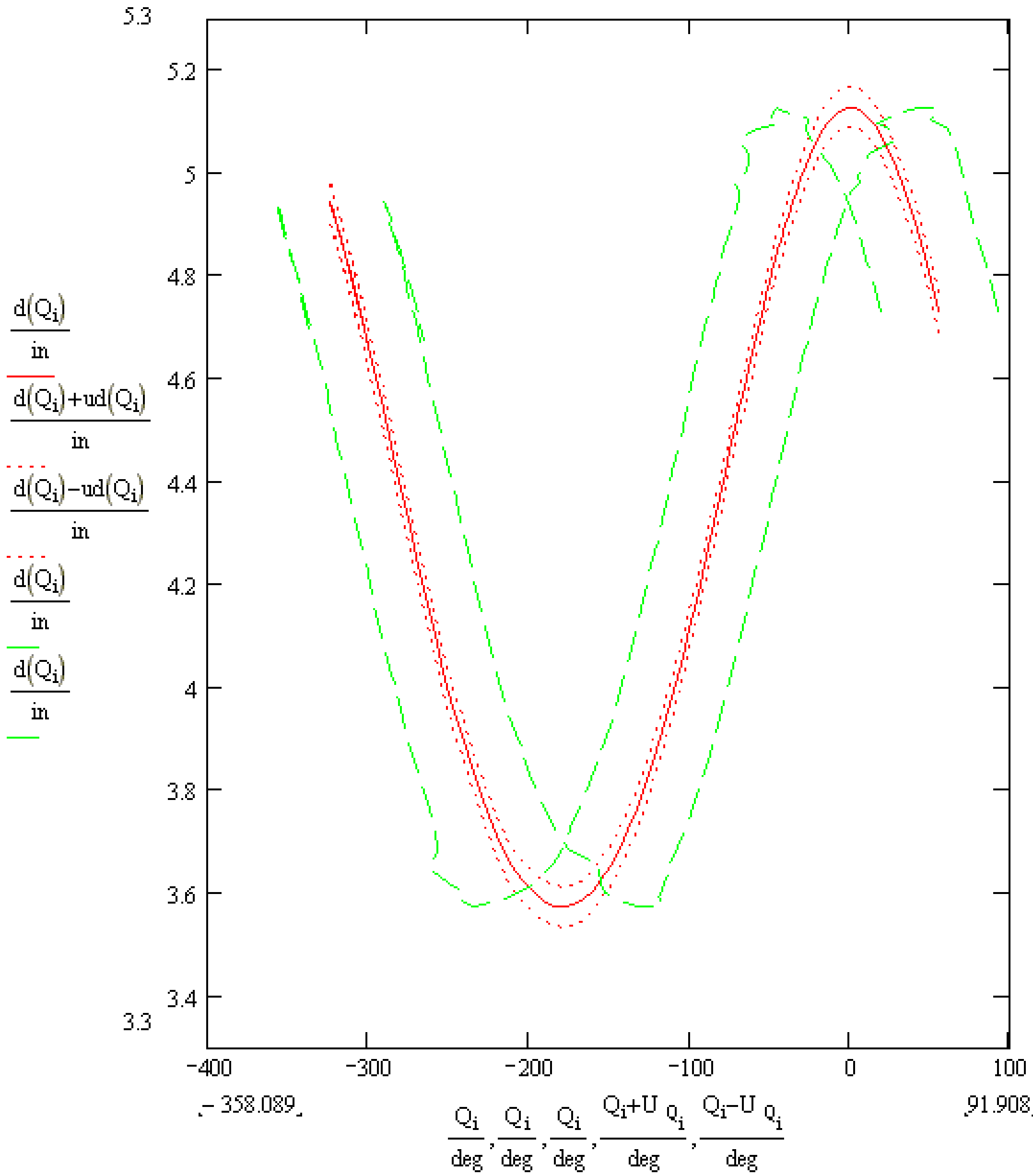

(b) Final Product 2

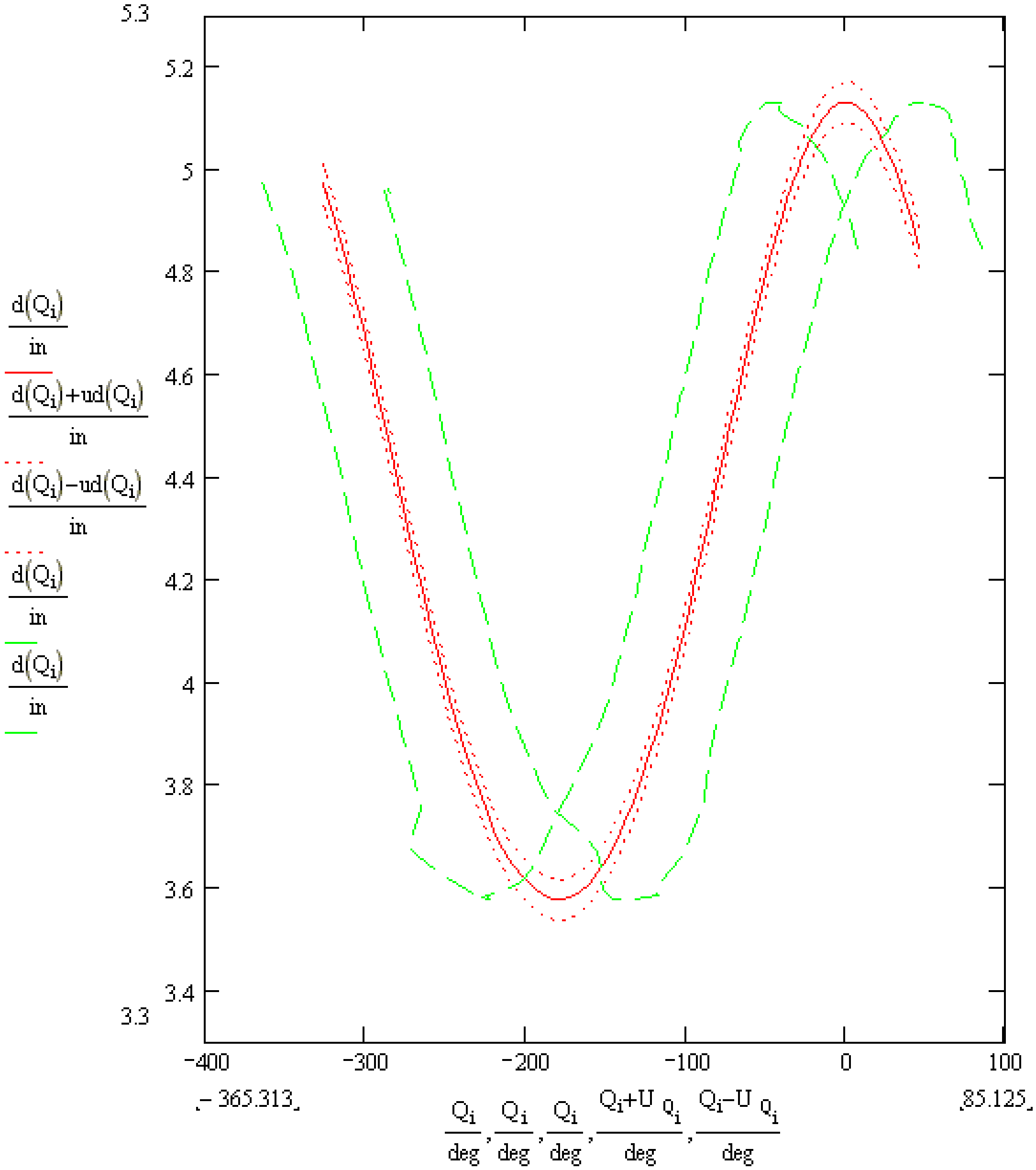

(c) Final Product 3

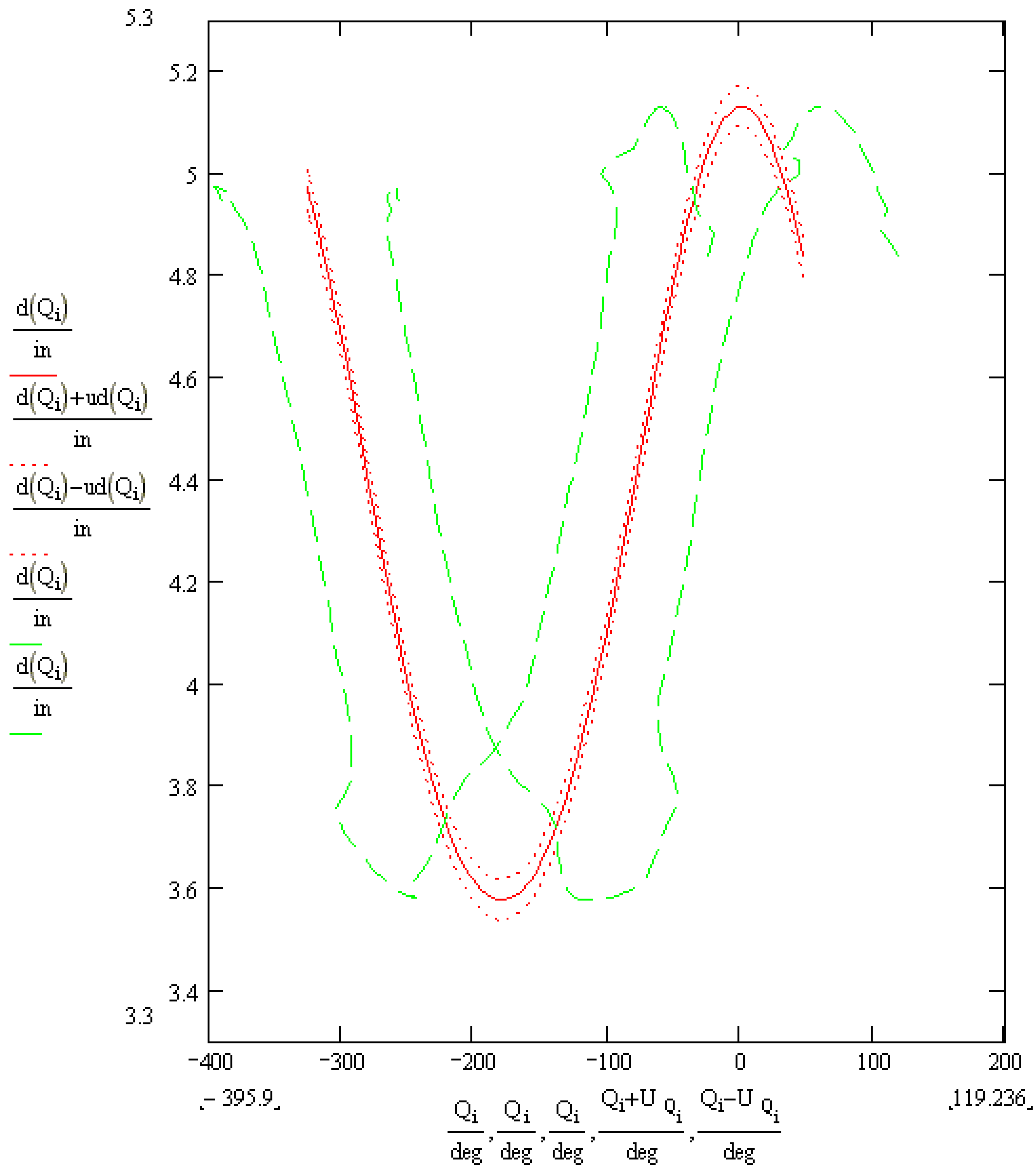

(d) Final Product 4

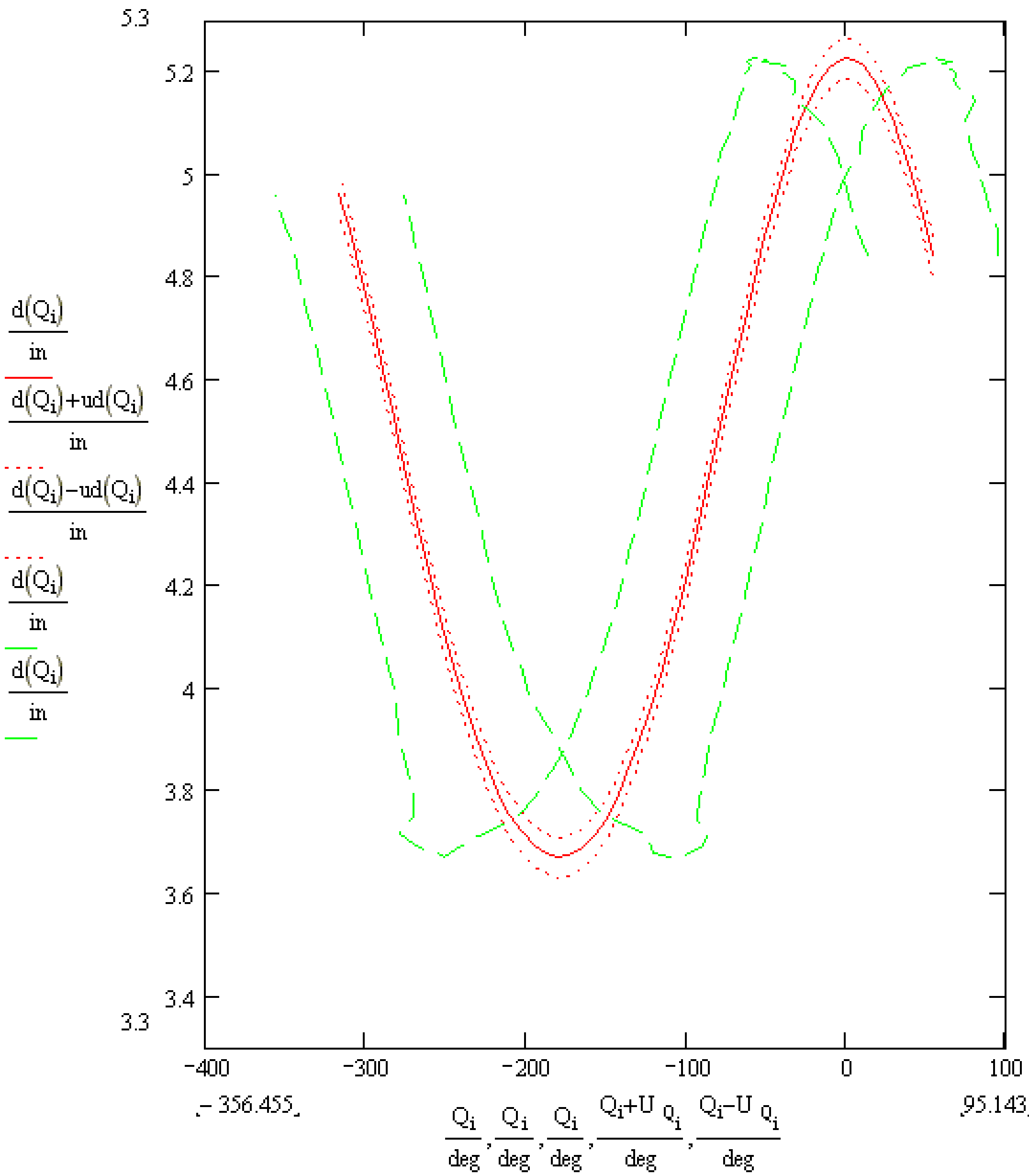

(e) Final Product 5

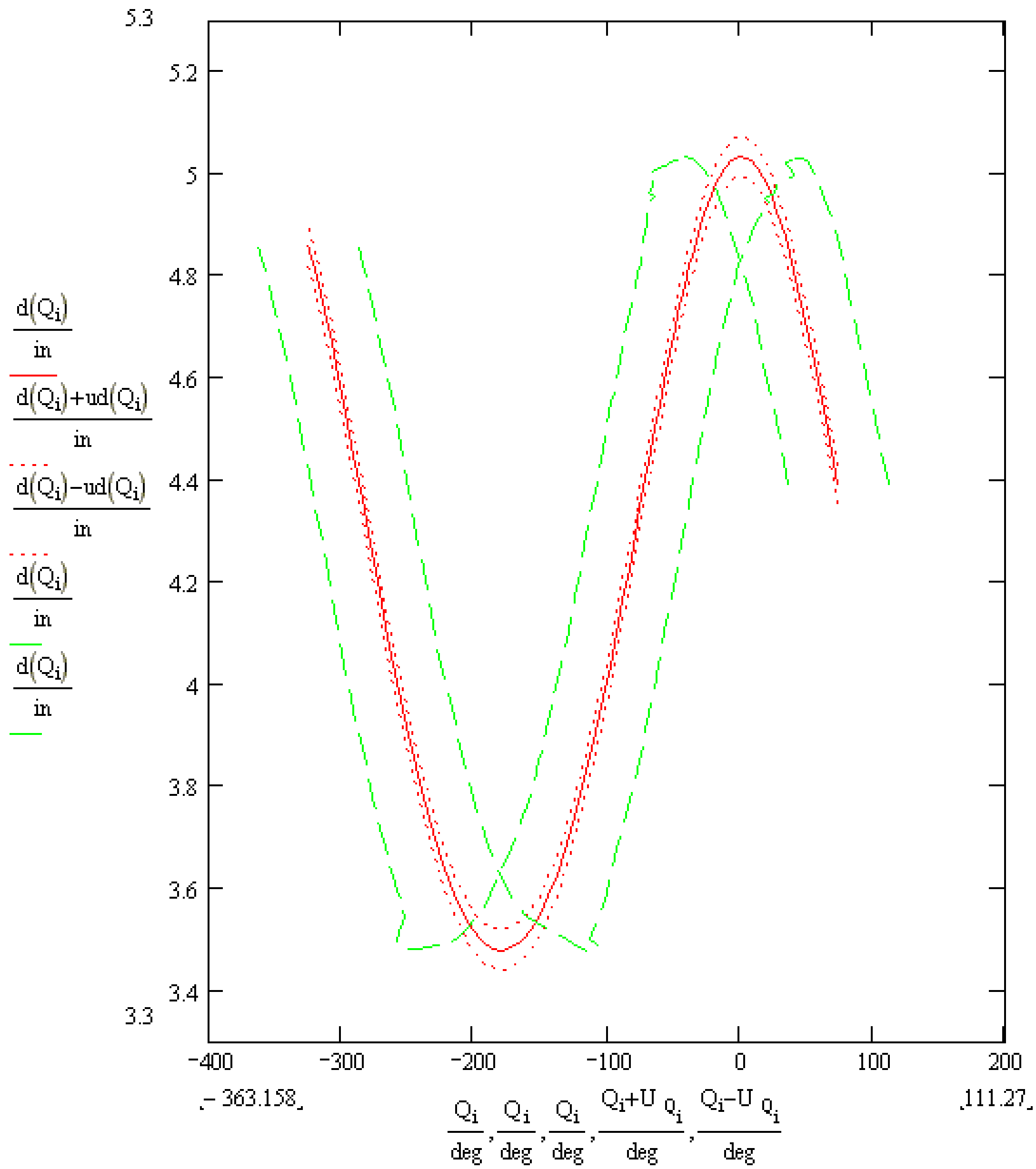

(f) Final Product 6

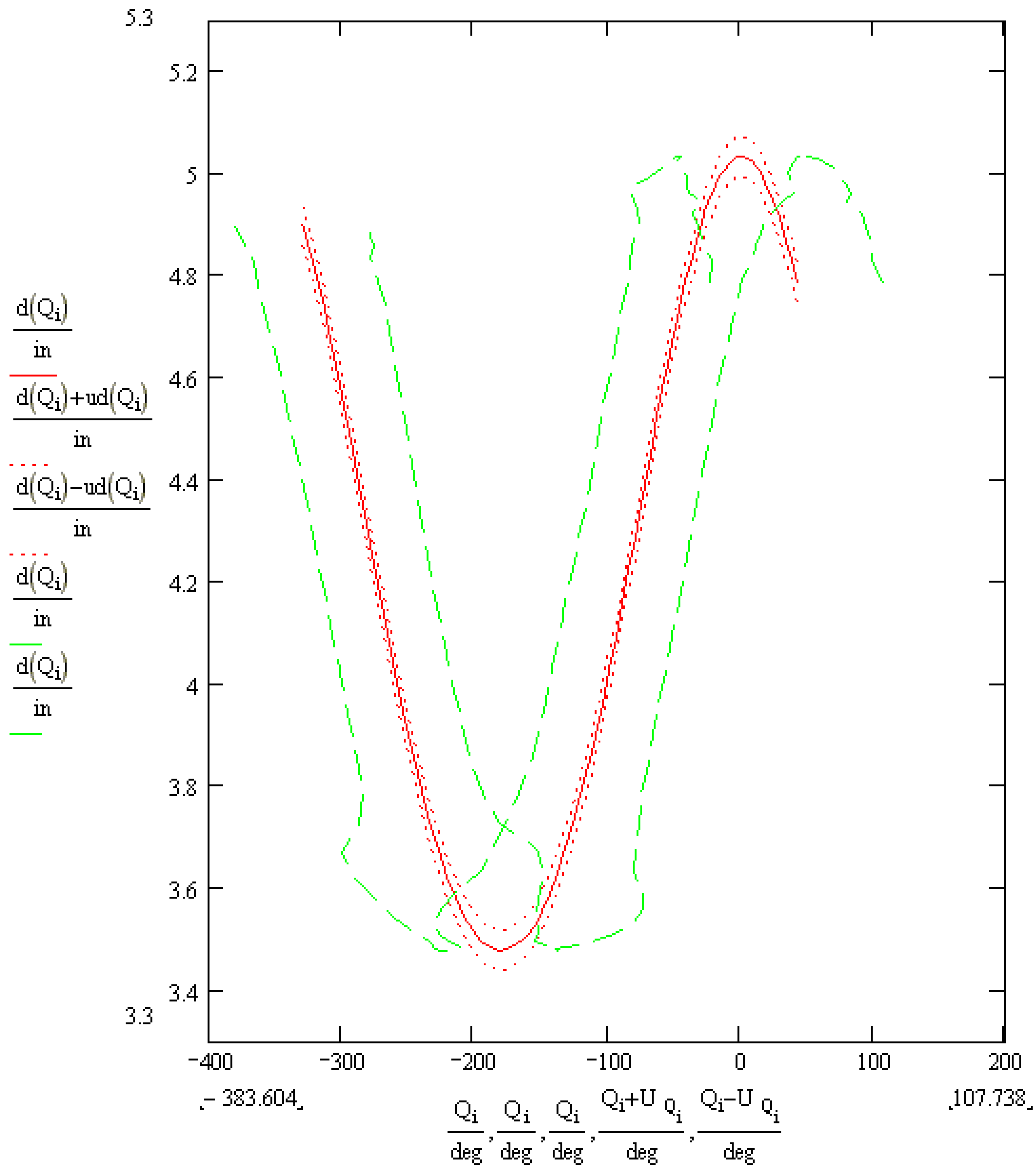

(g) Final Product 7

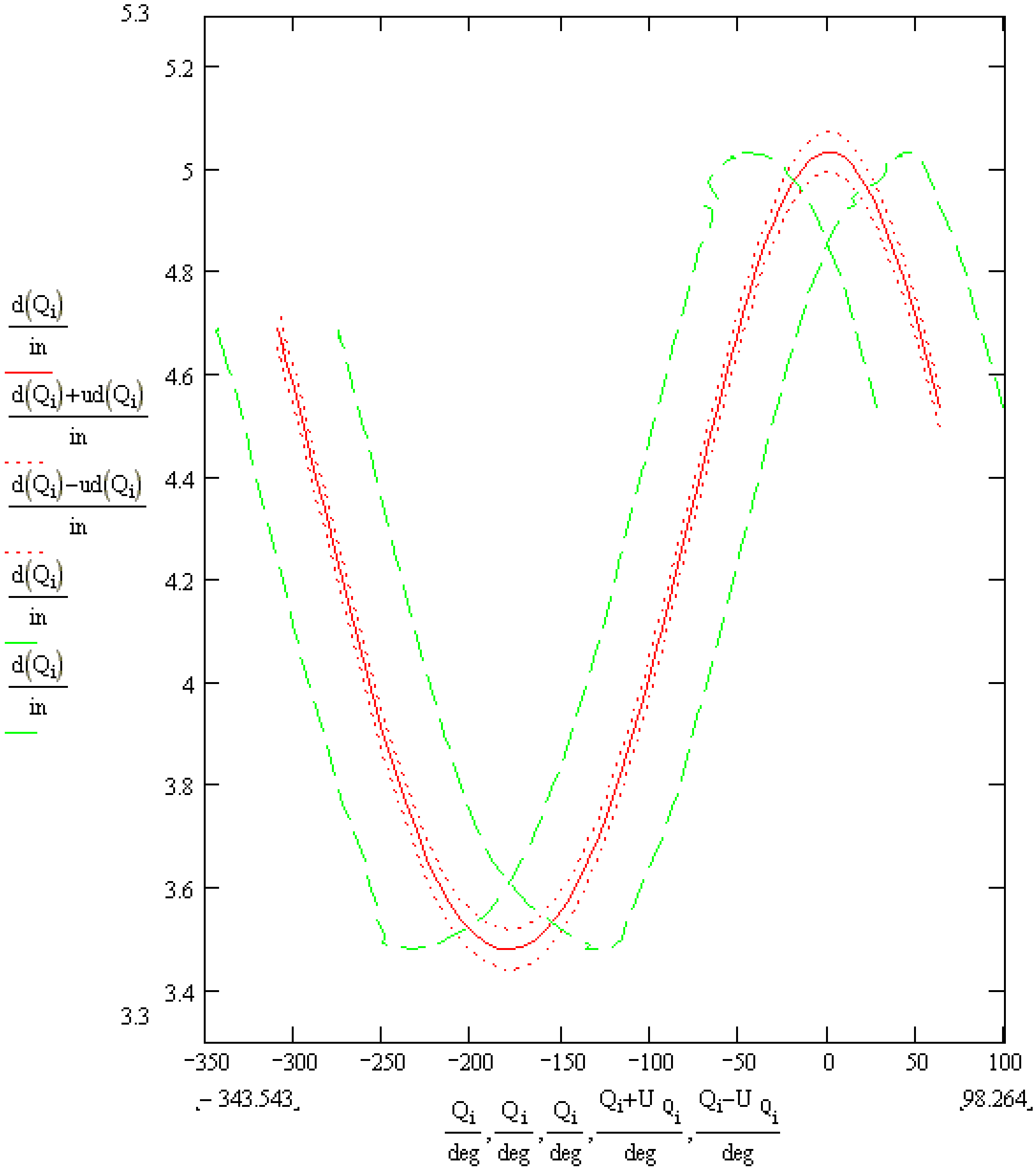

(h) Final Product 8

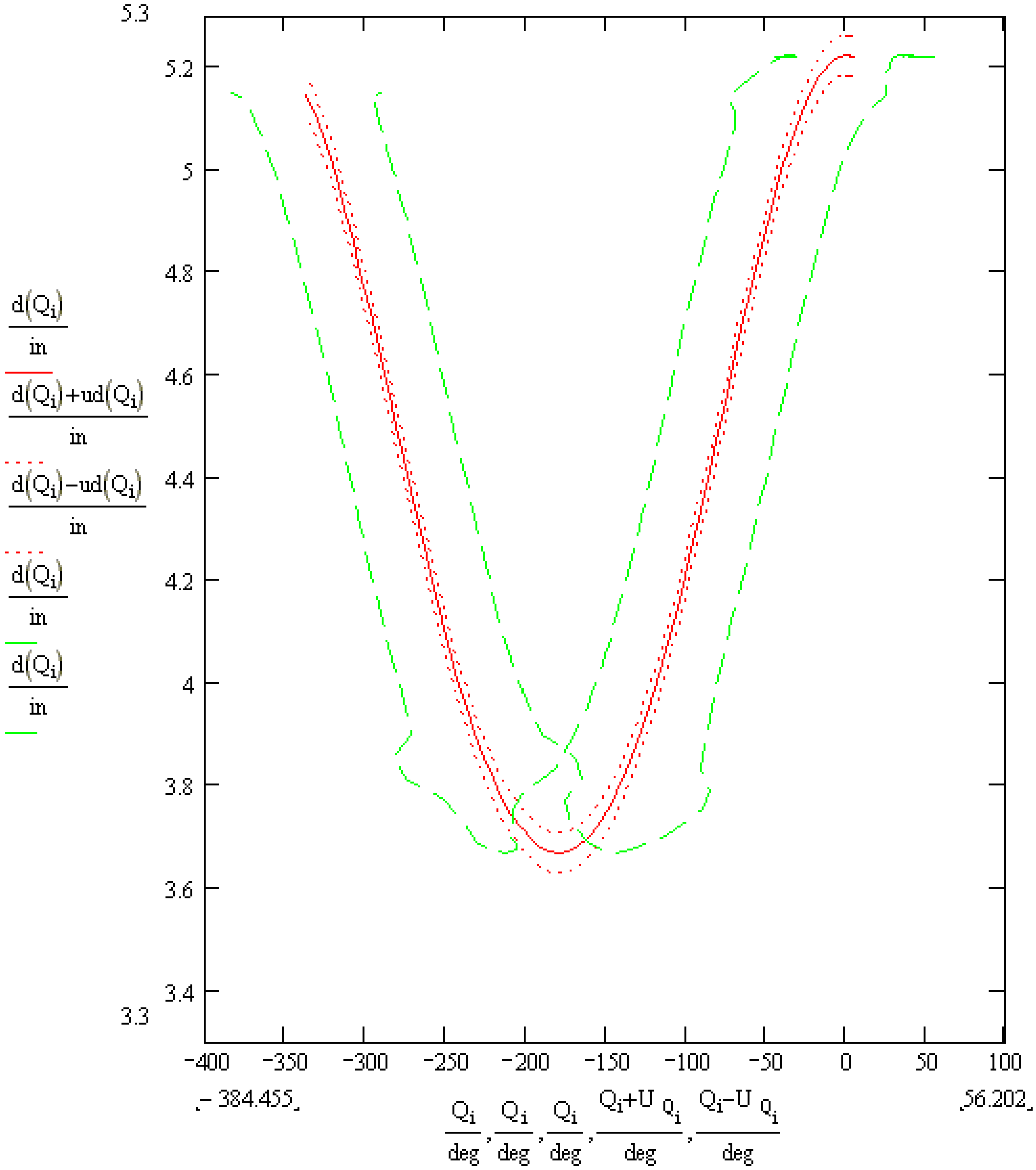

(i) Final Product 9

Figure 8.1 (a-i): Expected Results and Uncertainties of the Final Manufactured Product

CHAPTER IX

SUMMARY AND CONCLUSIONS

Summary

Research to examine uncertainty in the design process employs previous experience in experimental, model, and manufacturing uncertainty in an innovative approach for analyzing the entire design process. This research was initiated with a pilot project, a four-bar-slider mechanism. An in-house engine was used as the baseline design. From there, nine new connecting rods of various lengths and diameters were designed and manufactured. A kinematic model of the slider mechanism was developed to determine the piston displacement as a function of the crank angle. The connecting rods were used in an experiment to measure piston displacement. For the experiment, an air impact wrench was used to drive the crankshaft, a proximity sensor was used to find the initial angle, and a data acquisition system was used to take measurements regularly. The average engine speed was used to determine the crank angle for the model. The crank angle could not be measured with sufficient accuracy in order to compare the model and experimental results. It was proposed that design optimization techniques could be used to determine the instantaneous crank angle with better certainty to compare and validate the results and to predict the performance of the final manufactured connecting rod. To test this theory, the crank angle was determined using design optimization techniques to minimize the absolute error between the experiment and the model results. The crank angle determined from the design optimization process fell within the uncertainty bands from the original model uncertainty. In addition, the crank angle uncertainty was improved. Finally, the model, with a more exact estimate of the crank angle, was developed for the final manufactured product. Therefore, the first four objectives of this pilot project (Table 3.1), to complete the four stages of the design process and the uncertainty analyses, have been met. Also, the fifth objective, to determine the expected results and uncertainty of the final manufactured product has been met.

More research is required to determine a data reduction equation and the relative contribution of each design process stage (objectives 6 and 7). However, this pilot project has provided a direction for design process uncertainty research. In this analysis of the design process, an experimental quantity, the crank angle, was not measured with sufficient accuracy. The model was then used in an optimization process to determine this unknown quantity. The model function was used for the final manufactured product performance. The next step in this research would be to perform a two-variable optimization for both the slop and the crank angle where the experiment is already constructed to aid this comparison. Next, an uncertainty analysis could be performed to determine the relative importance of the model to the experiment. Unlike the optimization already explored, this would depend on the inaccuracies of both the model and the experiment. The uncertainty of the final manufactured product displacement would be a function of the model and the experimental uncertainty.

Conclusions

Several proposed hypothesis have resulted from this pilot project research. First, design optimization techniques could be employed to compare experimental and model uncertainty. Further, these techniques could be used to determine immeasurable experimental data or unknown model parameters. Also, the uncertainty in the final manufactured product can be determined using several trials of design optimization to determine the best estimate for unknown parameters. Next, the random uncertainties in distance measurements (e.g. lengths and diameters) could be replaced by the manufacturing uncertainty to determine the uncertainty of the final manufactured product. Finally, the manufacturing uncertainties could be included as additional random uncertainties in both the experiment and the model to determine the uncertainty in the final manufactured product. Further work is needed to more stringently test these hypotheses and advance research on uncertainty is design processes.

REFERENCES CITED

[1] Coleman, H. W. and Steele, W. G., *Experimentation and Uncertainty Analysis for Engineers*, Second Edition, John Wiley & Sons, Inc., New York, NY, 1999.

[2] Taylor, R. P., Luck, R., Hodge, B. K., and Steele, W. G., "Uncertainty Analysis of Diffuse-Gray Radiation Enclosure Problems," *Journal of Thermophysics and Heat Transfer*, Vol. 9, No. 1, Jan.-Mar. 1995, pp. 73-79.

[3] Taylor, R. P., Hodge, B. K., and Steele, W. G., "Series Piping System Design Program with Uncertainty Analysis," *Heating/Piping/Air Conditioning*, Vol. 75, No. 5, May 1993, pp. 87-93.

[4] Hudson, S.T., "Fastrac Engine ISP Uncertainty Analysis," NASA Marshall Space Flight Center report, MSFC memo TD73 99-017, October 29, 1999.

[5] Stern, F., Wilson, R.V., Coleman, H.W., and Paterson, E.G., "Verification and Validation of CFD Simulations," Iowa Institute of Hydraulic Research Report No. 407, September 1999.

[6] Griffin, L.W. and Huber, F.W., "Turbine Technology Team: An Overview of Current and Planned Activities relevant to the National Launch System," AIAA 92-3220.

[7] Huber, F.W., Johnson, P.D., Montesdeoca, X.A., Rowey, R.J., and Griffin, L.W., "Design of Advanced Turbopump Drive Turbines for National Launch Systems Application," AIAA 92-3221.

[8] Huber, F.W., Johnson, P.D., and Montesdeoca, X.A., "Baseline Design of the Gas Generator Oxidizer Turbine (GGOT) and Performance Predictions for the Associated Oxidizer Technology Turbine Rig (OTTR)," United Technologies Pratt & Whitney SZL:38875.doc to Scientific Research Associates, Inc., April 19, 1993.

[9] Griffin, L.W. and Huber, F.W., "Advancement of Turbine Aerodynamic Design Techniques," ASME 93-GT-370.

[10] de Jong, F.J., Chan, Y.T., and Gibeling, H.J., "Design of ETO Propulsion Turbine Using CFD Analysis—Final Report," Scientific Research Associates, Inc., Contract No. NAS8-38875, Document No. R95-9084-F, April 1995.

[11] Hudson, S.T., Johnson, P.D., and Branick, R.E., "Performance Testing of a Highly Loaded Single Stage Oxidizer Turbine with Inlet and Exit Volute Manifolds," AIAA 95-2405.

[12] Hudson, S.T., and Montesdeoca, X.A., "Aerodynamic Performance Test Results of Single Stage Oxidizer Turbine with Volute Manifolds," AIAA 97-3099.

[13] Taguchi, G., *Introduction to Quality Engineering*, Quality Resources, White Plains, NJ,1987.

[14] Taguchi, G., *System of Experimental Design: Engineering Methods to Optimize Quality and Minimize Cost*, Quality Resources, White Plains, NJ, 1987.

[15] Taguchi, G., *Introduction to Off-line Quality Control*, Central Japan Quality Control Association, 1985.

[16] Liaw, Leslie D., "Reliability-Based Optimization for Rodust Design," *International Journal of Vehicle Design,* v25, 1-2, 2001.

[17] Du, Xiaoping, Wang, Yijun, and Chen, Wei, "Methods for Robust Multildisciplinary Design," Structural Cynamics and Materials Conference, v1, III, 2000.

[18] Fenstermaker, Stephen, George, David, Kahng, Andrew B., Mantik, Stefanus, and Thielges, Bart, "Metrics: A Design Architecture for Design Optimization," *Design Automation Conference, 2000, DAC 2000, 37th Design Automation Conference*, June 5- Jun 9 2000, Los Angleles, CA.

[19] Ventresca, Carol, "Continuous Process Improvement Through Design Experiments and Multi-Attribute Desirability Optimization," *ISA Transactions*, v 32, n 1, May 1993.

[20] Bayazitoglu, Y., Peterson, J., "Optimization of Cost Subject to Uncertainty Constraints in Experiment Fluid Flow and Heat Transfer," ASME Journal of Heat Transfer, vol. 113, 1991.

[21] Shigley, Joseph Edward, Vicker, John J., Theory of Machines and Mechanisms, Second Edition, McGraw-Hill Inc., New York, NY, 1994.

APPENDIX A

MATHCAD WORKSHEETS

Model

Model Definition

Establish origin in MathCad: ORIGIN ≡ 1

The measured variables and associated uncertainties were determined using a sample of 10 measurements.

$$ml_{cs} := \begin{pmatrix} .777 \\ .778 \\ .777 \\ .776 \\ .777 \\ .778 \\ .778 \\ .776 \\ .779 \\ .777 \end{pmatrix} \cdot in \quad ml_1 := \begin{pmatrix} 2.504 \\ 2.502 \\ 2.5 \\ 2.501 \\ 2.499 \\ 2.498 \\ 2.505 \\ 2.503 \\ 2.502 \\ 2.501 \end{pmatrix} \cdot in \quad ml_2 := \begin{pmatrix} 3.993 \\ 3.999 \\ 4.003 \\ 4.006 \\ 4.003 \\ 4.003 \\ 4.002 \\ 3.999 \\ 4.002 \\ 3.999 \end{pmatrix} \cdot in \quad md_{cs} := \begin{pmatrix} .746 \\ .745 \\ .749 \\ .748 \\ .745 \\ .747 \\ .746 \\ .744 \\ .742 \\ .746 \end{pmatrix} \cdot in \quad md_{cr} := \begin{pmatrix} .743 \\ .752 \\ .754 \\ .757 \\ .759 \\ .758 \\ .751 \\ .752 \\ .758 \\ .752 \end{pmatrix} \cdot in \quad ml_p := \begin{pmatrix} 1.101 \\ 1.099 \\ 1.102 \\ 1.100 \\ 1.102 \\ 1.101 \\ 1.099 \\ 1.100 \\ 1.101 \\ 1.101 \end{pmatrix} \cdot in$$

Establish counters in MathCad: $N := 10$ $\quad j := 1..N$

The mean value will be used for each set of 10 measurements:

The large sample assumption, if N≥ 10: $t := 2$

$$l_{cs} := \frac{\sum_j ml_{cs_j}}{N} \quad l_1 := \frac{\sum_j ml_{1_j}}{N} \quad l_2 := \frac{\sum_j ml_{2_j}}{N} \quad d_{cs} := \frac{\sum_j md_{cs_j}}{N} \quad d_{cr} := \frac{\sum_j md_{cr_j}}{N} \quad l_p := \frac{\sum_j ml_{p_j}}{N}$$

$$l_{cs} = 0.777in \quad l_1 = 2.502in \quad l_2 = 4.001in \quad d_{cs} = 0.746in \quad d_{cr} = 0.754in \quad l_p = 1.101in$$

Assume perfect fit therefore slop is negligible: $s_x := 0 \cdot in$

The model equation:

$$d(\theta) := l_{cs} \cdot \cos(\theta) + \sqrt{\left(\frac{l_1 + l_2}{2}\right)^2 - l_{cs}^2 \cdot (\sin(\theta))^2} + l_p + s_x$$

Model Uncertainty

Partial derivatives of piston displacement with respect to each variable:

$$pl_{cs}(\theta) := \cos(\theta) + \frac{-l_{cs} \cdot (\sin(\theta))^2}{\sqrt{\left(\frac{l_1 + l_2}{2}\right)^2 - l_{cs}^2 \cdot (\sin(\theta))^2}} \qquad pl_{cs}(180 \cdot deg) = -1$$

$$pl_1(\theta) := \frac{1}{2}\cdot\frac{\frac{l_1+l_2}{2}}{\sqrt{\left(\frac{l_1+l_2}{2}\right)^2 - l_{cs}{}^2\cdot(\sin(\theta))^2}}$$ $pl_1(180\cdot\deg) = 0.5$

$$pl_2(\theta) := \frac{1}{2}\cdot\frac{\frac{l_1+l_2}{2}}{\sqrt{\left(\frac{l_1+l_2}{2}\right)^2 - l_{cs}{}^2\cdot(\sin(\theta))^2}}$$ $pl_2(180\cdot\deg) = 0.5$

$pl_p := 1$ $pl_p = 1$

$ps_x := 1$ $ps_x = 1$

The standard deviations from the ten measurements

$$Sl_{cs} := \left[\frac{1}{N-1}\cdot\sum_j \left(ml_{cs_j} - l_{cs}\right)^2\right]^{\frac{1}{2}}$$ $Sl_{cs} = 9.487\times 10^{-4}\,in$

$$Sl_1 := \left[\frac{1}{N-1}\cdot\sum_j \left(ml_{1_j} - l_1\right)^2\right]^{\frac{1}{2}}$$ $Sl_1 = 2.173\times 10^{-3}\,in$

$$Sl_2 := \left[\frac{1}{N-1}\cdot\sum_j \left(ml_{2_j} - l_2\right)^2\right]^{\frac{1}{2}}$$ $Sl_2 = 3.573\times 10^{-3}\,in$

$$Sl_p := \left[\frac{1}{N-1}\cdot\sum_j \left(ml_{p_j} - l_p\right)^2\right]^{\frac{1}{2}}$$ $Sl_p = 1.075\times 10^{-3}\,in$

$$Sd_{cr} := \left[\frac{1}{N-1}\cdot\sum_j \left(md_{cr_j} - d_{cr}\right)^2\right]^{\frac{1}{2}}$$ $Sd_{cr} = 4.789\times 10^{-3}\,in$

$$Sd_{cs} := \left[\frac{1}{N-1}\cdot\sum_j \left(md_{cs_j} - d_{cs}\right)^2\right]^{\frac{1}{2}}$$ $Sd_{cs} = 1.989\times 10^{-3}\,in$

The random uncertainty values based on the standard deviations:

$$rl_{cs} := \frac{t \cdot Sl_{cs}}{\sqrt{N}} \qquad rl_1 := \frac{t \cdot Sl_1}{\sqrt{N}} \qquad rl_p := \frac{t \cdot Sl_p}{\sqrt{N}} \qquad rl_2 := \frac{t \cdot Sl_2}{\sqrt{N}} \qquad rd_{cs} := \frac{t \cdot Sd_{cs}}{\sqrt{N}} \qquad rd_{cr} := \frac{t \cdot Sd_{cr}}{\sqrt{N}}$$

A micrometer was used to determine these measurements: $LC := .001 \cdot in$

The systematic uncertainty in these measurements:

$$sl_{cs1} := \frac{1}{2} \cdot LC \qquad sl_{p1} := \frac{1}{2} \cdot LC \qquad sl_1 := \frac{1}{2} \cdot LC \qquad sl_2 := \frac{1}{2} \cdot LC \qquad sd_{cs1} := \frac{1}{2} \cdot LC \qquad sd_{cr} := \frac{1}{2} \cdot LC$$

The second elemental source was the baseline design:

$$sl_{cs2} := rl_{cs} \qquad sd_{cs2} := rd_{cs} \qquad sl_{p2} := rl_p$$

The combined systematic uncertainty for the pre-designed pieces:

$$sd_{cs} := \sqrt{sd_{cs1}^2 + sd_{cs2}^2} \qquad sl_{cs} := \sqrt{sl_{cs1}^2 + sl_{cs2}^2} \qquad sl_p := \sqrt{sl_{p1}^2 + sl_{p2}^2}$$

The total uncertainty for the diameters:

$$ud_{cs} := \sqrt{sd_{cs}^2 + rd_{cs}^2} \qquad ud_{cr} := \sqrt{sd_{cr}^2 + rd_{cr}^2}$$

Slop uncertainty equations:

$$rs_x := \frac{d_{cr} - d_{cs}}{2} \qquad ss_x := \sqrt{\frac{1}{4} \cdot ud_{cr}^2 + \frac{1}{4} \cdot ud_{cs}^2}$$

The model uncertainty obtained from the experimental uncertainty equation

$$rd(\theta) := \left(pl_{cs}(\theta)^2 \cdot rl_{cs}^2 + pl_1(\theta)^2 \cdot rl_1^2 + pl_2(\theta)^2 \cdot rl_2^2 + pl_p^2 \cdot rl_p^2 + ps_x^2 \cdot rs_x^2\right)^{\frac{1}{2}}$$

$$sd(\theta) := \left(pl_{cs}(\theta)^2 \cdot sl_{cs}^2 + pl_1(\theta)^2 \cdot sl_1^2 + pl_2(\theta)^2 \cdot sl_2^2 + pl_p^2 \cdot sl_p^2 + ps_x^2 \cdot ss_x^2\right)^{\frac{1}{2}}$$

Finally, the combined uncertainty: $ud(\theta) := \sqrt{rd(\theta)^2 + sd(\theta)^2}$

The model equation:

$$d(\theta) := l_{cs} \cdot \cos(\theta) + \sqrt{\left(\frac{l_1 + l_2}{2}\right)^2 - l_{cs}^2 \cdot (\sin(\theta))^2} + l_p + s_x$$

Prepare for comparisons:

$$dm(\theta) := d(\theta) \qquad U_{dm}(\theta) := ud(\theta) \qquad S_{dm}(\theta) := sd(\theta) \qquad R_{dm}(\theta) := rd(\theta)$$

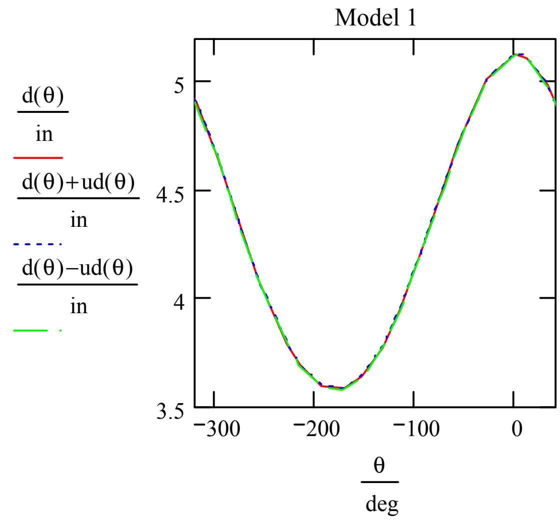

Figure A.1: Model Results and Uncertainty

MANUFACTURE

Manufacture Description

The uncertainty calculation including manufacturing tolerances

Specified Values for Manufacture: $l_{cr} := 3.25 \cdot in$ $d_p := .49 \cdot in$ $d_{cr} := .8 \cdot in$

Tolerances specified for new connecting rod: $tl_{cr} := .01 \cdot in$ $td_p := .005 \cdot in$

Exaggerated uncertainty in the diameter: $td_{cr} := .05 \cdot in$ $sd_{cr} := td_{cr}$

Data reduction equations for manufacture:

$$l1 := l_{cr} - \frac{d_{cr} + d_p}{2} \qquad l2 := l_{cr} + \frac{d_{cr} + d_p}{2}$$

Manufacturing Uncertainty

The uncertainty based on manufacturing tolerances:

$$sl_1 := \sqrt{tl_{cr}^{\ 2} + \left(\frac{1}{4}\right) \cdot td_{cr}^{\ 2} + \left(\frac{1}{4}\right) \cdot td_p^{\ 2}} \qquad sl_2 := \sqrt{tl_{cr}^{\ 2} + \left(-\frac{1}{4}\right) \cdot td_{cr}^{\ 2} + \left(-\frac{1}{4}\right) \cdot td_p^{\ 2}}$$

Other links will be manufactured also for final manufactured product:

$tl_{cs} := .01 \cdot in$ $tl_p := .005 \cdot in$ $td_{cs} := .005 \cdot in$ $sl_{cs} := tl_{cs}$ $sl_p := tl_p$ $sd_{cs} := td_{cs}$

EXPERIMENT

Experiment Definition

Linear Transducer Calibration

Establish the origin in Mathcad: ORIGIN≡ 1

Measured Variables:

The data table was input here.

$$V1 := DATA^{\langle 1\rangle} \quad V2 := DATA^{\langle 2\rangle} \quad V3 := DATA^{\langle 3\rangle}$$

$$V4 := DATA^{\langle 4\rangle} \quad V5 := DATA^{\langle 5\rangle}$$

Establish counters in Mathcad: $N := rows(V1)$

Mean Values:

$$V_1 := \frac{\sum_{j=1}^{N} V1_j}{N} \quad V_2 := \frac{\sum_{j=1}^{N} V2_j}{N} \quad V_3 := \frac{\sum_{j=1}^{N} V3_j}{N} \quad V_4 := \frac{\sum_{j=1}^{N} V4_j}{N} \quad V_5 := \frac{\sum_{j=1}^{N} V5_j}{N}$$

$$V_1 = 6.467 \quad V_2 = 5.916 \quad V_3 = 5.243 \quad V_4 = 4.364 \quad V_5 = 3.402$$

Standard Deviations:

$$SV_1 := \sqrt{\sum_{j=1}^{N} \frac{(V_1 - V1_j)^2}{N-1}} \quad SV_2 := \sqrt{\sum_{j=1}^{N} \frac{(V_2 - V2_j)^2}{N-1}}$$

$$SV_1 = 0.034 \quad SV_2 = 0.04$$

$$SV_3 := \sqrt{\sum_{j=1}^{N} \frac{(V_3 - V3_j)^2}{N-1}} \quad SV_4 := \sqrt{\sum_{j=1}^{N} \frac{(V_4 - V4_j)^2}{N-1}} \quad SV_5 := \sqrt{\sum_{j=1}^{N} \frac{(V_5 - V5_j)^2}{N-1}}$$

$$SV_3 = 0.138 \quad SV_4 = 0.187 \quad SV_5 = 0.026$$

Reestablish counters in MathCad: $N := 5 \quad j := 1..5$

Measured variables from calibration:

$$V := \begin{pmatrix} V_5 \\ V_4 \\ V_3 \\ V_2 \\ V_1 \end{pmatrix} \qquad d := \begin{pmatrix} 1.25 \\ 1 \\ .75 \\ .5 \\ .25 \end{pmatrix} \cdot in$$

Linear regression constants for calibration:

$$C_1 := \frac{N \cdot \sum_{j=1}^{N} (V_j \cdot d_j) - \left(\sum_{j=1}^{N} V_j\right) \cdot \left(\sum_{j=1}^{N} d_j\right)}{N \cdot \sum_{j=1}^{N} (V_j)^2 - \left(\sum_{j=1}^{N} V_j\right)^2} \quad C_2 := \frac{\left[\sum_{j=1}^{N} (V_j)^2\right] \cdot \left(\sum_{j=1}^{N} d_j\right) - \left(\sum_{j=1}^{N} V_j\right) \cdot \left(\sum_{j=1}^{N} V_j \cdot d_j\right)}{N \cdot \sum_{j=1}^{N} (V_j)^2 - \left(\sum_{j=1}^{N} V_j\right)^2}$$

Proximity Sensor Calibration

The 10 measurements used to find TDC.

$$m\theta_1 := \begin{pmatrix} 100 \\ 98.5 \\ 99 \\ 99 \\ 99 \\ 98.5 \\ 98 \\ 98.5 \\ 98.5 \\ 99 \end{pmatrix} \cdot deg \qquad m\delta\theta_1 := \begin{pmatrix} 103.5 \\ 103 \\ 103.5 \\ 104 \\ 104 \\ 103.5 \\ 104 \\ 103.5 \\ 103.5 \\ 104 \end{pmatrix} \cdot deg \qquad m\theta_2 := \begin{pmatrix} 99 \\ 99.5 \\ 100 \\ 99.5 \\ 100 \\ 99.5 \\ 100 \\ 99.5 \\ 99.5 \\ 100 \end{pmatrix} \cdot deg \qquad m\delta\theta_2 := \begin{pmatrix} 94.5 \\ 94 \\ 94.5 \\ 95 \\ 94.5 \\ 94.5 \\ 94 \\ 94 \\ 93 \\ 94.5 \end{pmatrix} \cdot deg$$

Reestablish counters in Mathcad: $N := \mathrm{rows}(m\theta_1)$ $\qquad j := 1..N$

Calculating the mean values:

$$\theta_1 := \frac{\sum_{j=1}^{N} m\theta_{1_j}}{N} \qquad \delta\theta_1 := \frac{\sum_{j=1}^{N} m\delta\theta_{1_j}}{N} \qquad \theta_2 := \frac{\sum_{j=1}^{N} m\theta_{2_j}}{N} \qquad \delta\theta_2 := \frac{\sum_{j=1}^{N} m\delta\theta_{2_j}}{N}$$

$\theta_1 = 98.8deg$ $\qquad \delta\theta_1 = 103.65deg$ $\qquad \theta_2 = 99.65deg$ $\qquad \delta\theta_2 = 94.25deg$

Calculating the standard deviations:

$$S\theta_1 := \sqrt{\frac{\sum_j \left(m\theta_{1_j} - \theta_1\right)^2}{N-1}} \qquad S\delta\theta_1 := \sqrt{\frac{\sum_j \left(m\delta\theta_{1_j} - \delta\theta_1\right)^2}{N-1}} \qquad S\theta_2 := \sqrt{\frac{\sum_j \left(m\theta_{2_j} - \theta_2\right)^2}{N-1}} \qquad S\delta\theta_2 := \sqrt{\frac{\sum_j \left(m\delta\theta_{2_j} - \delta\theta_2\right)^2}{N-1}}$$

$S\theta_1 = 0.537deg$ $\qquad S\delta\theta_1 = 0.337deg$ $\qquad S\theta_2 = 0.337deg$ $\qquad S\delta\theta_2 = 0.54deg$

Equation for θ_{TDC}:

$$\theta_{TDC} := \frac{\left(\theta_1 + \frac{\delta\theta_1}{2}\right) + \left(\theta_2 - \frac{\delta\theta_2}{2}\right)}{2} \qquad \theta_{TDC} = 101.575deg$$

$$m_{\theta 1} := \begin{pmatrix} 149 \\ 148.5 \\ 149 \\ 148.5 \\ 149 \\ 149 \\ 148.5 \\ 149 \\ 149 \\ 149 \end{pmatrix} \cdot deg \qquad \theta 1 := \frac{\sum_{j=1}^{N} m_{\theta 1_j}}{N} \qquad S_{\theta 1} := \left[\frac{1}{N-1} \cdot \sum_j \left(m_{\theta 1_j} - \theta 1\right)^2\right]^{\frac{1}{2}}$$

$\theta 1 = 148.85deg$ $\qquad S_{\theta 1} = 0.242deg$

The data reduction equation for the reference angle:

$$\theta_0 := \theta 1 - \left[\frac{\left(\theta_1 + \frac{\delta\theta_1}{2}\right) + \left(\theta_2 - \frac{\delta\theta_2}{2}\right)}{2}\right] \qquad \theta_0 = 47.275\mathrm{deg}$$

The Experimental Data:

The data tables were input into MathCad Here.

$t_1 := DATA^{\langle 1\rangle}\cdot s \qquad Vo_1 := DATA^{\langle 3\rangle} \qquad d_1 := \left(C_1 \cdot Vo_1 + C_2\right)$

$t_2 := DATA^{\langle 1\rangle}\cdot s \qquad Vo_2 := DATA^{\langle 3\rangle} \qquad d_2 := \left(C_1 \cdot Vo_2 + C_2\right)$

$t_3 := DATA^{\langle 1\rangle}\cdot s \qquad Vo_3 := DATA^{\langle 3\rangle} \qquad d_3 := \left(C_1 \cdot Vo_3 + C_2\right)$

$t_4 := DATA^{\langle 1\rangle}\cdot s \qquad Vo_4 := DATA^{\langle 3\rangle} \qquad d_4 := \left(C_1 \cdot Vo_4 + C_2\right)$

$t_5 := DATA^{\langle 1\rangle}\cdot s \qquad Vo_5 := DATA^{\langle 3\rangle} \qquad d_5 := \left(C_1 \cdot Vo_5 + C_2\right)$

$t_6 := DATA^{\langle 1\rangle}\cdot s \qquad Vo_6 := DATA^{\langle 3\rangle} \qquad d_6 := \left(C_1 \cdot Vo_6 + C_2\right)$

$t_7 := DATA^{\langle 1\rangle}\cdot s \qquad Vo_7 := DATA^{\langle 3\rangle} \qquad d_7 := \left(C_1 \cdot Vo_7 + C_2\right)$

$t_8 := DATA^{\langle 1\rangle}\cdot s \qquad Vo_8 := DATA^{\langle 3\rangle} \qquad d_8 := \left(C_1 \cdot Vo_8 + C_2\right)$

Establish experimental counters in MathCad: $P := \mathrm{rows}\left(d_1\right) \qquad i := 1..P$

Experimental Uncertainty

Linear Transducer Uncertainty:

200 measurements to determine calibration voltage uncertainty: $N := 20($

$RV_1 := \frac{(t \cdot SV_1)}{\sqrt{N}}$ $RV_2 := \frac{(t \cdot SV_2)}{\sqrt{N}}$ $RV_3 := \frac{(t \cdot SV_3)}{\sqrt{N}}$ $RV_4 := \frac{(t \cdot SV_4)}{\sqrt{N}}$ $RV_5 := \frac{(t \cdot SV_5)}{\sqrt{N}}$

$RV_1 = 4.763 \times 10^{-3}$ $RV_2 = 5.682 \times 10^{-3}$ $RV_3 = 0.02$ $RV_4 = 0.026$ $RV_5 = 3.67 \times 10^{-3}$

These uncertainty values are for the calibration voltages. They include the random uncertainty in the set displacements:

$$RV := \begin{pmatrix} RV_1 \\ RV_2 \\ RV_3 \\ RV_4 \\ RV_5 \end{pmatrix}$$

From Calibration Data: $SV := .001$ $R_V := t \cdot SV$

The random uncertainty in displacement was included in the random voltage through the procedure: $R_d := 0 \cdot in$

Calculating the systematic uncertainty in the micrometer used for calibratio

$LC := .001 \cdot in$ $S_d := \frac{1}{2} \cdot LC$

Assume zero systematic uncertainty in linear transducer: $S_V := 0$

Measured variables from calibration:

$$V := \begin{pmatrix} V_5 \\ V_4 \\ V_3 \\ V_2 \\ V_1 \end{pmatrix} \qquad d := \begin{pmatrix} 1.25 \\ 1 \\ .75 \\ .5 \\ .25 \end{pmatrix} \cdot in$$

Reestablish counters in MathCad: $N := 5$ $j := 1..5$

The partial derivatives of constants with respect to Xi:

$$dmx_j := \frac{\left(N \cdot d_j - \sum_{j=1}^{N} d_j\right) \cdot \left[N \cdot \sum_{j=1}^{N} (V_j)^2 - \left(\sum_{j=1}^{N} V_j\right)^2\right] \ldots \\ + \left[N \cdot \sum_{j=1}^{N} (V_j \cdot d_j) - \left(\sum_{j=1}^{N} V_j\right) \cdot \left(\sum_{j=1}^{N} d_j\right)\right] \cdot \left(2 \cdot \sum_{j=1}^{N} V_j - 2 \cdot N \cdot V_j\right)}{\left[N \cdot \sum_{j=1}^{N} (V_j)^2 - \left(\sum_{j=1}^{N} V_j\right)^2\right]^2}$$

$$dcx_j := \frac{\left[N \cdot \sum_{j=1}^{N} (V_j)^2 - \left(\sum_{j=1}^{N} V_j\right)^2\right] \cdot \left[\left(2 \cdot \sum_{j=1}^{N} d_j\right) \cdot V_j - \left(\sum_{j=1}^{N} V_j \cdot d_j\right) - \left(\sum_{j=1}^{N} V_j\right) \cdot d_j\right] \ldots \\ + \left[\left[\sum_{j=1}^{N} (V_j)^2\right] \cdot \left(\sum_{j=1}^{N} d_j\right) - \left(\sum_{j=1}^{N} V_j\right) \cdot \left(\sum_{j=1}^{N} d_j\right)\right] \cdot \left(2 \cdot \sum_{j=1}^{N} V_j - 2 \cdot N \cdot V_j\right)}{\left[N \cdot \sum_{j=1}^{N} (V_j)^2 - \left(\sum_{j=1}^{N} V_j\right)^2\right]^2}$$

The partial derivatives of the constants with respect to Yi:

$$dmy_j := \frac{N \cdot V_j - \sum_{j=1}^{N} V_j}{N \cdot \sum_{j=1}^{N} (V_j)^2 - \left(\sum_{j=1}^{N} V_j\right)^2} \qquad dcy_j := \frac{\sum_{j=1}^{N} V_j - V_j \cdot \sum_{j=1}^{N} V_j}{N \cdot \sum_{j=1}^{N} (V_j)^2 - \left(\sum_{j=1}^{N} V_j\right)^2}$$

Partial derivatives of the regression equation with respect to each variabl

$$dyx(x) := dmx_j \cdot x + dcx_j \qquad dyy(x) := dmy_j \cdot x + dcy_j \qquad dyxn := m$$

Uncertainty in d from the regression:

$$R_d(x) := \sqrt{\sum_{j=1}^{N} \left(dmy_j \cdot x + dcy_j\right)^2 \cdot R_d^{\,2} + \sum_{j=1}^{N} \left(dmx_j \cdot x + dcx_j\right)^2 \cdot \left(RV_j\right)^2 + dyxn^2 \cdot \left(R_V\right)^2}$$

$$S_d(x) := \sqrt{\sum_{j=1}^{N} \left(dmy_j \cdot x + dcy_j\right)^2 \cdot S_d^{\,2} + \sum_{j=1}^{N} \left(dmx_j \cdot x + dcx_j\right)^2 \cdot \left(S_V\right)^2 + dyxn^2 \cdot \left(S_V\right)^2}$$

$$U_{dn}(x) := \sqrt{R_d(x)^2 + S_d(x)^2}$$

The regression uncertainty is the total experimental uncertainty:

$$U_{de_i} := U_{dn}\left(Vo1_i\right) \qquad S_{de_i} := S_d\left(Vo1_i\right) \qquad R_{de_i} := R_d\left(Vo1_i\right)$$

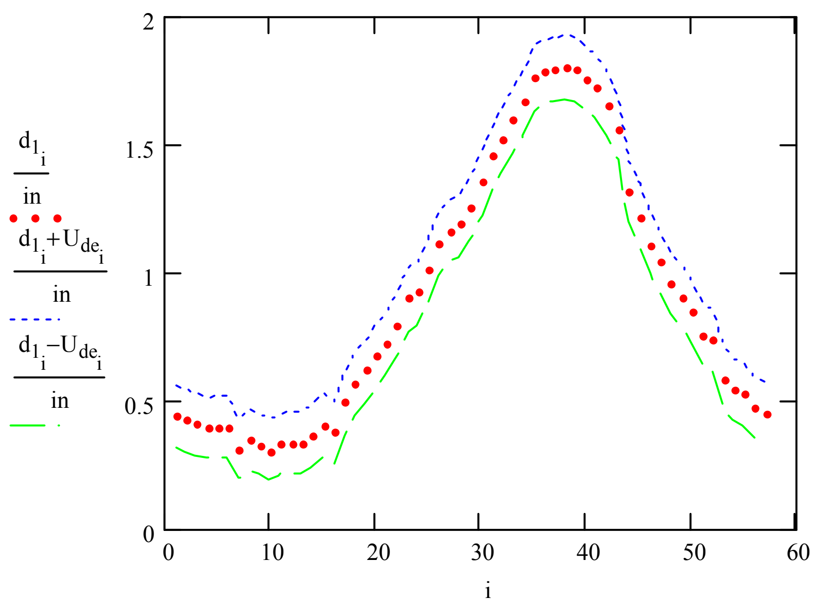

Figure A.2: Experimental Results and Uncertainty

Proximity Sensor Uncertainty

Reestablish counters in Mathcad: $N := \mathrm{rows}(m\theta_1)$ $j := 1..N$

Calculating the random uncertainties in the 10 measurements:

$P_{\theta 1} := t \cdot \frac{S\theta_1}{\sqrt{N}}$ $P_{\delta\theta 1} := t \cdot \frac{S\delta\theta_1}{\sqrt{N}}$ $P_{\theta 2} := t \cdot \frac{S\theta_2}{\sqrt{N}}$ $P_{\delta\theta 2} := t \cdot \frac{S\delta\theta_2}{\sqrt{N}}$

$P_{\theta 1} = 0.34\mathrm{deg}$ $P_{\delta\theta 1} = 0.213\mathrm{deg}$ $P_{\theta 2} = 0.213\mathrm{deg}$ $P_{\delta\theta 2} = 0.342\mathrm{deg}$

Estimate uncertainty in θ based on the degree wheel capabilities: $S_{\theta 1} := 1 \cdot \mathrm{deg}$

The random uncertainty in θ on: $P_{\theta 1} := 2 \cdot \frac{S\theta_1}{\sqrt{N}}$ $P_{\theta 1} = 0.34\mathrm{deg}$

The data reduction equation for the reference angle:

$$\theta_0 := \theta 1 - \left[\frac{\left(\theta_1 + \frac{\delta\theta_1}{2}\right) + \left(\theta_2 - \frac{\delta\theta_2}{2}\right)}{2}\right] \qquad \theta_0 = 47.275\mathrm{deg}$$

Calculating the random uncertainties in the 10 measurements:

$P_{\theta 1} := t \cdot \frac{S\theta_1}{\sqrt{N}}$ $P_{\delta\theta 1} := t \cdot \frac{S\delta\theta_1}{\sqrt{N}}$ $P_{\theta 2} := t \cdot \frac{S\theta_2}{\sqrt{N}}$ $P_{\delta\theta 2} := t \cdot \frac{S\delta\theta_2}{\sqrt{N}}$

$P_{\theta 1} = 0.34\mathrm{deg}$ $P_{\delta\theta 1} = 0.213\mathrm{deg}$ $P_{\theta 2} = 0.213\mathrm{deg}$ $P_{\delta\theta 2} = 0.342\mathrm{deg}$

Partial Derivatives of θ_0 with respect to each independent variable:

$p\theta_1 := -\frac{1}{2}$ $p\delta\theta_1 := -\frac{1}{4}$ $p\theta_2 := -\frac{1}{2}$ $p\delta\theta_2 := \frac{1}{4}$ $p_{\theta 1} := 1$

Using general uncertianty analysis, the uncertainty in the reference angle:

$$R_{\theta 0} := \sqrt{(p_{\theta 1} \cdot P_{\theta 1})^2 + (p\theta_1 \cdot P_{\theta 1})^2 + (p\delta\theta_1 \cdot P_{\delta\theta 1})^2 + (p\theta_2 \cdot P_{\theta 2})^2 + (p\delta\theta_2 \cdot P_{\delta\theta 2})^2} \qquad R_{\theta 0} = 0.407\mathrm{deg}$$

$$S_{\theta 0} := \sqrt{\begin{array}{l} S_{\theta 1}{}^2 + (p\theta_1 \cdot S_{\theta 1})^2 + (p\delta\theta_1 \cdot S_{\theta 1})^2 + (p\theta_2 \cdot S_{\theta 1})^2 + (p\delta\theta_2 \cdot S_{\theta 1})^2 + 2 \cdot p\theta_1 \cdot p\theta_2 \cdot S_{\theta 1}{}^2 \ldots \\ + 2 \cdot p\delta\theta_1 \cdot p\theta_2 \cdot S_{\theta 1}{}^2 + 2 \cdot p\delta\theta_2 \cdot p\theta_2 \cdot S_{\theta 1}{}^2 + 2 \cdot p\theta_1 \cdot p\delta\theta_2 \cdot S_{\theta 1}{}^2 + 2 \cdot p\delta\theta_1 \cdot p\delta\theta_2 \cdot S_{\theta 1}{}^2 \ldots \\ + 2 \cdot p\theta_1 \cdot p\theta_1 \cdot S_{\theta 1}{}^2 + 2 \cdot p\delta\theta_1 \cdot p_{\theta 1} \cdot S_{\theta 1}{}^2 + 2 \cdot p\delta\theta_2 \cdot p_{\theta 1} \cdot S_{\theta 1}{}^2 + 2 \cdot p\theta_1 \cdot p_{\theta 1} \cdot S_{\theta 1}{}^2 \ldots \\ + 2 \cdot p\theta_2 \cdot p_{\theta 1} \cdot S_{\theta 1}{}^2 \end{array}}$$

$U_{\theta 0} := \sqrt{R_{\theta 0}{}^2 + S_{\theta 0}{}^2}$ $U_{\theta 0} = 0.645\mathrm{deg}$ $S_{\theta 0} = 0.5\mathrm{deg}$

COMPARISONS

Note: The model manufacture and experiment manufacture comparisons follow t initial comparisons in the calculations.

Initial Comparisons

Identify values from experimental data:

$$t1_{P+1} := t1_P + (.005\cdot s) \qquad \omega := -184.61546\cdot\frac{deg}{s}$$

The constraint equation for theta as a function of engine speed and elapsed time:

$$\theta_i := \theta_0 + \sum_{j=1}^{i} \omega\cdot\left(t1_{j+1} - t1_j\right)$$

Recalculate experimental results with new frame of reference:

Reestablish counters in MathCad: $N := 8 \qquad j := 1..N$

The maximum and minimum displacement from the 8 cycles:

$$md_{min} := \begin{pmatrix} min(d_1) \\ min(d_2) \\ min(d_3) \\ min(d_4) \\ min(d_5) \\ min(d_6) \\ min(d_7) \\ min(d_8) \end{pmatrix} \qquad md_{max} := \begin{pmatrix} max(d_1) \\ max(d_2) \\ max(d_3) \\ max(d_4) \\ max(d_5) \\ max(d_6) \\ max(d_7) \\ max(d_8) \end{pmatrix}$$

The mean values of min and max d:

$$d_{min} := \frac{\sum_{j=1}^{N} md_{min_j}}{N} \qquad d_{max} := \frac{\sum_{j=1}^{N} md_{max_j}}{N}$$

$$d_{min} = 0.293in \qquad d_{max} = 1.797in$$

The standard deviations of the minimum and maximum displacements:

$$Sd_{min} := \sqrt{\sum_{j=1}^{N} \frac{\left(d_{min} - md_{min_j}\right)^2}{N-1}} \qquad Sd_{max} := \sqrt{\sum_{j=1}^{N} \frac{\left(d_{max} - md_{max_j}\right)^2}{N-1}}$$

$$Sd_{min} = 0.018in \qquad Sd_{max} = 4.33\times 10^{-3}\ in$$

The random uncertainties in the maximum and minimum displacements:

$$Rd_{min} := 2\cdot\frac{Sd_{min}}{\sqrt{N}} \qquad Rd_{max} := 2\cdot\frac{Sd_{max}}{\sqrt{N}}$$

The total displacement:

$$d_t := \frac{d_{min} + dm(0) + d_{max} + dm(\pi)}{2}$$

Converting all 8 experimental cycles:

$$de_1 := d_t - d_1 \qquad de_2 := d_t - d_2 \qquad de_3 := d_t - d_3 \qquad de_4 := d_t - d_4$$

$$de_5 := d_t - d_5 \qquad de_6 := d_t - d_6 \qquad de_7 := d_t - d_7 \qquad de_8 := d_t - d_8$$

The data reduction equation as a function of measured variables:

$$de_1 := \frac{d_{min} + dm(0) + d_{max} + dm(\pi)}{2} - d_1$$

Therefore the general uncertainty analysis equation is:

$$S_{dec_i} := \sqrt{\frac{1}{4}\cdot\left(S_{de_{38}}\right)^2 + \frac{1}{4}\cdot sd(0\cdot deg)^2 + \frac{1}{4}\left(S_{de_{10}}\right)^2 + \frac{1}{4}\cdot sd(180\cdot deg)^2 + \left(S_{de_i}\right)^2}$$

$$R_{dec_i} := \sqrt{\frac{1}{4}\cdot Rd_{min}^{\ 2} + \frac{1}{4}\cdot rd(0\cdot deg)^2 + \frac{1}{4}Rd_{max}^{\ 2} + \frac{1}{4}\cdot rd(180\cdot deg)^2 + \left(R_{de_i}\right)^2}$$

$$U_{dec} := \sqrt{S_{de}^{\ 2} + R_{de}^{\ 2}}$$

Rename variables: $d_{mc_i} := dm(\theta_i)$ $U_{dmc_i} := U_{dm}(\theta_i)$

Initial Comparisons Uncertainty

Estimate the uncertainty in average engine speed: $u_\omega := 300\cdot\frac{deg}{s}$

Uncertainty in reference angle becomes fossilized systematic: $S_\theta := U_{\theta 0}$

Partial derivative of crank angle with respect to engine speed and uncertainty equation for crank angle as a function of engine speed, reference angle, and elapsed time:

$p_{\omega_i} := i\cdot .005\cdot s$ $U_{\theta_i} := \sqrt{\left(p_{\omega_i}\right)^2\cdot u_\omega^{\ 2} + S_\theta^{\ 2}}$ $\Theta := \theta$

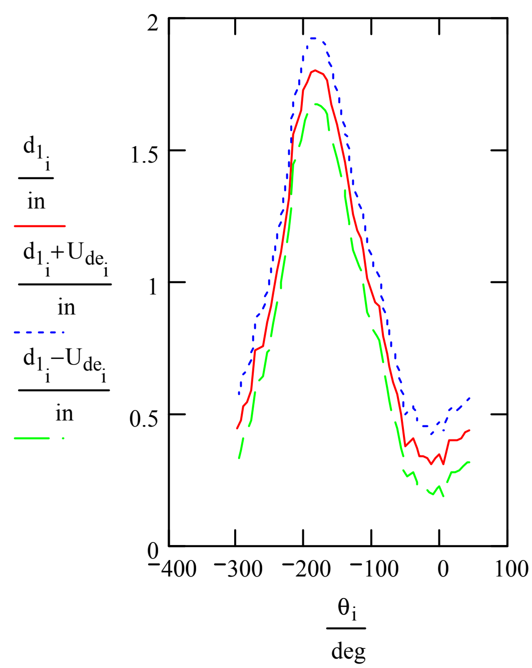

Figure A.3: Uncertainty in Experimental Displacement

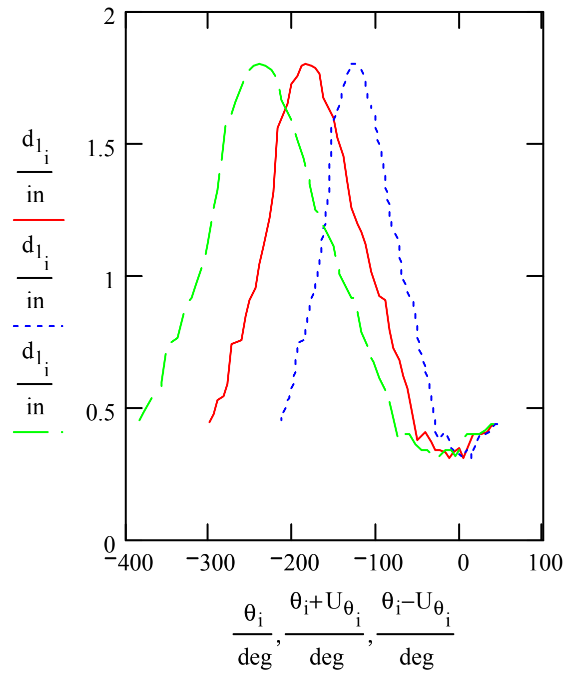

Figure A.4: Uncertainty in Experimental Crank Ang

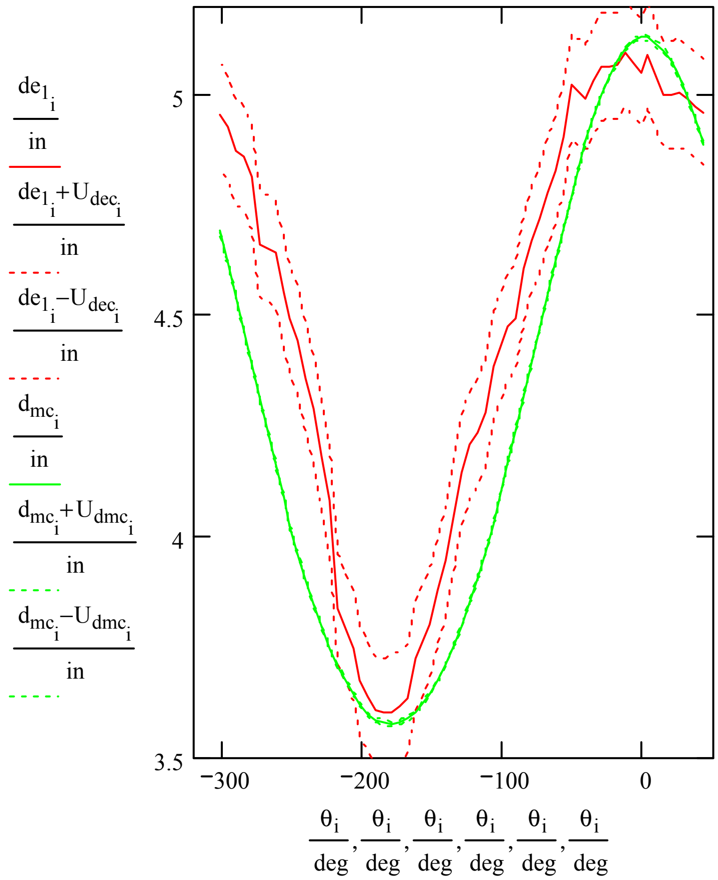

Figure A.5: Experimental Results with New Frame of Reference

Manufacturing Effects on the Model

The first elemental source was the baseline design:

$sl_{cs1} := rl_{cs}$ $\quad sd_{cs1} := rd_{cs}$ $\quad sl_{p1} := rl_{p}$

Manufacture is the second elemental source for the pre-designed links:

$sl_{cs2} := tl_{cs}$ $\quad sl_{p2} := tl_{p}$ $\quad sd_{cs2} := td_{cs}$

The root-sum-square method to combine elemental sources:

$sl_{cs} := \sqrt{sl_{cs1}^{2} + sl_{cs2}^{2}}$ $\quad sl_{p} := \sqrt{sl_{p1}^{2} + sl_{p2}^{2}}$ $\quad sd_{cs} := \sqrt{sd_{cs1}^{2} + sd_{cs2}^{2}}$

The total uncertainty for the diameters:

$ud_{cs} := \sqrt{sd_{cs}^{2} + rd_{cs}^{2}}$ $\quad ud_{cr} := \sqrt{sd_{cr}^{2} + rd_{cr}^{2}}$

Repeat slop uncertainty equations: $rs_{x} := \dfrac{d_{cr} - d_{cs}}{2}$ $\quad ss_{x} := \sqrt{\dfrac{1}{4} \cdot ud_{cr}^{2} + \dfrac{1}{4} \cdot ud_{cs}^{2}}$

The model uncertainty repeated:

$$rd(\theta) := \left(pl_{cs}(\theta)^2 \cdot rl_{cs}^{\ 2} + pl_1(\theta)^2 \cdot rl_1^{\ 2} + pl_2(\theta)^2 \cdot rl_2^{\ 2} + pl_p^{\ 2} \cdot rl_p^{\ 2} + ps_x^{\ 2} \cdot rs_x^{\ 2}\right)^{\frac{1}{2}}$$

$$sd(\theta) := \left(pl_{cs}(\theta)^2 \cdot sl_{cs}^{\ 2} + pl_1(\theta)^2 \cdot sl_1^{\ 2} + pl_2(\theta)^2 \cdot sl_2^{\ 2} + pl_p^{\ 2} \cdot sl_p^{\ 2} + ps_x^{\ 2} \cdot ss_x^{\ 2}\right)^{\frac{1}{2}}$$

Finally, the combined uncertainty: $ud(\theta) := \sqrt{rd(\theta)^2 + sd(\theta)^2}$

The model equation:

$$d(\theta) := l_{cs} \cdot \cos(\theta) + \sqrt{\left(\frac{l_1 + l_2}{2}\right)^2 - l_{cs}^{\ 2} \cdot (\sin(\theta))^2} + l_p + s_x$$

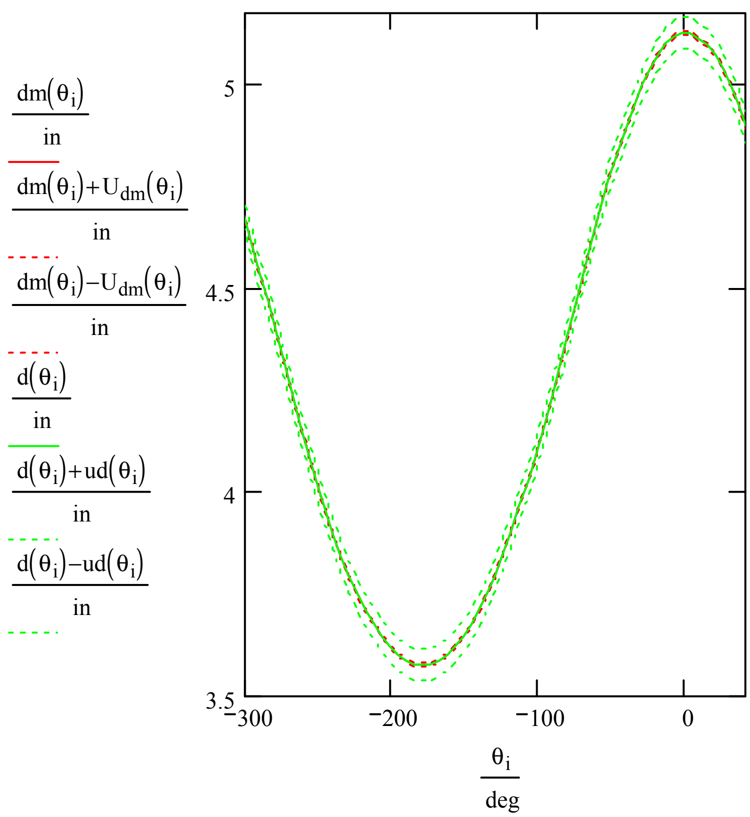

Figure A.6: Model Results with and without Manufacturing Effects

Manufacture Effects on the Experiment

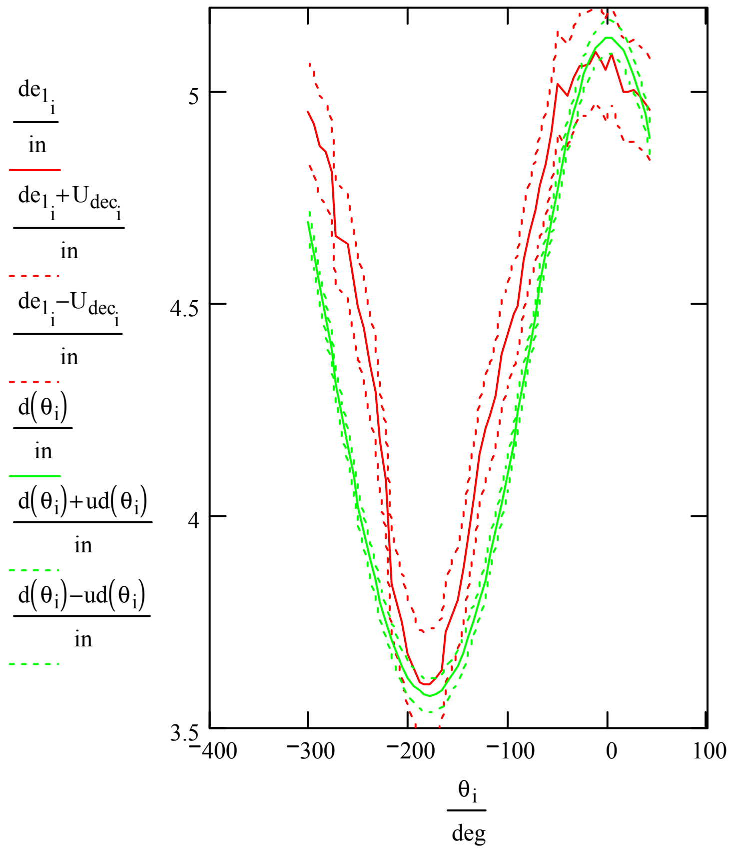

Figure A.7: Model results with Manufacture Effects and Experimental Results

Final Comparisons

Nondimensionalize for design optimization:

$$nl_{cs} := \frac{l_{cs}}{in} \quad nl_1 := \frac{l_1}{in} \quad nl_2 := \frac{l_2}{in} \quad nde := \frac{de_1}{in} \quad nl_p := \frac{l_p}{in} \quad nU_{de} := \frac{U_{dec}}{in}$$

Design optimization techniques to minimize the absolute error:

$$F(z, nde) := \left| nde - \left[nl_{cs} \cdot \cos(z) + \sqrt{\left(\frac{nl_1 + nl_2}{2}\right)^2 - nl_{cs}^{\,2} \cdot (\sin(z))^2} + nl_p \right] \right|$$

Establish tolerances:

$$\tau := .382 \quad \varepsilon := 0.0001 \quad N := \frac{\ln(\varepsilon)}{\ln(1-\tau)} + 3 \quad N = 22.138 \quad N := 23 \qquad i := 2..(N-2)$$

Reestablish counters in Mathcad, the algorithm must be partitioned into 3 groups to ensure that the algorithm finds the accuratee value of theta.

$j := 1..10$

The golden section algorithm:

$$
\begin{aligned}
X1(nde) := \;&\; X_{l_1} \leftarrow 0 \\
&\; F_{l_1} \leftarrow F\left(X_{l_1}, nde\right) \\
&\; X_{u_1} \leftarrow 3.1 \\
&\; F_{u_1} \leftarrow F\left(X_{u_1}, nde\right) \\
&\; X1_1 \leftarrow (1-\tau)\cdot X_{l_1} + \tau\cdot X_{u_1} \\
&\; F_{l_1} \leftarrow F\left(X1_1, nde\right) \\
&\; X2_1 \leftarrow \tau\cdot X_{l_1} + (1-\tau)\cdot X_{u_1} \\
&\; \left(F2_1 \leftarrow F\left(X2_1, nde\right)\right) \\
&\; \text{for } i \in 2..(N-2) \\
&\quad \text{if } F\left(X1_{i-1}, nde\right) > F\left(X2_{i-1}, nde\right) \\
&\qquad X_{l_i} \leftarrow X1_{i-1} \\
&\qquad F_{l_i} \leftarrow F\left(X_{l_i}, nde\right) \\
&\qquad X_{u_i} \leftarrow X_{u_{i-1}} \\
&\qquad F_{u_i} \leftarrow F\left(X_{u_i}, nde\right) \\
&\qquad X1_i \leftarrow X2_{i-1} \\
&\qquad F1_i \leftarrow F\left(X1_i, nde\right) \\
&\qquad X2_i \leftarrow \tau\cdot X_{l_i} + (1-\tau)\cdot X_{u_i} \\
&\qquad F2_i \leftarrow F\left(X2_i, nde\right) \\
&\quad \text{otherwise} \\
&\qquad X_{u_i} \leftarrow X2_{i-1} \\
&\qquad F_{u_i} \leftarrow F\left(X_{u_i}, nde\right) \\
&\qquad X_{l_i} \leftarrow X_{l_{i-1}} \\
&\qquad F_{l_i} \leftarrow F\left(X_{l_i}, nde\right) \\
&\qquad X2_i \leftarrow X1_{i-1} \\
&\qquad F2_i \leftarrow F\left(X2_i, nde\right) \\
&\qquad X1_i \leftarrow (1-\tau)\cdot X_{l_i} + \tau\cdot X_{u_i} \\
&\qquad F1_i \leftarrow F\left(X1_i, nde\right) \\
&\; X1_{21}
\end{aligned}
$$

$pu := nde + nU_{de}$

$pl := nde - nU_{de}$

$p := nde$

$\theta u_j := X1\left(pu_j\right)$

$\theta l_j := X1\left(pl_j\right)$

$\theta_j := X1\left(p_j\right)$

$j := 10..38$

$$
X1(nde) := \left|
\begin{array}{l}
X_{l_1} \leftarrow -3.14 \\
F_{l_1} \leftarrow F\left(X_{l_1}, nde\right) \\
X_{u_1} \leftarrow 0 \\
F_{u_1} \leftarrow F\left(X_{u_1}, nde\right) \\
X_{1_1} \leftarrow (1-\tau)\cdot X_{l_1} + \tau\cdot X_{u_1} \\
F_{l_1} \leftarrow F\left(X_{1_1}, nde\right) \\
X_{2_1} \leftarrow \tau\cdot X_{l_1} + (1-\tau)\cdot X_{u_1} \\
\left(F_{2_1} \leftarrow F\left(X_{2_1}, nde\right)\right) \\
\text{for } i \in 2..(N-2) \\
\quad \left|
\begin{array}{l}
\text{if } F\left(X_{1_{i-1}}, nde\right) > F\left(X_{2_{i-1}}, nde\right) \\
\quad \left|
\begin{array}{l}
X_{l_i} \leftarrow X_{1_{i-1}} \\
F_{l_i} \leftarrow F\left(X_{l_i}, nde\right) \\
X_{u_i} \leftarrow X_{u_{i-1}} \\
F_{u_i} \leftarrow F\left(X_{u_i}, nde\right) \\
X_{1_i} \leftarrow X_{2_{i-1}} \\
F_{1_i} \leftarrow F\left(X_{1_i}, nde\right) \\
X_{2_i} \leftarrow \tau\cdot X_{l_i} + (1-\tau)\cdot X_{u_i} \\
F_{2_i} \leftarrow F\left(X_{2_i}, nde\right)
\end{array}
\right. \\
\text{otherwise} \\
\quad \left|
\begin{array}{l}
X_{u_i} \leftarrow X_{2_{i-1}} \\
F_{u_i} \leftarrow F\left(X_{u_i}, nde\right) \\
X_{l_i} \leftarrow X_{l_{i-1}} \\
F_{l_i} \leftarrow F\left(X_{l_i}, nde\right) \\
X_{2_i} \leftarrow X_{1_{i-1}} \\
F_{2_i} \leftarrow F\left(X_{2_i}, nde\right) \\
X_{1_i} \leftarrow (1-\tau)\cdot X_{l_i} + \tau\cdot X_{u_i} \\
F_{1_i} \leftarrow F\left(X_{1_i}, nde\right)
\end{array}
\right.
\end{array}
\right. \\
X_{1_{21}}
\end{array}
\right.
$$

$$\theta u_j := X1\left(pu_j\right)$$

$$\theta l_j := X1\left(pl_j\right)$$

$$\theta_j := X1\left(p_j\right)$$

$$j := 38..P$$

$$
X1(nde) := \left|
\begin{array}{l}
X_{l_1} \leftarrow -6.2 \\
F_{l_1} \leftarrow F\left(X_{l_1}, nde\right) \\
X_{u_1} \leftarrow -3.14 \\
F_{u_1} \leftarrow F\left(X_{u_1}, nde\right) \\
X1_1 \leftarrow (1-\tau)\cdot X_{l_1} + \tau\cdot X_{u_1} \\
F1_1 \leftarrow F\left(X1_1, nde\right) \\
X2_1 \leftarrow \tau\cdot X_{l_1} + (1-\tau)\cdot X_{u_1} \\
\left(F2_1 \leftarrow F\left(X2_1, nde\right)\right) \\
\text{for } i \in 2..(N-2) \\
\quad \left|
\begin{array}{l}
\text{if } F\left(X1_{i-1}, nde\right) > F\left(X2_{i-1}, nde\right) \\
\quad \left|
\begin{array}{l}
X_{l_i} \leftarrow X1_{i-1} \\
F_{l_i} \leftarrow F\left(X_{l_i}, nde\right) \\
X_{u_i} \leftarrow X_{u_{i-1}} \\
F_{u_i} \leftarrow F\left(X_{u_i}, nde\right) \\
X1_i \leftarrow X2_{i-1} \\
F1_i \leftarrow F\left(X1_i, nde\right) \\
X2_i \leftarrow \tau\cdot X_{l_i} + (1-\tau)\cdot X_{u_i} \\
F2_i \leftarrow F\left(X2_i, nde\right)
\end{array}
\right. \\
\text{otherwise} \\
\quad \left|
\begin{array}{l}
X_{u_i} \leftarrow X2_{i-1} \\
F_{u_i} \leftarrow F\left(X_{u_i}, nde\right) \\
X_{l_i} \leftarrow X_{l_{i-1}} \\
F_{l_i} \leftarrow F\left(X_{l_i}, nde\right) \\
X2_i \leftarrow X1_{i-1} \\
F2_i \leftarrow F\left(X2_i, nde\right) \\
X1_i \leftarrow (1-\tau)\cdot X_{l_i} + \tau\cdot X_{u_i} \\
F1_i \leftarrow F\left(X1_i, nde\right)
\end{array}
\right.
\end{array}
\right. \\
X1_{21}
\end{array}
\right.
$$

$$\theta u_j := X1\left(pu_j\right)$$

$$\theta l_j := X1\left(pl_j\right)$$

$$\theta_j := X1\left(p_j\right)$$

Reestablish counters in Mathcad: $i := 1..P \quad n_i := 1 \cdot i \quad N := P \quad j := 1..P$

Using the values of crank angle found in the design optimization process, a curve fit:

$$F(z) := \begin{pmatrix} z^4 \\ z^3 \\ z^2 \\ z \\ 1 \end{pmatrix}$$

$i := 1..P \quad n_i := 1 \cdot i \quad r := 1.3, 1.32..1.64$

$$C := \mathrm{linfit}(n, \theta, F) \qquad C = \begin{pmatrix} 2.625 \times 10^{-6} \\ -2.822 \times 10^{-4} \\ 8.582 \times 10^{-3} \\ -0.176 \\ 1.053 \end{pmatrix}$$

$$Q := C_1 \cdot n^4 + C_2 \cdot n^3 + C_3 \cdot n^2 + C_4 \cdot n + C_5$$

Final Comparisons Uncertainty

The experimental uncertainty bands were optimized also: $U_{\theta exp} := \dfrac{\theta u - \theta l}{2}$

Uncertainty estimate from the design optimization: $B_Y := .01$

The uncertainty in "i" was assumed to be negligible: $S_n := 0 \quad R_n := 0$

The uncertainty in the experimental displacement was converted to a random uncertainty in the crank angle: $R_Y := U_{\theta exp}$

Jitter Program used to estimate the partial derivatives:

$$\delta\theta := .01 \qquad q(z) := F(z)^T \qquad Q(z, c_1, c_2, c_3, c_4, c_5) := c_1 \cdot z^4 + c_2 \cdot z^3 + c_3 \cdot z^2 + c_4 \cdot z + c_5$$

$$\theta u(i,j) := \theta_i \cdot \left[1 + (\delta\theta \cdot \mathrm{identity}(P))_{i,j} \right] \qquad \theta l(i,j) := \theta_i \cdot \left[1 - (\delta\theta \cdot \mathrm{identity}(P))_{i,j} \right]$$

```
Qu := | for j ∈ 1..P
      |   | for i ∈ 1..P
      |   |    θ_i ← θu(i, j)
      |   | C ← linfit(n, θ, F)
      |   | Qu_j ← Q(n_i, C_1, C_2, C_3, C_4, C_5)
      | Qu

Ql := | for j ∈ 1..P
      |   | for i ∈ 1..P
      |   |    θ_i ← θl(i, j)
      |   | C ← linfit(n, θ, F)
      |   | Ql_j ← Q(n_i, C_1, C_2, C_3, C_4, C_5)
      | Ql
```

$$d\theta fit_j := \frac{Qu_j - Ql_j}{2 \cdot \delta\theta}$$

The total uncertainty in the improved estimate of the crank angle:

$$U_Q := \sqrt{\sum_{i=1}^{P} \left(d\theta fit_i\right)^2 \cdot R_Y{}^2 + \sum_{i=1}^{P} \left(d\theta fit_i\right)^2 \cdot B_Y{}^2 + 2 \cdot \sum_{i=1}^{P-1} \sum_{k=i+1}^{P} d\theta fit_i \cdot d\theta fit_k \cdot B_Y{}^2}$$

The curve fit equation repeated: $Q := C_1 \cdot n^4 + C_2 \cdot n^3 + C_3 \cdot n^2 + C_4 \cdot n + C_5$

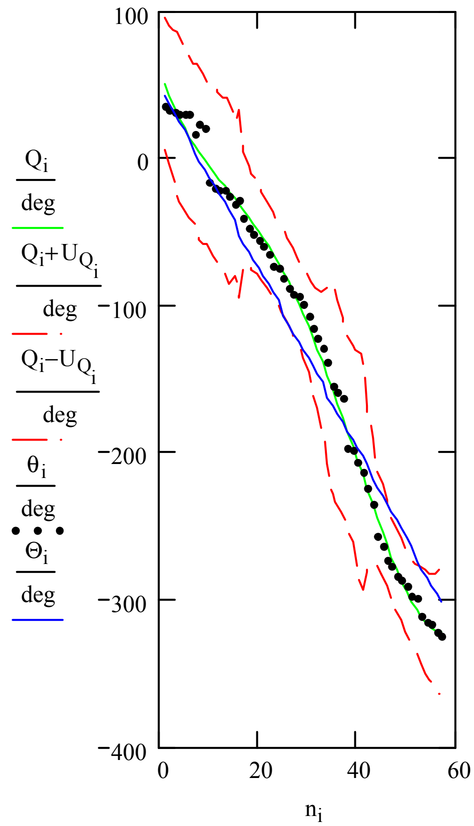

Figure A.8: Crank Angle Comparisons

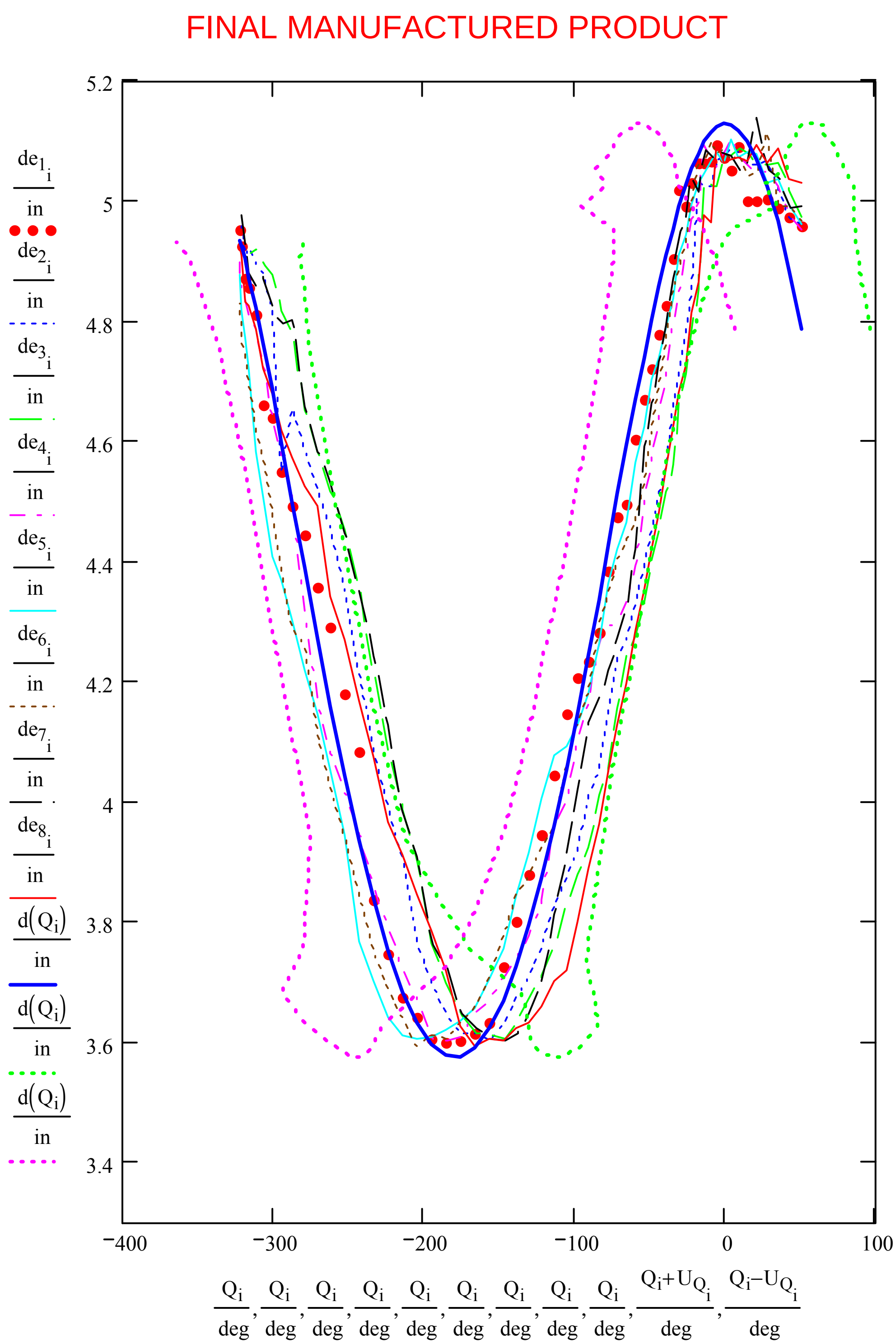

Figure A.9: Eight Cycles and Final Manufactured Product

FINAL MANUFACTURED PRODUCT UNCERTAINTY

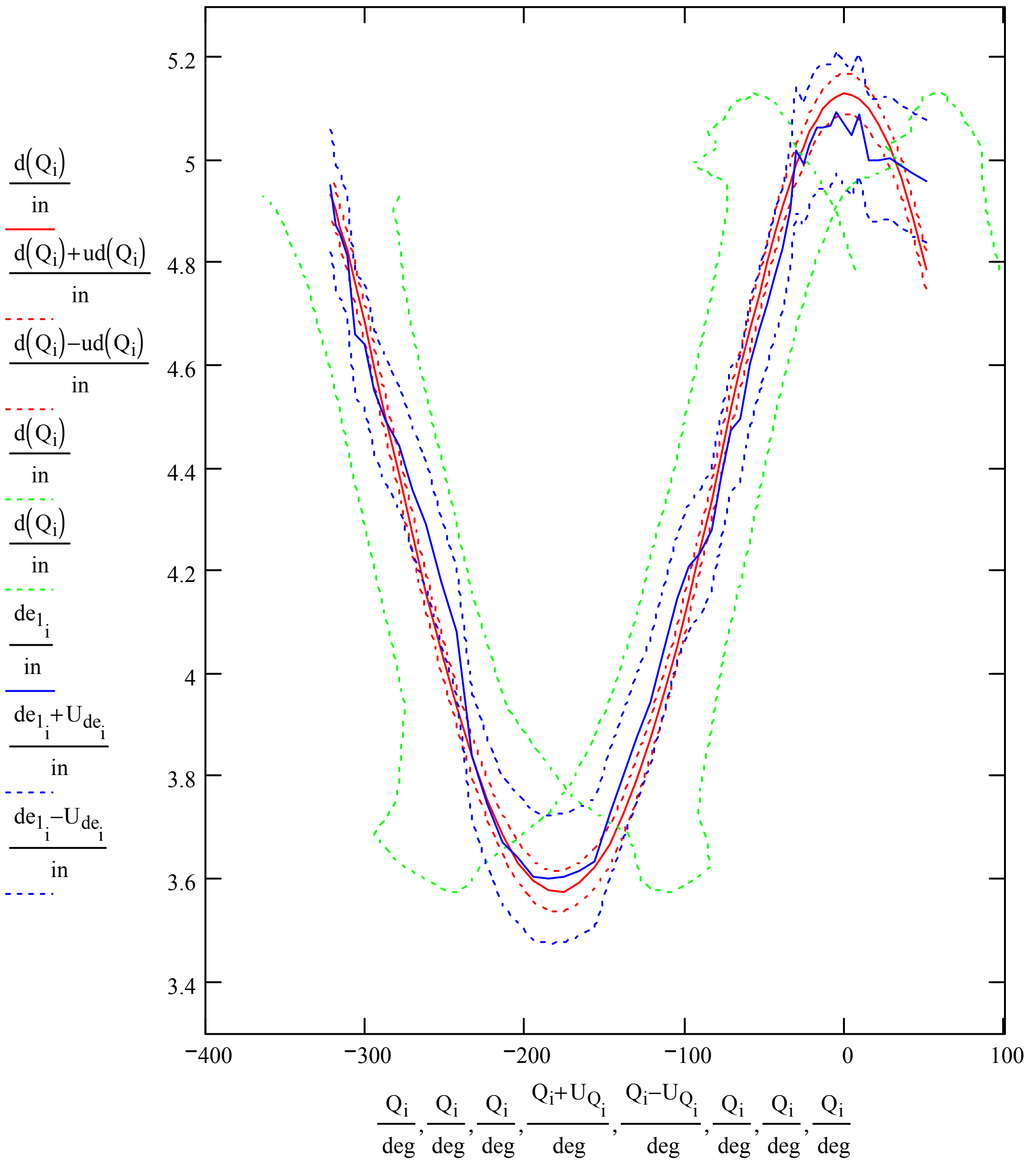

Figure A.10: Final Manufactured Product Uncertainty